ISBN 978-82-326-0356-5 (printed version)
ISBN 978-82-326-0357-2 (electronic version)
ISSN 1503-8181

Doctoral theses at NTNU, 2014:217

Zeinab Amrollahi Biyouki

Thermodynamic analysis of CO_2 capture processes for power plants

NTNU
Norwegian University of
Science and Technology
Faculty of Engineering
Science and Technology
Department of Energy and
Process Engineering

NTNU – Trondheim
Norwegian University of
Science and Technology

Doctoral Thesis

Zeinab Amrollahi Biyouki

Doctoral theses at NTNU, 2014:217

NTNU

NTNU – Trondheim
Norwegian University of
Science and Technology

Zeinab Amrollahi Biyouki

Thermodynamic analysis of CO_2 capture processes for power plants

Thesis for the degree of Philosophiae Doctor

Trondheim, August 2014

Norwegian University of Science and Technology
Faculty of Engineering Science and Technology
Department of Energy and Process Engineering

NTNU – Trondheim
Norwegian University of
Science and Technology

NTNU
Norwegian University of Science and Technology

Thesis for the degree of Philosophiae Doctor

Faculty of Engineering Science and Technology
Department of Energy and Process Engineering

ISBN 978-82-326-0356-5 (printed version)
ISBN 978-82-326-0357-2 (electronic version)
ISSN 1503-8181

Doctoral theses at NTNU, 2014:217

Printed by Skipnes Kommunikasjon as

To Mohammad and Mahsa

To Fatemeh and Reza

Abstract

This thesis work presents an evaluation of various processes for reducing CO_2 emissions from natural-gas-fired combined cycle (NGCC) power plants. The scope of the thesis is to focus mainly on post-combustion chemical absorption for NGCC. For the post-combustion capture plant, an important interface is the steam extraction from the steam turbine in order to supply the heat for solvent regeneration. The steam extraction imposes a power production penalty. The thesis includes analysis and comparison between several chemical absorption processes configurations integrated with NGCC.

The objectives of the present work were to use thermodynamic analysis on various chemical absorption process configurations to evaluate, quantify and justify improved design of NGCC with post-combustion CO_2 capture. The thermodynamic evaluation of the processes gave insight to the detailed distribution of process irreversibilities and supports the state-of-the-art process configuration with the lowest energy penalty due to addition of CO_2 capture to the power plant.

The reference power plant without CO_2 capture has a power production of 384 MW and a net electric efficiency of 56.4% (LHV) with CO_2 emissions of ≈ 362 g CO_2/ net kWh electricity. The power plant design was carried out using the computational tool GTPRO. The aim of the CO_2 capture plant was to remove 90% of the CO_2 emissions present in the flue gas. To assess and analyse the various chemical absorption process configurations, the UniSim Design software was used, which contains the Amines Property Package. This special property package has been designed to aid the modelling of alkanolamine treating units in which CO_2 is removed from gaseous streams. The downstream compression of the captured CO_2 was also simulated using UniSim Design.

The investigated process configurations were comprised of chemical absorption process with absorber inter-cooling, split-flow process and lean vapour recompression (LVR) process. Several design parameters were modified for each of the process configurations to achieve low energy consumption and consequently low work demand. The inter-cooling of the absorber column led to increased solvent rich loading. Consequently, the solvent circulation rate and reboiler energy requirement was decreased. In the split-flow configuration, due to splitting of the rich solvent into two streams, the amount of rich solvent entering the bottom section of the stripper was reduced. Therefore, less reboiler energy was required to remove CO_2 from the solvent to reach the same solvent lean loading as of the reference chemical absorption process. In the configuration with lean vapour recompression (LVR), the lean solvent stream was utilised as a low temperature heat source in order to add exergy input in the form of steam to the stripper column and thus reduce the reboiler duty. The reboiler duty for the CO_2 capture was decreased from 3.74 MJ/kgCO_2 in the reference chemical absorption process to 2.71 MJ/kgCO_2 for the case of LVR with absorber inter-cooling. The net electric efficiency of the reference process with CO_2 capture was calculated to 49.5% (LHV). With the improved process design, the highest net power plant efficiency was calculated to 50.2 % (LHV) for the case of LVR with absorber inter-cooling.

Moreover, exergy analysis was performed to identify the irreversibilities associated with the integration of power plant with various CO_2 capture and compression processes. Particularly, the second law of thermodynamics was used as a tool to evaluate and quantify the reduction of energy penalty associated with CO_2 capture for each process modification. Defining the work input for a theoretical reversible CO_2 capture process as the minimum required work was functional step in

characterising the difference of the work input of theoretical reversible processes and the real irreversible processes. Exergy efficiency of the reference chemical absorption process was calculated to 21.3 % versus 25 % for the case of LVR with absorber inter-cooling. Through exergy balance for every CO_2 capture process configuration, the exchange of exergy content of material and energy streams was assessed.

Using the combination of power plant efficiency and exergy analysis as tools, a pre-combustion reforming combined cycle (IRCC) process with chemical absorption CO_2 capture process was investigated. A rational efficiency of 43.8% was achieved, which indicates the share of input exergy utilised for work production by the power cycle in addition to the exergy of the pure compressed CO_2 stream. The highest amount of irreversibility was contributed by the gas turbine and mainly by the combustor. The irreversibility which is inherent in the combustion process corresponded to a large fraction of original exergy of the fuel. This could be partially compensated by increase the preheating of the fuel supplied to the combustor. Also preheating the inlet streams to auto-thermal reactor (ATR) was found advantageous in decreasing the ATR irreversibilities.

Preface

The thesis is submitted to the Norwegian University of Science and Technology (NTNU), for partial fulfilment of the requirements for the degree of *philosophiae doctor* (PhD). The work was carried out at the Department of Energy and Process Engineering at the Faculty of Engineering Science and Technology under the supervision of Professor Olav Bolland.

The Ph.D. thesis forms a part of the BIGCO2 project, performed under the strategic Norwegian research program Climit. It was founded by the partners: Statoil, GE Global Research, Statkraft, Aker Clean Carbon, Shell, TOTAL, ConocoPhillips, ALSTOM, the Research Council of Norway (178004/I30 and 176059/I30) and Gassnova (182070).

Acknowledgements

First of all, I would like to thank my supervisor Professor Olav Bolland for the opportunity of working on this interesting research topic. He supported me by his guidance and advice along the time as well as encouraged my independence. He inspired me for preforming high quality research and blessed me by his valuable suggestions and comments.

I would like to express my gratitude toward Professor Ivar Ståle Ertesvåg for his exceptional guidance and constant help. He was always eager and open for discussions and willing to share his profound knowledge on the subject matter.

My gratitude and thanks to Dr. Lars Olof Nord for sharing his IRCC model and conducting research together during my PhD work. He inspired me in finding solutions for problems through our valuable and countless discussions.

Also I would like to thank Dr. Rahul Anantharaman for his fruitful discussions during my PhD work.

I was privileged by having friends among NTNU PhD fellows. Among them, I would like to express my feelings and gratitude toward Bita Najmi and Aldo Bischi for their presence and support during this time. We shared our challenges and experiences together and the friendship we build out of it is priceless for me. Thanks for being there with me.

I thank my family and friends in Iran, specially my parents and sisters, whom always been present, supportive and motivating.

Mahsa, you are my true inspiration to finish this work. Having you is the best gift of my life and you could always count on me.

Finally, I would like to thank Mohammad for his unconditional love and encouragement. He walked this difficult path with me and raised me in the moments of fall. Thank you for your patience and support and coming this far with me.

Table of Contents

Nomenclature

C	Ratio between formed CO_2 and fuel, 44
E	Energy (MJ/kg CO_2)
f	CO_2 capture ratio
h	Specific enthalpy (J/kg)
I	Irreversibility (J/s)
LHV	Lower heating value (J/kg)
K	Equilibrium ratio *(k-value)*
$\dot{m}$	Mass flow rate (kg/s)
P	Pressure (bar)
P	Power (W)
$\dot{Q}$	Heat transfer rate (J/s)
$\tilde{R}$	Universal gas constant (J/(mol·K)
s	Specific entropy (J/kg)
T	Temperature (K)
$\dot{W}_x$	Shaft work rate (J/s)
x	Mole fraction (liquid phase)
y	Mole fraction (vapour phase)
$\Delta G^0_{reaction}$	Gibbs function of reaction (KJ/s)
$\Delta H^0_{reaction}$	Standard enthalpy change (heat) of reaction (kJ/s)
$\Delta S^0_{reaction}$	Standard entropy change of reaction (kJ/s·K)

Greek Letters

α	Ratio of incremental power reduction to incremental heat output ($MJ_{electrical}/MJ_{Heat}$)
η	Efficiency
E	Exergy (J)
ε	Specific exergy (J/kg)
$\tilde{\varepsilon}$	Specific molar exergy (J/mol)
ψ	Rational efficiency
γ	Extent of process. chemical reaction/ phase change

Subscripts

0	environmental state
aux	auxiliary
act	actual
C	compressor
CC	CO_2 capture and compression
comp	compression
cond	condensate
G	gas
g	generator
L	liquid
i	*i*-th component of a mixture
in	input
out	output
m, mech	mechanical
NG	natural gas
ph	physical
pp	power plant
rev	reversible
reb	reboiler
Ref	reference
SF	supplementary firing
st	steam
ST	steam turbine
th	thermal
T	turbine
WO-extr	without steam extraction; reference power plant without CO_2 capture
W-extr	with steam extraction; power plant with CO_2 capture and compression

Abbreviations

CCS	CO_2 Capture and Storage
GT	Gas Turbine
HHV	Higher Heating Value
ESA	Electrical Swing Adsorption
HP	High Pressure
HPT	High Pressure Turbine
HRSG	Heat Recovery Steam Generator
IGCC	Integrated Gasification Combined Cycle
IP	Intermediate Pressure
IPT	Intermediate Pressure Turbine
IRCC	Integrated Reforming Combined Cycle
LHV	Lower Heating Value
LP	Low Pressure
LPT	Low Pressure Turbine
LVR	Lean vapour recompression
MEA	Monoethanolamine
NG	Natural Gas
NGCC	Natural Gas Combined Cycle
PR	Peng Robinson
PSA	Pressure Swing Adsorption
ST	Steam Turbine
TIT	Turbine Inlet Temperature
TSA	Temperature Swing Adsorption
VLE	Vapour Liquid Equilibrium

1 Introduction

1.1 Motivation for carbon capture and sequestration

It is a long time that scientists believe greenhouse gases control the atmosphere climate change. Arrhenius (1896) was the first scientist who speculated that the changes in the levels of carbon dioxide in the atmosphere could substantially lead to the greenhouse effect and the surface temperature change. He predicted that emissions of carbon dioxide from the burning of fossil fuels and other combustion processes would cause global warming and he estimated the impact of anthropogenic emissions of CO_2.

Figure 1-1 depicts the global annual temperature change since 1880. Even with variation over the years, the general trend is clearly upwards. Although recently some cooler environment temperatures raised the idea of a global cooling trend, but as the graph shows, even several years of cooling doesn't mean a long-term warming trend is over.

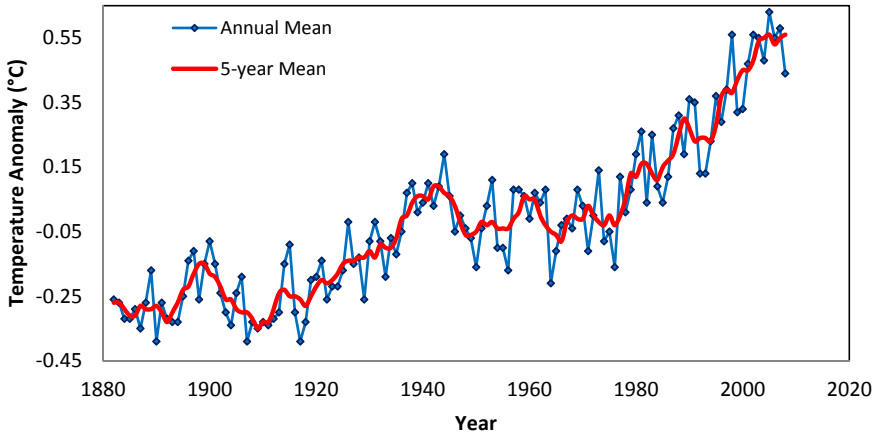

Figure 1-1: Global Annual mean surface air temperature anomalies, 1880 to present, with the base period 1951-1980. The dotted line is the annual mean and the solid red line is the five-year mean. The figure is updated based on Figure 1A in Hansen et al. (2006). Data available from Goddard Institute for Space Studies, 2011, NASA.

Carbon dioxide from fossil fuel combustion is the largest contributor to greenhouse gas emissions worldwide. According to IEA report 2010, 43% of CO_2 emissions from fuel combustion were produced from coal, 36% from oil and 20% from natural gas. Emissions of CO_2 from natural gas in 2010 represented 6.18 Gt CO_2, 4.5% higher than in the previous year. As of 2010, fossil fuels produce 31 gigatonne CO_2 annually. (Figure 1-2)

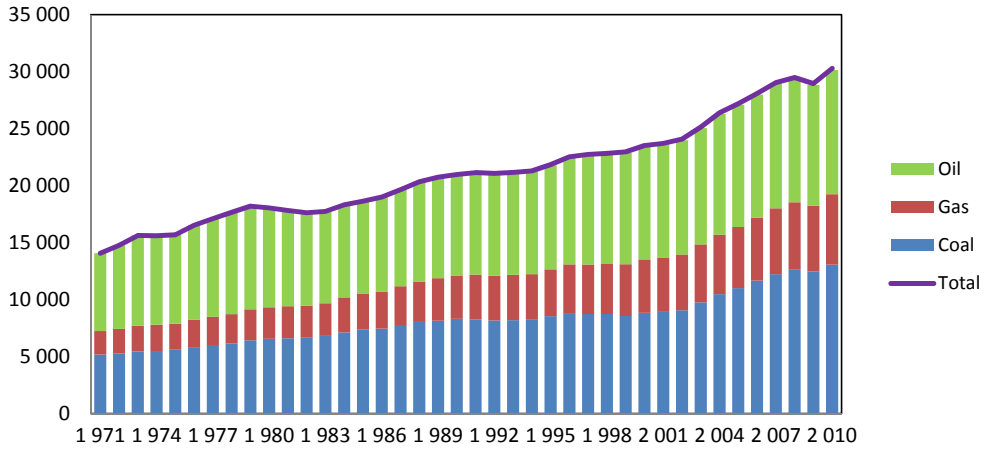

Figure 1-2: CO_2 emissions by fuel. IEA, 2010

Until now, the carbon dioxide from the combustion of fossil fuels has been emitted to the atmosphere and an insignificant amount of that is being captured. This has contributed to a nearly 39% increase of the CO_2 content of the atmosphere since the beginning of industrial revolution, from 280 ppm to 392 ppm today (Conway et al., 2011, NOAA/ESRL). Figure 1-3 shows the global averaged monthly mean CO_2 data that is provided by Global Monitoring Division of NOAA/ESRL from the measurement of carbon dioxide and other greenhouse gases for several decades at a distributed network of air sampling sites (Conway, 1994).

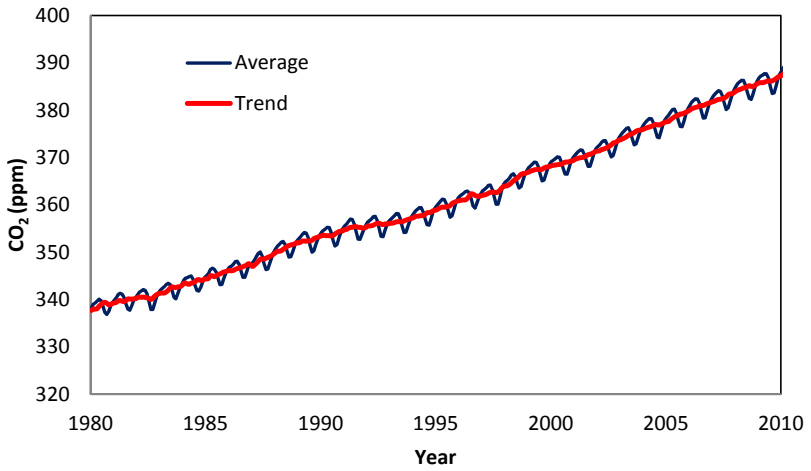

Figure 1-3: Plot of monthly mean carbon dioxide (ppm) globally averaged over marine surface sites. Data available from Conway et al., 2011, NOAA/ESRL. The black line represents the monthly mean values, centred on the middle of each month. The red line represents the same, after correction for the average seasonal cycle.

To stop or slow down this increasing trend, serious decisions should be taken in developing a sustainable energy infrastructure which eliminates the environmental impacts of carbon dioxide mitigation to the atmosphere.

1.1.1 CO_2 emissions by fuel

Fossil fuels are the dominant sources of primary energy worldwide, providing nearly 81% of the world demand (IEA, 2009). Among the fossil fuels, coal power generation with 42 percent of the total power generation is a favourable source since it is relatively inexpensive and compared to other fossil fuels. World Energy Outlook (IEA, 2012) reports that the growth in energy demand will increase the share of CO_2 emissions related to fossil fuel power generation from 41 percent energy at 2007 to 44 percent by 2030. (Figure 1-4)

Natural gas providing nearly 21% of the total power generation worldwide remains an important fuel for electricity generation since it is less expensive with natural gas than with oil as the primary energy source, and natural-gas-fired generating plants are less capital-intensive than plants that use coal, nuclear, or most renewable energy sources.

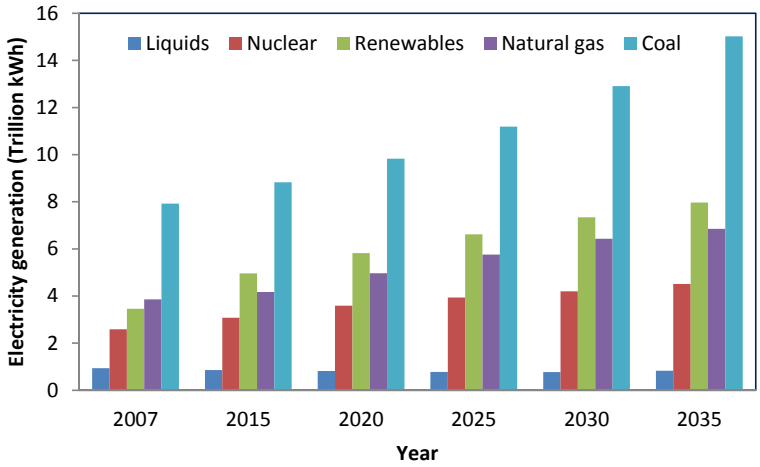

Figure 1-4: Plot of world net electricity generation by fuel, 2007-2035. Data available from International Energy Outlook, 2010.

CO_2 emissions from power generation also depend on the type of consumed fuel or energy and its carbon intensity. Figure 1-5 shows the effects of fuel switch for power generation on CO_2 mitigation for the fossil fuels, renewables and nuclear power. Electricity generation using natural gas instead of coal, for example, can reduce the CO_2 emissions because of the lower C content of natural gas. Also, there is a direct correlation between power plant efficiency, saving the energy and the amounts if the CO_2 emissions. For example, switching from coal to gas increases the efficiency of the power plant specially when used together with the more efficient combined-cycle results in even higher efficiencies (IEA, 2008). As shown in Figure 1-5, gas-fired combined-cycle plants produce less CO_2

per kWh electricity output than other fossil fuel technologies because of the relatively high thermal efficiency of the technology and the high hydrogen-carbon ratio of methane. Both effects, using low carbon-fuel and high energy efficiency are toward the global warming mitigation. However the limited sources of natural gas worldwide and its price would have dominant effect of the usage of this fuel and consequently would affect the CO_2 emissions trends.

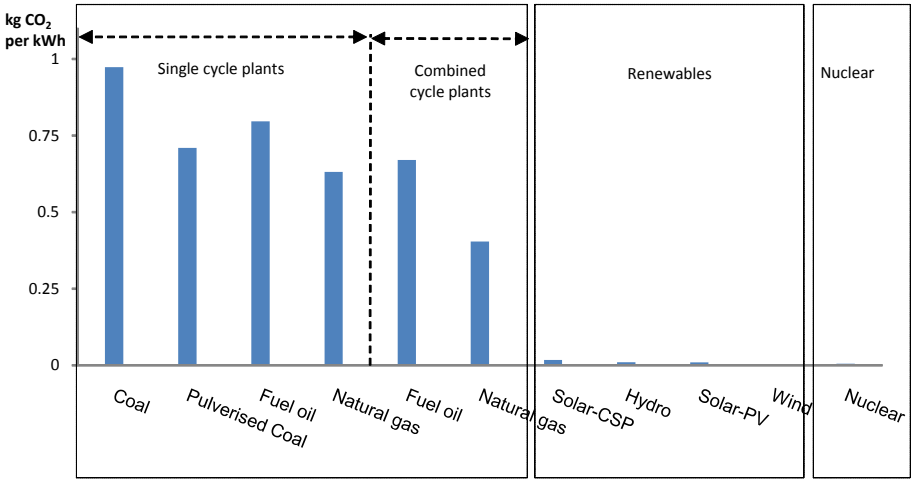

Figure 1-5: Lifecycle greenhouse gas emission estimates for electricity generators fossil fuels data for available from climate change 2007, IPCC; for renewables and nuclear from IEA, Energy Technology Perspectives, 2010

Another option of energy supply would be switching to renewables and nuclear power instead of fossil fuels which are as illustrated by Figure 1-5 can considerably reduce CO_2 emissions. Some forms of renewable energy are now competitive in various market conditions, like wind power which is growing at the rate of 30% annually worldwide with the installed capacity of 158 (GW) in 2009 (GWEC, 2010). Also global photovoltaic (PV) installations surpassed 21 GW cumulatively (Russell, 2010). However high cost of renewables makes them generally uncompetitive with fossil fuel.

CO_2 capture and storage (CCS) is the only pathway which allows the world to continue the usage of fossil fuels while reducing their combustion-associated emissions. Furthermore, the most near-term method of CO_2 capture is post-combustion capture for existing fossil fuel plants followed by long-term, large-scale sequestration to the isolate the CO_2 from the atmosphere.

1.2 Introduction to carbon capture

There are three major approaches to capture CO_2.The summary comes in following paragraphs;

1.2.1 Post-combustion capture

In post-combustion capture, CO_2 is removed from the combustion product - flue gas - before emission to the atmosphere. This capture method is an extension to the flue gas treatment for the SO_x and NO_x removal, however, the higher concentration of CO_2 (typically 4-15%, depending on the fuel type)

made CO_2 removal more challenging. Post-combustion CO_2 capture using absorption is the most developed candidate for gas-fired power plants. Neither the oxyfuel combustion nor the pre-combustion approaches are well suited for gas-fired power plants (Herzog et al., 2009). Furthermore, post-combustion capture is compatible to retrofit into the existing power plants without requiring fundamental change in basic combustion technology as well as it is near-term solution for new power plants.

Moreover, this method offers flexibility to the power plant. Because it is not highly integrated into the power plant process and is designed as an add-on to the power plants, in case of capture plant failure and shut down, the power plant can still operate. Figure 1-6 depicts a schematic of post-combustion capture.

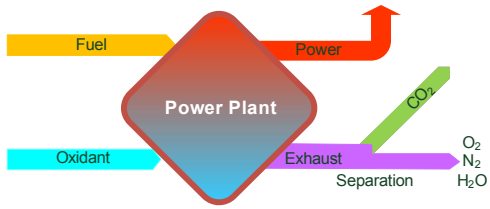

Figure 1-6: Schematic of post-combustion CO_2 capture

Several technologies have been developed to remove CO_2 from flue gases of the power plants which include but not limited to: absorption with solvents, membrane purification, adsorption and cryogenic distillation.

1.2.1.1 Absorption

Absorption is a well-established process of separation as the physical or chemical process in which CO_2 enters liquid bulk phase and is absorbed by the liquid volume. The process takes place in columns in which turbulent flow promotes rapid CO_2 transfer from gas to liquid. Also reaction happens between the CO_2 and the aqueous absorbents in liquid phase. Further on, density differences simplifies the separation of remaining gas and liquid containing CO_2.

To recover the captured CO_2 the loaded solvent is pumped to a stripper in which it is exposed to steam that heats up the solvent and regenerate it. The stripped liquid is pumped back to the absorber while the steam/CO_2 mixture is cooled to condense the steam, leaving high-purity CO_2 suitable for compression and, after transportation to an appropriate site, sequestration.

Aqueous alkanolamine solutions are the most used solvents for chemical absorption processes (monoethanolamine, MEA, being the most widely known). This will be further elaborated in chapter 2.2.2. Other fluids with alkaline character, such as chilled or ambient temperature ammonia or ammonium carbonate are investigated for chemical absorption processes in pilot plants (by Alstom in Pleasant Prairie, USA and Technology centre Mongstad).

Hot potassium carbonate solution is used by early industrial systems for recovering CO_2 from gas streams (Sanyal et al., 1988). It reacts with dissolved CO_2 to form potassium bicarbonate. But most recently amines are preferred for industrial CO_2 recovery processes (Kohl et al., 1997).

Chapter 2 gives more technical background information regarding various chemical absorption solvents and reviews the various chemical absorption process-configuration alternatives.

Physical absorption is a successfully established process for gaseous streams with high CO_2 partial pressures. The nonreactive organic solvents physically dissolve the CO_2 which is then stripped by merely reducing the pressure (low heat consumption). The solvents have no absorption limitation and the CO_2 loading capacity is determined by the vapor-liquid equilibrium of the mixture, which is governed by the pressure and temperature. At high CO_2 partial pressures, the CO_2 loading capacity of the solvent is higher for a physical solvent than for a chemical solvent. Methanol (Rectisol process), Dimethyl ether of polyethylene glycol (SELEXOL), N-Methyl-2-pyrrolidone (Purisol), and propylene carbonate (Fluor Solvent) are among the (industrial) commercial physical solvents (Kohl et al., 1997).

There is another class of absorption processes usually referred to as hybrid solvents, which offer a combination of chemical and physical absorption. The hybrid solvent which is a blend of an amine with a physical solvent, combines the bulk removal capabilities of physical solvent with amine's reactive ability to achieve very low residual CO_2 in a single removal step. Typical processes are Sulfinol, Amisol and Selefining process (Kohl et al., 1997, Collot, 2003).

Other innovative absorption processes are found in the literature such as combination of mixed amines with other activating materials such as membranes. In this method, porous membranes are used as platforms for absorption and stripping. Shimada et al. (2006) research investigated the absorption /desorption of CO_2 into/from aqueous solution of a secondary amine using a membrane contained contactor. CORAL, a hybrid absorption solvent (Feron et al., 2004), contains a mixture of salts and amino acids, and flue gases are carried out through poly-olefin membrane contactors. Similarly, a novel concept based on reverse osmosis membrane as an application to post-combustion CO_2 capture with ammonia absorption has been developed recently (Li et al., 2011).

1.2.1.2 Cryogenic separation

Cryogenic separation is an air separation process, where gaseous components of a mixture are separated by condensation. The thermodynamic process is based on a closed-cycle operated refrigeration system consisting of a compressor, a Joule–Thompson valve (JTV), multi-stage heat exchangers and expanders. Cryogenic separation is widely used for purification of CO_2 from the streams that already have high CO_2 concentrations (>50%) and it is not generally considered as a method for separation of CO_2 from flue gases (Wilcox, 2012). However, its application is expected in oxyfuel separation processes to obtain pure oxygen. Through cryogenic separation, the liquid CO_2 is directly produced at a relatively low pressure which is avoiding high energy consumption for compressing gaseous CO_2 to very high pressures. However, substantial energy consumption for refrigeration step and CO_2 solidification under low-temperature process are the main challenges for further research and development (Zhang et al., 2006). A novel cryogenic separation process has been developed recently which uses two-stage compression to increase the CO_2 pressure. Thus the liquefaction temperature will be increased which leads to lower energy consumption in refrigeration step and prevent equipment from freezing (Lively et al., 2012).

1.2.1.3 Membrane separation

Membrane technology is among the novel processes under development for separation of CO_2 from flue gases with clear benefits such as low cost of operation as well as safe and environmentally friendly nature of the process. Chemical species permeate selectively with different rates (based on sizes of the permeating molecules and/or solubility and/or diffusion coefficients), through the polymeric membranes. This process is mostly pressure-driven, which makes the separation of CO_2 from flue gases of NGCC challenging, due to low partial pressure of CO_2 in flue gases of NGCC. Other factors which identifies the suitability of membranes in CO_2 separation from flue gases are CO_2/N_2 selectivity >70 and minimum permeability of 100 GPU (Gas Permeation Unit).[1] (Huang et al., 2008)

The majority of investigations on application of membranes for the post-combustion CO_2 capture is on coal-fired power plants (Favre et al., 2011, Merkel et al., 2010, Zhao et al., 2008, 2010), which shows less applicability of membrane contactors for post-combustion CO_2 capture of natural-gas fired power plants. In general, polymeric membranes for CO_2 separation achieved high technology readiness when considering the availability and fabrication readiness of the membranes. However, they are unsuitable for post-combustion capture from natural-gas-fired power plants due to high air-to-fuel ratios producing large amounts of exhaust gas containing highly diluted, low concentrated CO_2 (Carapellucci et al., 2004).

1.2.1.4 Adsorption

Physical adsorption

These processes are based on physical adsorption of CO_2 (without forming chemical bond only weak interactions such as van der Waals forces) to the surface of a variety of nonreactive sorbents including carbonaceous materials and crystalline materials known as zeolites. Under certain conditions i.e. either Pressure Swing Adsorption (PSA), Temperature Swing Adsorption (TSA) or Electrical Swing Adsorption (ESA), the regeneration process continues with release of CO_2 from the adsorbents. Fundamentally, zeolites show better results to remove CO_2 from flue gases since their CO_2/N_2 selectivities are higher than carbonaceous materials (Activated carbon molecular sieves). However, their capacities are lower and their performance would fall down in presence of steam (Siriwardane et al., 2001, Lu et al. 2008).

Adsorption systems are well developed for the separation of CO_2 from natural gas streams (Kohl et al., 1997) but for post-combustion CO_2 capture from natural gas-fired power plants, (less than 5% CO_2 concentration), adsorbents with improved properties that can operate during multi cycle tests at higher temperature, in the presence of steam are yet under development and demonstration (Siriwardane et al., 2005, Phan et al., 2009, Merel et al., 2008). Furthermore, for lower CO_2 concentration, combined temperature and vacuum PSA (Ishibashi et al., 1996) and also TSA were proposed (Merel et al., 2006). In recent studies, ESA process for capture CO_2 from NGCC has been evaluated; the main disadvantage of this method comparing to TSA is that the temperature increase is achieved by using electric power while in the case of TSA, waste heat is employed (Grande and Rodrigues, 2008). To conclude, adsorbents are considered as a future alternative, potentially less-

[1] $1\ GPU = 10^{-6} cm^3(STP)/(cm^2 s\ cm\ Hg)$, (Huang et.al, 2008)

energy-intensive CO_2 separation technology comparing to amine chemical absorption (Choi et al., 2009).

Chemical sorbents

One of the techniques under development for the removal of CO_2 is chemisorption with regenerable sorbents. Chemisorbents include, but not limited to, metal-oxide-based adsorbents such as CaO, MgO, K_2CO_3, Na_2CO_3 Li_2ZrO_3 and Li_4SiO_4, and hydrotalcite-like compounds and organic and organic-inorganic hybrid adsorbents. Alkali metal carbonates (such as K_2CO_3) and hydrotalcite-like compounds (HTs) are intermediate temperature adsorbents (absorption temperatures between 200 and 400 °C), while CaO, Li_2ZrO_3, and Li_4SiO_4 adsorbents are high temperature adsorbents (Choi et al., 2009, Hutson et al., 2008, Liang et al., 2004).

Alkali metal-based oxides such as CaO, MgO, and Al_2O_3 are investigated for CO_2 capture due to availability, good tolerability over temperature ranges and relatively lower costs compared to zeolites. These oxides can be used under a range of temperatures from room temperature to 850 °C. However there are still some challenges in the regeneration of these sorbents.

Among these sorbents, $CaO/CaCO_3$ is widely investigated due to its availability in natural minerals and high adsorption capacity. Originally Shimizu (1999) proposed the carbonation-calcination cycle as a post-combustion system which involved the calcination of the sorbent in a fluidized bed, by firing a fraction of the fuel with O_2/CO_2 mixtures. Furthermore, it offers possibilities for power plant configurations of utilizing the available high heat level, potential of low capture cost and very low efficiency penalties, due to steam generation from high amount of released heat and it could be used for both coal and natural gas fired power plants (Manovic et al., 2008, Romeo et al., 2010, Abanades, 2008, Berstad et al., 2012).

1.2.2 Oxyfuel combustion capture

This CO_2 separation method involves the combustion of fuel with nearly pure O_2 to get CO_2 enriched flue gas. Since nitrogen is the major component of power plant flue gas, post-combustion capture is essentially about nitrogen and CO_2 separation. In the absence of nitrogen, CO_2 capture from flue gases would be greatly simplified, and this is the basic idea of oxyfuel combustion CO_2 capture method. High purity (≥95%) oxygen is delivered in two forms; either as a gas stream, produced by the external cryogenic separation of O_2 from air or as a solid oxide in a chemical looping which is internally integrated process. Either way, oxygen is introduced to the power plant for the combustion of fuel. Since the fuel is burnt in presence of pure oxygen, the flame temperature is excessively high, so H_2O and/or CO_2 process streams would be recycled to the combustor to moderate the combustion temperature. Figure 1-7 depicts a schematic of oxyfuel combustion.

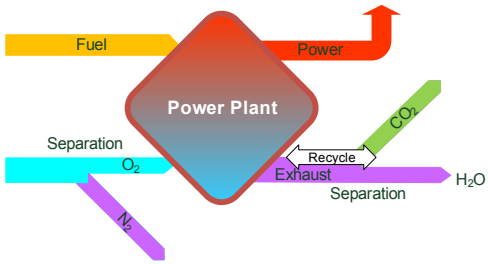

Figure 1-7: Schematic of oxyfuel combustion CO_2 capture

The advantages of oxyfuel combustion cycles are the great variety of fuels which can be used (natural gas, syngas from coal or biomass gasification, etc.), low NO_x generation and reaching high CO_2 capture ratios. The combustion with pure oxygen leads to a working fluid consisting mainly of steam and CO_2, which allows relatively easy and cost-effective CO_2 separation by steam condensation. It should be mentioned that, the oxyfuel combustion cycles need development of specific turbomachinery components with improved materials/coatings that has higher durability against temperature degradation in presence of high concentrations of CO_2 and H_2O. Moreover, the high cost of air separation unit is another obstacle in commercialization of new oxyfuel plants with CO_2 capture. Fortunately, the new working fluid of steam and CO_2 allows new power plant cycles of highest efficiency, so that the additional efforts for oxygen supply can be largely compensated (Dillon et al., 2005, Coraggio et al., 2011). Oxyfuel cycles are based on different concepts and designs if CO_2 is used as the working fluid, including the O_2/CO_2 cycle (Kvamsdal et al., 2007, Zhang et al., 2008), the MATIANT (Mathieu et al, 1999), if H_2O is the working fluid such as the CES Cycle (Anderson et al., 2008), and if CO_2/H_2O are working fluids such as the Graz Cycle (Jericha et al., 2004). Furthermore, new technologies with the attempts to lower the penalty due to oxygen separation have been developed, such as chemical-looping combustion (Ishida et al., 1996) and the AZEP concept (Griffin et al, 2005). Chemical looping combustion (CLC) is similar to the sorbent-based oxygen production method discussed earlier; though here, the oxygen-carrying sorbent which typically is a metal oxide would be contacted with a fuel, and that combustion takes place. Then the exhaust stream contains only CO_2 and H_2O, as in other oxyfuel schemes (Rubin et al. 2012).

1.2.3 Pre-combustion capture

The pre-combustion capture method refers to the capture of CO_2 prior to combustion. The fuel (natural gas/coal) is converted to syngas (CO + H_2, by means of steam reforming/partial oxidation /auto-thermal reforming/gasification). The resulting syngas undergoes water-gas shift reaction where CO_2 H_2 is formed, and then CO_2 is separated right before hydrogen-rich gas turbine fuel is sent to combustor of the power plant. Figure 8 depicts a schematic of pre-combustion CO_2 capture.

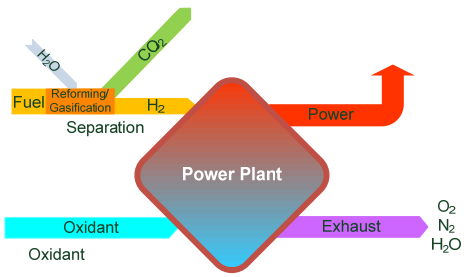

Figure 1-8: Schematic of pre-combustion CO_2 capture

There are numerous pre-combustion configurations found in the literature (Sekar et al, 2007, Bouallou et al., 2007, Ertesvåg et al., 2005, Lozza et al. 2002 a, b). This method is a viable option for the integrated coal gasification combined cycle (IGCC) plants, and applicable to all integrated gasification systems where hydrogen is the final syngas product, such as integrated gasification fuel cell system (IGFC). Among the technical solutions developed for CO_2 capture from natural gas fired power plants, Eide and Baily (2005) described pre-combustion based on different available reforming technologies. The conversion, net electrical efficiency, thermodynamics, reliability and operability and economic analysis of various natural gas pre-combustion combined cycle power plants was assessed. The demonstration of such power plants has yet to be performed (Amann et al. 2009, Ertesvåg et al. 2005, Hoffman et al. 2009, Lozza et al. 2002 a ,b, Nord et al. 2009, Romano et al., 2010). These cycles need lower energy requirements for CO_2 capture process and are less expensive. However, their total low power plant efficiency makes them less competitive with the amine absorption post-combustion capture from natural gas fired power plant.

1.3 Thesis scope of work

As mentioned in chapter 1.1.1, power plants burning natural gas as fuel produce lower CO_2 emissions. Also switching from coal to natural gas, results in higher efficiency power plants. Yet, the majority of studies focus on CO_2 capture plants integrated with coal-fired power plant. And detailed assessment of the integration of the optimized CO_2 capture plants with natural gas fired power plants needs to be performed. Hence, the current thesis is focusing on post-combustion chemical absorption for natural gas-fired combined cycle (NGCC) power plant.

Since the most widely-studied solvent for CO_2 capture chemical absorption processes is MEA, it was decided to use a 30% MEA solution in all of the simulations. A base case process configuration and a number of alternative process configurations were investigated with the same solvent material/aqueous solution concentration. The thesis includes analysis and comparison between several chemical absorption process configurations integrated with NGCC.

1.4 Thesis objectives

The main objective of this thesis is to evaluate, quantify and justify improved design of power processes with post-combustion CO_2 capture using thermodynamic analysis on various chemical absorption process configurations.

The thermodynamic evaluation of the processes gives insight to the detailed distribution of process irreversibilities and supports the state-of-the-art process configuration with the lowest energy penalty due to addition of CO_2 capture to the power plant. Specifically, the thesis objectives were listed as below:

- Develop optimized process modifications of CO_2 capture chemical absorption integrated to NGCC with low energy consumptions and reduced power energy penalty
- Detailed understanding of various penalties associated to different CO_2 process modifications by performing first law of thermodynamics analysis
- Quantification of the irreversibilities occurring in different parts of the CO_2 processes and comparing those for various process modifications.
- Identification of the irreversibilities associated with the integration of power plant with various CO_2 capture configurations by performing second law analysis

1.5 Thesis outline

This thesis comprises 5 chapters including 3 papers which analyse different process configurations of chemical absorption post-combustion CO_2 capture for natural gas fired combined-cycle power plant. Chapter 1 of this thesis introduces the motivation and a general background of CO_2 capture methods and the viable options for post-combustion CO_2 capture of natural gas fired power plants. Chapter 2 gives the technical background, subsystem description of the post-combustion chemical absorption for the NGCC power plant and the various chemical absorption process configurations analyzed in this thesis. Chapter 3 describes the ground definitions and methodologies used for the thesis work. Chapter 4 summarizes the results of the thesis, including power plant efficiency analysis and exergy analysis of the models. Chapter 5 details conclusions and main thesis contributions. It also includes the further suggestions for the future work to be carried on.

1.6 List of papers

- **Paper 1**

Amrollahi, Z., Ertesvåg, I. S.,Bolland, O.,2011. Thermodynamic analysis on post-combustion CO_2 capture of natural-gas-fired power plant. *International Journal of Greenhouse Gas Control,* 5**,** 422-426.

A chemical absorption, post-combustion CO_2 capture unit is simulated and an exergy analysis has been conducted, including irreversibility calculations for all process units. By pinpointing major irreversibilities, new proposals for efficient energy integrated chemical absorption process are suggested. Further, a natural-gas combined-cycle power plant with a CO_2 capture unit has been analyzed on an exergetic basis. By defining exergy balances and black-box models for plant

units, investigation has been made to determine effect of each unit on the overall exergy efficiency. Simulation of the chemical absorption plant was done using UniSim Design software with Amines Property Package. For natural-gas combined-cycle design, GT PRO software (Thermoflow, Inc.) has been used. For exergy calculations, spreadsheets are created with Microsoft Excel by importing data from UniSim and GT PRO. Results show the exergy efficiency of 21.2% for the chemical absorption CO_2 capture unit and 67% for the CO_2 compression unit. The total exergy efficiency of CO_2 capture and compression unit is 31.6%.

Author's contribution: Zeinab Amrollahi conceived the concept of the paper, run the simulations. She interpreted the results and made the conclusions in cooperation with other authors. Zeinab wrote the paper with comments from other authors.

- **Paper 2**

Amrollahi, Z., Ertesvåg, I. S., Bolland, O.,2010. Thermodynamic analysis of a Post Combustion CO_2 Capture Process. *Proceedings of ECOS 2010,* 4, 133-139

A chemical absorption, post-combustion CO_2 capture unit is simulated and an exergy analysis was conducted, including irreversibility calculations for all process units. With pinpointing major irreversibilities, new proposals for efficient energy integrated chemical absorption process were suggested. Moving further to the whole natural gas combined cycle plant with a CO_2 capture unit, it has been analyzed on an exergetic basis. By defining exergy balances and black-box models for plant components, investigation has been made to determine effect of each component on overall exergy efficiency. Simulation of chemical absorption plant was done using UniSim Design software with Amine Property Package which maintains thermodynamic data. For overall power plant design, GT PRO software (Thermoflow, Inc.) was used for simulation of a natural gas combined cycle. For exergy calculations, spreadsheets were created with Microsoft Excel by importing data from UniSim and GT PRO. By pinpointing major irreversibilities, new proposal for energy-efficient integrated chemical absorption process is suggested. Results show that for current chemical absorption plant, the exergetic efficiency compared to the reversible separation work lies between 15% and 22%.

Author's contribution: Zeinab Amrollahi conceived the concept of the paper, run the simulations. She interpreted the results and made the conclusions in cooperation with other authors. Zeinab wrote the paper with comments from other authors.

- **Paper 3**

Amrollahi, Z., Nord, L.O., Ertesvåg, I. S., Bolland, O.,2010. Identifying areas for improvement and development in a pre-combustion CO_2 capture cycle. *Conference paper. GHGT-10.*

This paper discusses the thermodynamic efficiency of an integrated reforming combined cycle (IRCC) process as one of the proposed pre-combustion CO_2 capture processes. By simulating an IRCC plant with CO_2 capture, for thermodynamic evaluation, exergy of streams and irreversibilities were calculated. The exergy analysis of the system, pinpoint major irreversibilities and exergy losses. Simulation of the IRCC plant with CO2 capture was done using Aspen Plus software. For gas turbine and steam cycle design, GT PRO software (Thermoflow, Inc.) was used. For exergy calculations,

ExerCom software (JACOBS consultancy) was used to calculate the exergy of streams and irreversibilities of each unit operation. To decrease the exergy losses in the gas turbine combustor, fuel pre-heating up to 500°C, would decrease the gas turbine irreversibility up to 11%. Additionally, preheating the inlet streams to the auto-thermal reformer would be beneficial in decreasing its exergy losses.

Author's contribution: Zeinab Amrollahi conceived the concept of the paper. She got access to an available Aspen plus simulation for IRCC with CO_2 capture and run the main simulations; then compiling the results to Exercom software helped in finding out the exergy results. She interpreted the results and made the conclusions in cooperation with other authors. Zeinab wrote the paper with comments from other authors.

- **Paper 4**

Amrollahi, Z., Ystad, P. A. M., Ertesvåg, I. S., Bolland, O., 2012. Optimized process configurations of post-combustion CO2 capture for natural-gas-fired power plant – Power plant efficiency analysis. *International Journal of Greenhouse Gas Control,* 8**,** 1-11.

Carbon dioxide was removed by chemical absorption processes from the flue gases of natural-gas-fired combined-cycle power plant. The main challenge of chemical absorption processes is reducing the energy requirement. The paper discusses the selection of most important parameters necessary to obtain 90% capture ratio and the lowest energy consumption for the CO_2 capture and compression plants. The integrated capture processes with power plant were evaluated by using the net power-plant efficiency. Several chemical absorption process configurations were analyzed and the design parameters were compared for the different cases. The findings show decreased reboiler energy consumption for the Base case chemical absorption process configuration with 3.74 MJ/kg CO_2 to 2.71 MJ/kg CO_2 for the modified chemical absorption process configuration of lean vapor recompression with absorber inter-cooling. The net power plant efficiency with CO_2 capture and compression was increased from 49.4 percent (LHV) for the Base case chemical absorption process to 50.2 percent (LHV) for the chemical absorption process with absorber inter-cooling and lean vapor recompression. The power output reduction due to CO_2 capture and compression was decreased from 48 MW for the Base case chemical absorption process to 42.5 MW for the case with absorber inter-cooling and lean vapor recompression.

Author's contribution: Zeinab Amrollahi conceived the concept of the paper, run the simulations. She interpreted the results and made the conclusions in cooperation with other authors. Zeinab wrote the paper with comments from other authors.

- **Paper 5**

Amrollahi, Z., Ertesvåg, I. S., Bolland, O., 2011. Optimized process configurations of post-combustion CO_2 capture for natural-gas-fired power plant - Exergy analysis. *International Journal of Greenhouse Gas Control,* 5, 1393-1405.

Several chemical absorption CO_2 capture process configurations were analyzed and compared according to their associated exergy losses. The total work demand was decreased from 1.39 MJ/kg CO_2 for the Base case chemical absorption process configuration to 1.23 MJ/kg CO_2 for the modified

chemical absorption process configuration of lean vapor recompression with absorber inter-cooling (best case). Considering the minimum work requirement of separation processes, the exergy efficiency of capture and compression plants was increased from 31.6 percent for the Base case chemical absorption process to 35.6 percent for the best case. Respectively, irreversibilities were reduced from the 1.60 MJ/kg CO_2 for the Base case to 1.29 MJ/kg CO_2 for the case with absorber inter-cooling and lean vapor recompression. The rational efficiency for the natural-gas-fired combined cycle power plant with CO_2 capture and compression shows an increase from 48.5 percent for the Base case chemical absorption process configuration to 49.5 percent for the best case.

Author's contribution: Zeinab Amrollahi conceived the concept of the paper, run the simulations. She interpreted the results and made the conclusions in cooperation with other authors. Zeinab wrote the paper with comments from other authors.

1.7 Detailed working process

The findings of this thesis work would be based on the results of research papers one to five (Appendix A).The core of this thesis is to use thermodynamic analysis on various chemical absorption process configurations to evaluate, quantify and justify improved design of power processes with post-combustion CO_2 capture. The thermodynamic evaluation of the processes gave insight to the detailed distribution of process irreversibilities and supported the state-of-the-art process configuration with the lowest energy penalty due to addition of CO_2 capture to the power plant. These have been fulfilled through the following steps;

1.7.1 Base case development

The first step was to simulate the base case chemical absorption integrated to the reference NGCC, and optimize it to reach the goal of highest power plant efficiency i.e. the lowest energy penalty due to the addition of CO_2 capture plant. The base case optimized process configuration was achieved by numerous parametric variations and the optimization target was toward the reduction of reboiler energy consumption and the total work demand of the CO_2 capture plant, and the highest net power plant efficiency. As described in paper 1 and 4, the UniSim process tool was chosen for chemical absorption process simulations (developed by, Honeywell, 2008) and GTPRO (developed by Thermoflow, 2009) was chosen for power plant model. Further on, exergy analysis has been used to obtain insight for the irreversibilities occurring in the base case chemical absorption plant and overall exergy balance calculations was used to identify the overall exergy efficiency for the base case capture plant integrated to NGCC power plant. The findings from this step were used as a reference case for comparison in assessing other process configurations that are addressed in this thesis (Papers 2, 4 and 5).

1.7.2 Process modifications

As the next step, it was necessary to explore and investigate several process modifications with lower energy consumptions and consequently reduction in the power energy penalty due to addition of capture plant. Process configurations as described in papers 2 and 4 were developed and their integration to the power plant was investigated. Parametric variations were performed to reach the optimized processes; optimization target was toward the reduction of reboiler energy consumption

and the total capture plant work demand, and the highest net power plant efficiency. It should be noted that the different models were consistent in terms of boundary and input/ output conditions they utilized; this resulted to achieve a consistent comparison of the performance of different process modifications. Further on, here again, exergy analysis was used to detect and demonstrate the changes of irreversibility rates in the main process sections for various process configurations (Papers 2 and 5). Moreover, overall exergy analysis was performed to identify the irreversibilities associated with the integration of power plant with various CO_2 capture and compression processes. Particularly, the second law of thermodynamics was used as a tool to evaluate and quantify the reduction of energy penalty associated with CO_2 capture for each process modification. The results of this step is used to conclude on the combined first and second law analysis on CO_2 capture processes for NGCC power plants as tabulated in papers 4 and 5.

1.7.3 A pre-combustion case

A combination of power plant (1st law) and exergy analysis (2nd law) have been used to investigate a pre-combustion reforming combined cycle (IRCC) process with chemical absorption CO_2 capture plant. (Paper 3) By using exergy analysis, the major irreversibilities and exergy loses were pinpointed. The findings from this paper gave ideas for reducing exergy losses as well as increasing the power plant efficiency.

1.7.4 Achievements

As described step-wise in previous sections, the following actions have been performed in the current thesis to fulfil the objectives stated in chapter 1.4.

- Optimization of base case chemical absorption process (Papers 1, 2, 4 and 5)
- Developing modified chemical absorption process configurations that yields to distinct improvement in power plant efficiency (First method available in the toolbox, referring Figure 1-9) Results are tabulated in Papers 2 and 4.
- Assessment and comparison of the proposed process configurations using exergy method (2nd law of thermodynamics, Referring Figure 1-9). Results are tabulated in Papers 1, 2 and 5.
- Understating and insight to the irreversibilities in the chemical absorption process by exergy analysis. Results are discussed in Paper 5.

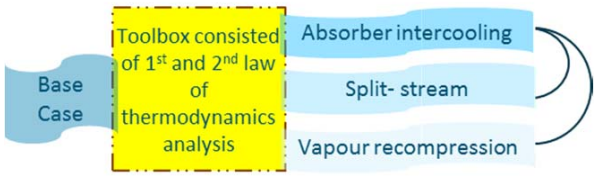

Figure 1-9: Schematic method description for the current thesis

References:

Abanades, C., 2008. Calcium Sorbent Cycling for Simultaneous CO_2 Capture and Clinker Production. Published by the Global Climate and Energy Project. http://gcep.stanford.edu.

Amann, J. M., Kanniche M., Bouallou Ch. , 2009. Reforming natural gas for CO_2 pre-combustion capture in combined cycle power plant. Clean Technologies and Environmental Policy 11(1), 67-76.

Anderson, R. E., MacAdam, S., Viteri, F., Davies, D. O., Downs, J. P., Paliszewski, A., 2008. Adapting Gas Turbines to Zero Emission Oxy-Fuel Power Plants. ASME Conference Proceedings, 2008**,** 781-791.

Arrhenius, S., 1896. On the Influence of Carbonic Acid in the Air upon the Temperature of the Ground. Philosophical Magazine and Journal of Science, Series 5, 41, 237-276.

Berstad, D., Anantharaman, R., Jordal, K., 2012. Post-combustion CO_2 capture from a natural gas combined cycle by $CaO/CaCO_3$ looping. International Journal of Greenhouse Gas Control, 11, 25-33.

Bouallou, C.,Kanniche, M., 2007. CO_2 capture study in advanced integrated gasification combined cycle. Applied Thermal Engineering, 27, 2693-2702.

Carapellucci, R., Milazzo, A., 2004. Carbon dioxide removal via a membrane system in a natural gas combined-cycle plant. Proceedings of the Institution of Mechanical Engineers, Part A: Journal of Power and Energy, 218, 219-229.

Choi, S., Drese, J. H., Jones, C.W., 2009. Adsorbent Materials for Carbon Dioxide Capture from Large Anthropogenic Point Sources. ChemSusChem, 2, 796-854.

Climate Change 2007: Mitigation of Climate Change, 2007. Working Group III contribution to the Intergovernmental Panel on Climate Change. Fourth Assessment Report, IPCC.

Collot, A.G., 2003, Prospects for Hydrogen from Coal, IEA Coal Research, the Clean Coal Center, UK

Conway, T.J., Tans, P.P., 2011. NOAA/ESRL. www.esrl.noaa.gov/gmd/ccgg/trends.

Conway, T.J., Tans, P.P., Waterman, L.S., Thoning, K.W., Kitzis, D.R., Masarie, K.A., Zhang, N., 1994. Evidence of Interannual Variability of the Carbon Cycle from the NOAA/CMDL Global Air Sampling Network, Journal of Geophysical Research-Atmospheres*,* 99(D11), 22831-22855.

Coraggio, G., Tognotti, L., Cumbo, D., Rossi, N., Brunetti, J., 2011. Retrofitting oxy-fuel technology in a semi-industrial plant: Flame characteristics and NO_x production from a low NO_x burner fed with natural gas. Proceedings of the Combustion Institute, 33, 3423-3430.

Eide, L. I., Bailey D. W., 2005. Capture pre-combustion. Oil & Gas Science and Technology - Rev. IFP 60(3), 475-484.

Ertesvåg, I. S., Kvamsdal, H. M., Bolland, O., 2005. Exergy analysis of a gas-turbine combined-cycle power plant with pre-combustion CO_2 capture. Energy 30, 5-39.

Favre, E., 2011. Membrane processes and post-combustion carbon dioxide capture: Challenges and prospects. Chemical Engineering Journal, 171, 782-793.

Feron, H.M., Asbroek, N. T., 2004. New Solvents Based On Amino-Acid Salts For CO_2 Capture from Flue Gases. Proceedings of 7th International Conference on Greenhouse gas control technologies.

GCEP Energy Assessment Analysis, 2005.An Assessment of Carbon Capture Technology and Research Opportunities. Published by the Global Climate and Energy Project. http://gcep.stanford.edu.

Global Wind Energy Council, 2010. Global wind power boom continues despite economic woes. http://www.gwec.net

Goddard Institute for Space Studies, NASA, accessed 2011. http://data.giss.nasa.gov/gistemp/graphs/

Grande, C. A., Rodrigues, A. E., 2008. Electric Swing Adsorption for CO2 removal from flue gases. International Journal of Greenhouse Gas Control, 2, 194-202.

Griffin, T., Sundkvist, S. G., Asen, K., Bruun, T., 2005. Advanced Zero Emissions Gas Turbine Power Plant. Journal of Engineering for Gas Turbines and Power, 127, 81-85.

GT PRO version 19, 2009, Thermoflow Inc

Hansen, J., Sato, Mki., Ruedy, R., Lo, K., Lea, D.W., Medina-Elizade, M., 2006. Global Temperature Change. The Proceedings of the National Academy of Sciences USA (PNAS), 103, 14288-14293.

Herzog, H., Meldon, J., Hatton, A., 2009.Advanced Post-Combustion CO_2 Capture, prepared for Clean Air Task Force. http://web.mit.edu/mitei/docs/reports/herzog-meldon-hatton.pdf

Hoffmann S., Bartlett M., Finkenrath, M., Evulet A., Ursin T.P., 2009. Performance and Cost Analysis of Advanced Gas Turbine Cycles With Pre-combustion CO_2 Capture. Journal of Engineering for Gas Turbines and Power-Transactions of the ASME 131.

Huang, J., Zou, J., Ho, W.S.W., 2008. Carbon Dioxide Capture Using a CO_2-Selective Facilitated Transport Membrane. Industrial & Engineering Chemistry Research, 47, 1261-1267.

Hutson, N., Attwood, B., 2008. High temperature adsorption of CO_2 on various hydrotalcite-like compounds. Adsorption, 14**,** 781-789.

International Energy Agency, 2010. Energy Technology Perspectives, Key graphs. http://www.iea.org/techno/etp/etp10/key_ Abanades s.pdf

International Energy Agency, 2010. CO_2 Emissions from Fuel Combustion Highlights. http://www.iea.org/co2highlights/CO2highlights.pdf

International Energy Agency, 2009. World Energy Outlook 2009. http://www.iea.org/textbase/nppdf/free/2009/WEO2009.pdf

International Energy Agency, 2008. Energy Technology Perspectives. http://www.iea.org/textbase/nppdf/free/2008/etp2008.pdf

Ishibashi, M., Ota, H., Akutsu, N., Umeda, S., Tajika, M., Izumi, J., Yasutake, A., Kabata, T.,Kageyama, Y. , 1996. Technology for removing carbon dioxide from power plant flue gas by the physical adsorption method. Energy Conversion and Management, 37, 929-933.

Ishida, M., Jin, H., Okamoto, T., 1996. A fundamental study of a new kind of medium material for chemical-looping combustion. Energy and Fuels, 10, 958-963.

Jericha, H., Gottlich, E., Sanz, W., Heitmeir, F., 2004. Design Optimization of the Graz Cycle Prototype Plant. Journal of Engineering for Gas Turbines and Power, 126, 733-740.

Kehlhofer, R., Rukes, B., Hannemann, F., Stirnimann, F, 2009. Combined-Cycle Gas and Steam Turbine Power Plants (3rd Edition). PennWell.

Kvamsdal, H. M., Jordal, K., Bolland, O., 2007. A quantitative comparison of gas turbine cycles with CO_2 capture. Energy, 32, 10-24.

Li, X., Remias, J. E., Neathery, J. K., Liu, K., 2011. NF/RO faujasite zeolite membrane-ammonia absorption solvent hybrid system for potential post-combustion CO_2 capture application. Journal of Membrane Science, 366, 220-228.

Liang, Y., Harrison, D. P., Gupta, R. P., Green, D. A., Mc Michael, W. J., 2004. Carbon Dioxide Capture Using Dry Sodium-Based Sorbents. Energy & Fuels, 18, 569-575.

Lively, R. P., Koros, W. J., Johnson, J. R., 2012. Enhanced cryogenic CO_2 capture using dynamically operated low-cost fiber beds. Chemical Engineering Science, 71, 97-103.

Lozza, G.,Chiesa, P., 2002. Natural Gas Decarbonization to Reduce CO_2 Emission From Combined Cycles---Part I: Partial Oxidation. Journal of Engineering for Gas Turbines and Power, 124**,** 82-88.

Lozza G., Chiesa P., 2002. Natural Gas Decarbonization to Reduce CO_2 Emission from Combined Cycles-Part II: Steam-Methane Reforming. Journal of Engineering for Gas Turbines and Power 124(1): 89-95.

Lu, C., Bai, H., Wu, B., SU, F., Hwang, J. F., 2008. Comparative Study of CO_2 Capture by Carbon Nanotubes, Activated Carbons, and Zeolites. Energy & Fuels, 22, 3050-3056.

Manovic, V., Anthony, E. J., 2008. Thermal Activation of CaO-Based Sorbent and Self-Reactivation during CO_2 Capture Looping Cycles. Environmental Science & Technology, 42, 4170-4174.

Mathieu, P.,Nihart, R., 1999. Zero-Emission MATIANT Cycle. Journal of Engineering for Gas Turbines and Power, 121, 116-120.

Mérel, J., Clausse, M., Meunier, F., 2006. Carbon dioxide capture by indirect thermal swing adsorption using 13X zeolite. Environmental Progress, 25, 327-333.

Merel, J., Clausse, M., Meunier, F., 2008. Experimental Investigation on CO_2 Post-Combustion Capture by Indirect Thermal Swing Adsorption Using 13X and 5A Zeolites. Industrial & Engineering Chemistry Research, 47, 209-215.

Merkel, T.C., Lin, H., Wei, X., Baker, R., 2010. Power plant post-combustion carbon dioxide capture: An opportunity for membranes. Journal of Membrane Science, 359, 126-139.

Nord, L. O., Anantharaman, R., Rausand, M., Bolland, O., 2009. A qualitative reliability and operability analysis of an integrated reforming combined cycle plant with CO_2 capture. International Journal of Greenhouse Gas Control, 3, 411-421.

Parsons, J. E., Sekar, R. C., Herzog, H. J., Jacoby, H. D., 2007. Future carbon regulations and current investments in alternative coal-fired power plant technologies. Energy Policy, 35, 1064-1074.

Phan, A., Doonan, C. J., Uribe-romo, F. J., Knobler, C. B., O'keeffe, M., Yaghi, O. M., 2009. Synthesis, Structure, and Carbon Dioxide Capture Properties of Zeolitic Imidazolate Frameworks. Accounts of Chemical Research, 43, 58-67.

Romeo, L. M., Usón, S., Valero, A., Escosa, J. M., 2010. Exergy analysis as a tool for the integration of very complex energy systems: The case of carbonation/calcination CO_2 systems in existing coal power plants. International Journal of Greenhouse Gas Control, 4**,** 647-654.

Romano, M. C., Chiesa, P., Lozza, G., 2010. Pre-combustion CO_2 capture from natural gas power plants, with ATR and MDEA processes. International Journal of Greenhouse Gas Control, 4, 785-797.

Rubin, E. S., Mantripragada, H., Marks, A., Versteeg, P., Kitchin, J., 2012. The outlook for improved carbon capture technology. Progress in Energy and Combustion Science, 38, 630-671.

Russell, J., 2010. Record Growth in Photovoltaic Capacity and Momentum Builds for Concentrating Solar Power Vital Signs, June 03, 2010.

Sanyal, D., Vasishtha, N.,Saraf, D. N., 1988. Modeling of Carbon-Dioxide Absorber Using Hot Carbonate Process. Industrial & Engineering Chemistry Research, 27, 2149-2156.

Shimada, K., Seekkuarachchi, I.N., Kumazawa, H, 2006. Absorption of CO_2 into aqueous solutions of sterically hindered methyl aminoethanol using a hydrophobic microroporous hollow fiber contained contactor. Chemical Engineering Communications, 193,1, 38-54.

Shimizu, T., Hirama, T., Hosoda, H., Kitano, K., Inagaki, M.,Tejima, K., 1999. A Twin Fluid-Bed Reactor for Removal of CO_2 from Combustion Processes. Chemical Engineering Research and Design, 77, 62-68.

Siriwardane, R.V., Shen, M.S., Fisher, E.P., 2005. Adsorption of CO_2 on zeolites at moderate temperatures. Energy Fuels, 19, 1153–1159.

Siriwardane, R.V., Shen, M.S., Fisher, E.P., Poston, J.A., 2001. Adsorption of CO_2 on molecular sieves and activated carbon. Energy Fuels, 15, 279–284.

Zhang, N., Lior, N., 2006. A novel near-zero CO_2 emission thermal cycle with LNG cryogenic exergy utilization. Energy, 31,1666-79

Zhang, N., Lior, N., 2008. Two novel oxy-fuel power cycles integrated with natural gas reforming and CO_2 capture. Energy, 33, 340-351.

Zhao, L., Riensche, E., Menzer, R., Blum, L., Stolten, D., 2008. A parametric study of CO_2/N_2 gas separation membrane processes for post-combustion capture. Journal of Membrane Science, 325, 284-294.

Zhao, L., Riensche, E., Blum, L., Stolten, D., 2010. Multi-stage gas separation membrane processes used in post-combustion capture: Energetic and economic analyses. Journal of Membrane Science, 359, 160-172.

UniSim design user guide, 2008, Honeywell, R380 Release

Wilcox, J. 2012. Cryogenic Distillation and Air Separation. Carbon Capture. Springer New York.

2 Post-combustion CO_2 capture; description of sub-systems

The post-combustion CO_2 capture process is a downstream process to the power plant which involves the removal of CO_2 from the flue gases of the power plant by means of different separation principles such as physical/chemical absorption, adsorption and solid sorbents, membrane separation and cryogenic separation. The sub-systems in the current CO_2 capture analysis are defined in this section;

2.1 Natural Gas Fired Combined Cycle Power Plant

A Natural gas fired combined-cycle power plant consists of one or more gas turbine generators equipped with heat recovery steam generators and a steam turbine which enhances the efficiency of electricity generation. The heat from the gas turbine exhaust is captured through heat recovery steam generator (HRSG) and steam is produced which powers a steam turbine (ST) generator to produce additional electric power.

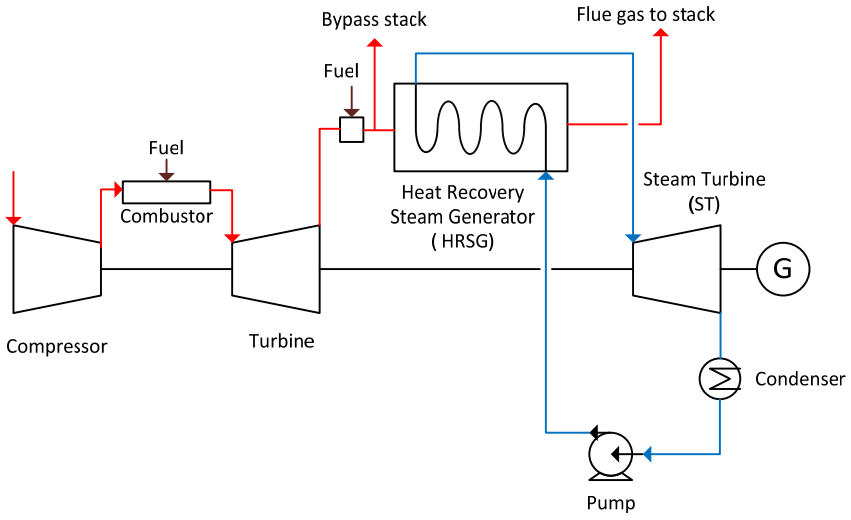

Figure 2-1: Schematic of the operation of natural gas fired combined cycle power plant

Air at atmospheric condition is compressed in the compressor to the range of 10-35 bar; pressurized air enters into a mixture with fuel and undergoes combustion. This results in turbine inlet temperatures as high as 1300-1400 °C. Through the turbine, the expansion process of gases takes place in a few stages and the energy conserved in hot gases leads to power generation. The gas turbine exit temperature is typically in the range 550 – 640°C.

2.1.1 Combined cycle thermal efficiency

Generally, for any thermodynamic process that involves heat transfer and work generation (consumption), the fraction of the heat input that is converted to net work output is a measure of the performance. This ratio is called thermal efficiency and defined as below:

$$\eta_{th} = \frac{\text{Net work output}}{\text{Heat supplied}}$$

Specifically for a combined cycle efficiency is determined from:

$$\eta_{CC} = \frac{P_{GT} + P_{ST} - P_{AUX}}{\dot{Q}_{GT} + \dot{Q}_{SF}}$$

According to the above formula, the net natural gas fired power plant efficiency (LHV based) shall be calculated as:

$$\eta_{net,pp} = \frac{((\dot{W}_T - \dot{W}_C)_{GT} + \dot{W}_{ST})\eta_m \eta_g - \dot{W}_{aux}}{(\dot{m}LHV)_{NG}}$$

Combined cycle power plants currently entering service can convert about 50 percent of the chemical energy of natural gas into electricity (HHV basis). The net electric power efficiency of a NGCC is typically in the range of 55% to 60% LHV-based (Kehlhofer et al., 2009). Compared to simple cycle gas turbine power plants, combined cycles have higher efficiencies, which are related to use of heat available from the GT exhaust gas. Additionally, combined cycles are characterized by low initial cost, high reliability, operational flexibility, quick part-load starting, suitability for both base-load and cyclic operation, and relatively low carbon dioxide emissions. Combined cycle power plants employ more than one thermodynamic cycle; Brayton cycle for the gas turbine and Rankine for the steam plant. Hereafter, key design parameters and equations expressing the total work and efficiencies are presented for both of the cycles.

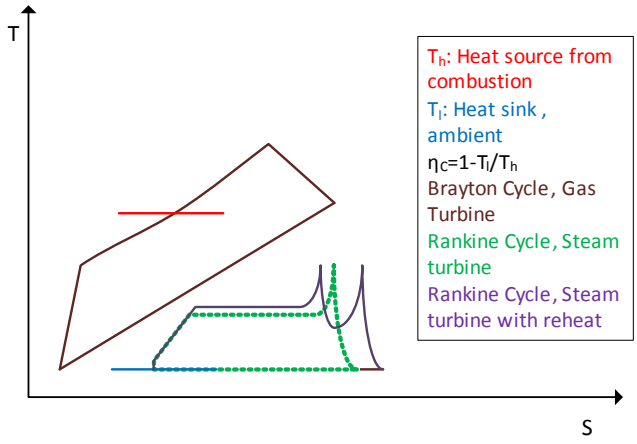

Figure 2-2 Combined Cycle Power plant on T-S diagram

2.1.2 Gas Turbine

The efficiency of the Gas Turbine (GT) is highly dependent on the inlet temperature (TIT) and pressure of the gas entering the turbine. The former is constrained due to formation of more NOx at higher combustion temperatures and gas turbine blade construction materials. However with more effective cooling and better materials, TITs as high as 1490°C for industrial gas turbines are achieved. Compressor pressure ratio will also affect the GT power output. Among the state of the art gas turbines, GE H system turbine exploits pressure ratio of 23:1; Alstom's turbines have operated with a pressure ratio of about 30:1 (Bolland, 2009).

It should be noted that the ambient temperature, affects both the GT compressor work and the fuel consumption. A decrease in ambient temperature increases both specific power output and cycle efficiency although the cycle efficiency is less affected than the power output (Sarvanamuttoo et al., 2001).

One main parameter in GT performance is the fuel supplied to the combustion chamber which in our case is natural gas. Critical properties such as Wobbe index, chemical composition and compounds are the key factors which is defined and set for a GT fuel. The Wobbe index that is an indication of interchangeability of fuels is actually the correct representation of the heating value of natural gas arriving, from the gas line, at the orifice where the appliance (burner) is located. And the compounds of the natural gas are restricted according to the hydrogen, higher hydrocarbons (>C3), hydrogen sulfide and mercaptans concentrations.

2.1.3 Steam cycle; HRSG and steam turbine

The HRSG generates steam using water by utilizing GT exhaust gas heat. The flue gas from the HRSG is sent to stack. The generated steam drives a steam turbine and shaft power will be produced. The steam turbine exhaust goes to the condenser. The condensed water is pumped back again to the HRSG.

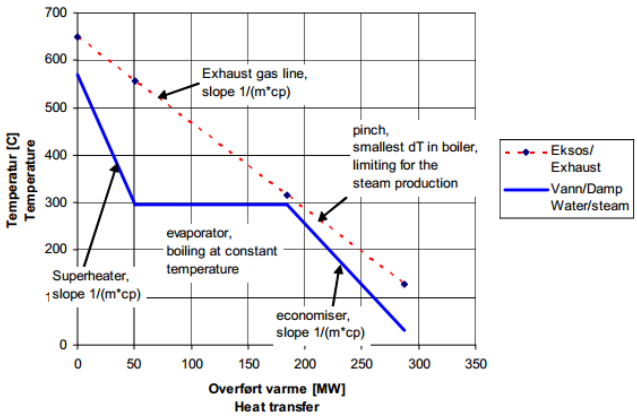

Figure 2-3: T-H diagram for dual pressure combined cycle plant (Bolland, 2009)

T-H diagrams present the gas and steam conditions in an HRSG. The enthalpy rise of the steam compared to the feed water inlet is equal to the enthalpy drop of the exhaust gases entering the HRSG. Higher efficiencies will be achievable by designing the steam cycle with dual and triple pressure cycles with reheat because the average temperature difference, at which heat is transferred, is decreased. For these cycles, the steam will be produced at three different levels of high pressure (HP), intermediate pressure (IP) and low pressure (LP) in HRSG in corresponding boilers- HPB, IPB and LPB, superheated in corresponding steam drums (HPS, IPS, LPS) and sent for further expansion to the corresponding turbine sections HPT, IPT and LPT.

A low gas turbine exhaust temperature leads to less steam being produced in the HRSG. In a combined cycle, if the compressor pressure ratio is increased to get higher GT efficiency, that will then counter-effect the steam cycle efficiency and may lead to drop in overall efficiency. In practice, industrial gas turbines working with compressor pressure ratios around 15, gives exhaust gas temperatures 550-600°C, which is suitable for both simple and combined cycle applications. Another attempt to increase the temperature of exhaust gases entering the steam cycle is to introduce supplementary firing. This will be fruitful for increasing peak loads for certain periods, but will affect the capital cost and size of the plant (Sarvanamuttoo et al., 2001).

2.1.4 Steam Extraction for CO_2 capture plant

For the post-combustion capture plant, an important interface is the steam extraction from the steam turbine or the HRSG in order to supply heat for solvent regeneration. If the heat demand is supplied by steam extraction from the HRSG, in order to provide enough steam that must be extracted from all three pressure levels. This leads to a large exergy loss because the process conditions (temperature and pressure) of IP and HP steam are higher than what is required for solvent regeneration. For the chemical absorption CO_2 capture plant with MEA, the temperature of the solvent in the reboiler should be in the range of 120°C - 122°C due to degradation problem (Section 2.2.2.1). This defines the supply temperature of the steam to the reboiler to be at least 130°C at saturated conditions considering 10°C as the differential temperature approach. The pressure of this saturated steam corresponds to 2.7 bar. Therefore, the steam supply conditions to the reboiler should stay above the aforementioned. For this thesis work, the steam at 4 bar and 145°C is determined for the supply to the reboiler in order to cater for piping pressure losses between the steam turbine and CO_2 capture plant.

To maintain the steam with mentioned process condition to the reboiler, the extraction point from ST will be higher than 4 bar. At these conditions, the steam could be extracted from the crossover pipe before the low pressure (LP) turbine cylinder. The steam expanded in the IPT flows through the crossover pipe, is mixed with LP steam produced in the HRSG and expands further in the LPT.

When extracting superheated steam from the IP/LP crossover, it should be saturated with water injection and will be supplied to the reboiler at the exact temperature and pressure that is required for the regeneration process. The steam condition changes are illustrated in Figure 2-4.

The change in the operating conditions of both IP and LP turbine is disadvantageous due to lower power generation in the steam turbine. Some manufacturers utilize LP crossover throttle valves to regulate the extraction steam pressure. An LP crossover extraction valve can adjust the extraction pressure, which allows for more efficient operation in part-load conditions (Karimi, 2011).

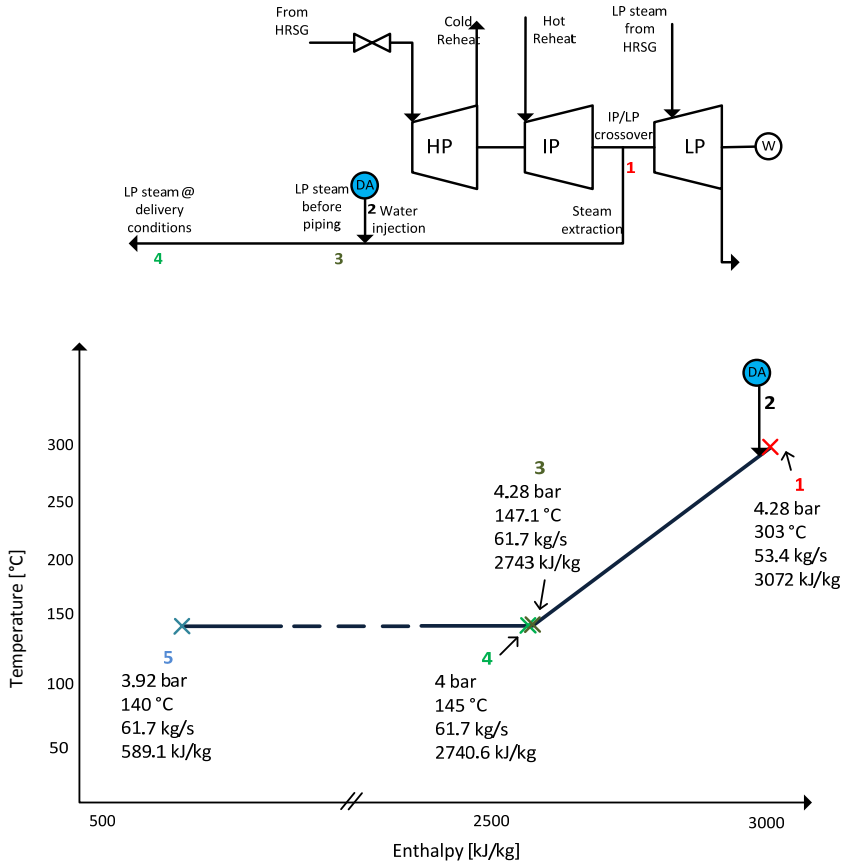

Figure 2-4: Illustrative T-H diagram showing steam conditions from the extraction point (No. 1) to the reboiler supply point (No. 4). The de-superheating water (No. 2) which is injected to the superheated steam to decrease the temperature, has the following conditions: 134.8 bar, 145.3 °C, 8.28 kg/s, 620.4 kJ/kg

The other option for providing steam employs the steam extraction from the LP boiler drum which provides steam at a temperature and pressure closest to what the solvent regeneration process needs. However, in this case the mass flow of steam will be not sufficient for the purpose of solvent regeneration. The main effect of this steam extraction is the loss of steam turbine power output and plant efficiency loss. This will be explained later in this section.

2.1.5 Power penalty

A steam turbine steam extraction imposes a power production penalty. This penalty can be quantified using α-value, which is the ratio between the power output reduction of the power plant due to steam extraction and the equivalent heat acquired from the extracted steam to provide the reboiler heat requirement;

$$\alpha = \frac{P_{\text{pp WO-extr}} - P_{\text{pp W-extr}}}{Q_{\text{Reboiler}}} \quad , \quad Q_{\text{Reboiler}} = \dot{m}_{st}(h_{st,in} - h_{cond,out})$$

where $\dot{m}_{st}$ denotes the steam mass flow extracted from the steam turbine and supplied to the reboiler, $h_{st,in}$ is the enthalpy of steam to the reboiler and $h_{cond,out}$ the enthalpy of returning condensate .

The turbine power output will vary dependent on where in the steam cycle steam is extracted. If the steam was not extracted, it could alternatively have been expanded in the steam turbine. While increasing the extraction steam pressure, turbine power output will be decreased. According to Figure 2-5, steam extraction pressure grows more rapidly versus saturation temperature for higher pressures. This means for steam extraction at higher pressures and fixed condenser pressure, the slope of changes to α-value is less than for lower extraction pressures. In the other words, the small change in extraction pressure has a greater impact on the lost power generation for low pressures compared to at higher pressures.

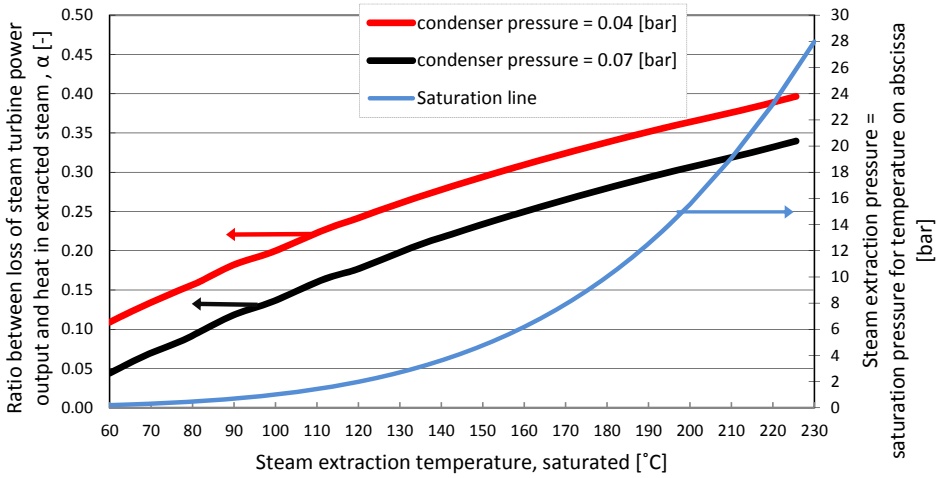

Figure 2-5: α-value mapping diagram as a function of steam extraction temperature and pressure (after Bolland et al., 2003)

The condensate pressure returning to steam cycle, also affects the net power plant output. For a constant reboiler duty, the higher the condensate pressure, the lower would be the power loss due to extraction. This is shown in Figure 2-5.

Furthermore, as Figure 2-5 depicts, in case of low steam extraction pressure the α-value is low and with that the power generation penalty of extracting steam from the turbine is small. The steam is therefore preferably extracted at lowest pressures possible within the conditions for the simulation.

2.2 Amine chemical absorption processes

2.2.1 Technology status

CO_2 removal by absorption and stripping processes with aqueous amine solution is a well-established and widely-defined technology. Many plants nowadays remove CO_2 from natural gas, hydrogen or other gases with low oxygen content. A number of technology suppliers currently offer commercial amine-based processes; Fluor Daniel Econamine FG Plus process with 30 wt% MEA concentration, the KEPCO/MHI KM-CDR based on proprietary sterically-hindered amine-based solvents (the KS series), the ABB/Lummus Kerr-McGee process with 15-20 wt% aqueous MEA solution, the Aker Clean Carbon with aqueous amine solutions, the Cansolv CO_2 capture system with tertiary amine and promoter, the HTC Purenergy Process with mixed amines, Babcock and Wilcox OptiCap process based on blend of existing solvents (probably amine-based) and other chemicals, Toshiba newly developed amine-based carbon capture system and the Hitachi amine based capture process (Herzog et al. 2009) .

To date, four coal-fired power plants (up to 43 MW) have ABB commercial flue gas CO_2 capture units. Fluor Daniel and MHI have current commercial capture facilities at three natural gas-fired power plants and they offer commercial guarantees for post-combustion capture at coal-fired power plants as well. The currently operating Lummus systems employ a solution of 20 percent MEA in water, while the Fluor systems use a solvent with a 30 percent amine concentration. More than 10 plants use KS-1, a proprietary hindered amine, with flue gases produced by combustion of clean fuel. Several demonstration capture projects for coal-fired power plants are on their way to completion during recent years in Canada, Germany and USA (Mills, 2012).

The largest demonstration facility for testing and improving post-combustion CO_2 capture technologies for natural gas-fired power plant is the CO_2 Technology Centre Mongstad (TCM) in Norway. It verifies two CO_2 capture technologies of Alstom chilled ammonia (80,000 ton/year CO_2) and Aker Clean Carbon amine-based capture (20,000 ton/year CO_2). Flue Gases to the capture processes are delivered either from a Residue Catalytic Cracker (RCC) and Natural Gas Combined Heat and Power (CHP) plant with 350 MW heat and 280 MW electricity output. Higher amine concentrations are beneficial in reducing the energy penalty of CO_2 capture since there is less water in the solution that has to be pumped and heated in the regeneration process. Capital cost also is reduced since higher amine concentrations lead to smaller equipment sizes. On the other hand, amines such as MEA are highly corrosive, so higher amine concentrations require chemical additives or more costly materials of construction to prevent corrosion. Tradeoffs among these factors underline some of the differences in capture system designs offered by different vendors. The systems and solvents currently offered commercially by Fluor (Econamine FG+) (with energy consumption ≈ 3.0 MJ/kgCO_2) and MHI (KS-1) (with energy consumption ≈ 2.8 MJ/kgCO_2) suggest reductions of roughly 20-25 percent in capture energy requirements relative to conventional system designs using MEA (Jansen et al., 2008).

2.2.2 Conventional chemical absorption process

An absorber is a process equipment where an absorbent (solvent) flows countercurrent to a gas stream for the purpose of removing one or more constituents (absorbate) from the gas stream. Most absorbers are vertical with the liquid entering at the top and the gas at the bottom. The amount of the contact that must be provided in this absorber tower depends on the system, the relative flow rate of the gas and the solvent and the concentrations involved. Solvent in this study is aqueous Monoethanolamine (MEA) and the absorbate is CO_2. The process flow diagram of a conventional chemical absorption plant is shown in Figure 2-6.

Flue gas enters the bottom of the absorber column and flows upward through the absorber, counter-current to the solvent. CO_2 gets into reaction with solvent (MEA) and is transferred from the rich gas to MEA. The dry gas which is mainly O_2 and N_2 and H_2O leaves the top of the absorber column to a scrubber for further separation of H_2O. At scrubber H_2O is removed from dry gas and returned to the H_2O cycle in the absorption system. Lean MEA enters on the top tray of the absorber, flows downward and picks and reacts with CO_2. Rich MEA leaves the bottom of the absorber column, passes through a heat exchanger with increase in flow temperature and flows to the top of the stripper. In stripper, heat is added to around 120°C and CO_2 is removed from the overhead of the stripper; here the driving force for separation of CO_2 from the solution with MEA is the partial pressure difference and the stripping heat that is delivered by the stripping vapour which is moving upwards in the stripper column. This stripping vapour is generated in the reboiler that exchanges the latent heat of the LP steam provided from power plant to evaporate the water and CO_2 from the solution with MEA. The hot lean MEA is recycled from the bottom of the stripper to the top of the absorber via the heat exchanger. Additional cooler may be used to cool down the solvent to lower temperatures (40-70°C). At the top of the stripper column, the gas goes to the condenser where the steam condenses and CO_2 exits for several stages of compression (Kohl et al., 1997).

CO_2 is soluble in the water itself, however for industrial application, amines and other organic solvents are chosen due to greater CO_2 solubilities. Hot potassium carbonate solutions that react with dissolved CO_2 to form potassium bicarbonate are among the traditional solutions for removal of CO_2. However, amine systems are favoured for industrial systems (Kohl et al., 1997). Flue gas mixtures from NGCC, inherit near-atmospheric pressures, therefore aqueous solutions with amines (in our case MEA) is deployed for CO_2 removal.

The main variables to control the absorption process are the solvent circulation rate and the amount of vapour-liquid contact; the main variables for controlling a stripper with a given feed composition and condition at fixed pressure are the temperatures at the top and bottom of the column, the feed location and the amount of vapour-liquid contact. Also the concentration of CO_2 in lean MEA (lean solvent loading) is a key parameter for design an efficient CO_2 absorption process (Kohl et al., 1997).

The parameters affecting solvent circulation rate of MEA are the partial pressure of CO_2 in the flue gas and the lean solvent loading. As mentioned earlier, the performance of absorption process will be improved by increasing the solvent circulation rate and/or decreasing MEA lean loading. However increasing solvent circulation rate leads to higher reboiler duties and these two parameters are subject to tradeoff once designing the process.

Abu Zahra et al. (2009) performed a parametric study on the effect of changing CO_2 lean MEA loading on solvent circulation rate. CO_2 lean MEA loading was varied to find the optimum solvent loading for a minimal thermal energy requirement. Additionally, MEA circulation rate was varied to achieve the same CO_2 removal capacity. From the results of this study it's clear that the thermal energy requirement decreases with increasing lean solvent loading until a minimum energy requirement is attained, however this minimum point was achieved by increasing the solvent circulation rate. This shows the complex effects of these parameters once aiming for lowest thermal energy requirement.

Furthermore, CO_2 loading is another key parameter that specifies the amount of CO_2 absorbed in molecular form by the solvent. In the current study it was defined as the ratio of CO_2 mole fraction and MEA mole fraction in the solution,

$$\text{Loading} = \frac{x_{CO_2}}{x_{MEA}}$$

The main burden of an amine absorption post-combustion system to a power plant is the parasitic loss of power. As discussed in chapter 2.1.4, LP steam is provided to the reboiler to transfer its latent heat to the rich CO_2 solution, and strip the solution from CO_2. Furthermore, there is the demand of electrical energy for flowing the gas and liquid fluids through the process by means of running blower and pump(s). CO_2 compression system also imposes additional work demand to the total power generation.

The main stream of research for chemical absorption post-combustion CO_2 capture focuses on novel solvents that need less regeneration energy. The solvents will be reviewed in the 2.2.2.1, however the thesis, exploits and elaborates various process modifications to the conventional absorption system.

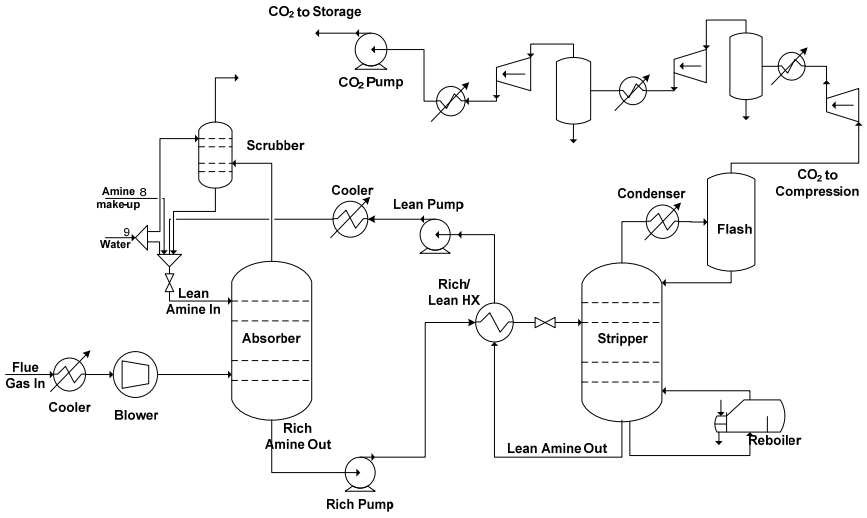

Figure 2-6: Standard process for post-combustion chemical absorption system with flue gas water-wash system and CO_2 compression

2.2.2.1 Solvents

Amines are water-soluble organic chemicals that contain reactive nitrogen atoms that react selectively and rapidly with acid gases such as CO_2, even at low partial pressures. Historically, use of MEA (monoethanolamine) for acid gas removal was patented 1930s. Since then acid gas removal from natural gas was the main stream for development of solvents specifically MEA.

Though MEA is the most popular amine used for flue gas cleaning, there are problems related to corrosiveness which results in more expensive construction materials compared to potassium carbonates, and volatilization and degradation of MEA. The problem of degradation shows itself more in the presence of O_2 and SO_2, which is the case for flue gases from power plants. To be able to solve these issues, inhibitors are used to resist solvent degradation and equipment corrosion. Moreover, in order to prevent severe degradation phenomena, fresh amine make-up should be injected from time to time. On the other hand, the increased solvent circulation rate, leads to larger equipment size and increased regeneration energy.

As mentioned earlier, the considerable amount of heat requirement to strip CO_2 from MEA solutions leads to parasitic loss of power when integrating a CO_2 capture system to a power plant. This motivated researchers to improve and develop alternative reactants other than MEA (Bonenfant et al., 2003) and/or mixed solvents that require less heat of regeneration.

Alkanolamines are divided into three different categories, primary amines such as MEA, secondary amines such as diethanolamine (DEA) and tertiary amines such as s methyldiethanolamine (MDEA) and TEA. Tertiary amines are interesting since they have high capacity for CO_2 absorption and low heat of absorption due to enhanced bicarbonate formation. This leads to lower solvent circulation rates and less thermal energy requirement for regeneration. (Yang et al., 2008) However, low rates of CO_2 absorption make them infeasible to use for CO_2 capture unless the absorption rates could be increased. This could be achieved by using mixed amines such as MEA/MDEA solution instead of a single MEA (Idem et al., 2006) or using promoted MDEA by the additive piperazine (PZ). Piperazine has higher volatility than MDEA and limited solubility in water, but considerably accelerates CO_2 absorption rates and offers energy savings up to 15% (Oyenekan, 2007).

Hindered amines such as 2-amino-2- methyl-1-propanol (AMP) are known to have high cyclic capacity, which means that they bind more CO_2 per molecule than other amines such as MEA and the reaction rates are much higher than of MDEA (Sartori et al., 1983). Hindered amines perform better absorption in high CO_2 molar composition in flue gas, such as 8-15 % (Hook, 1997) which makes them viable solvents for CO_2 capture from flue gases of coal-fired power plants. They have low degradation and volatility but their major drawback is the lower reaction rates comparing to MEA Investigations show significantly lower energy requirement and the larger size of the absorber column for AMP. The low reaction rates of AMP could be improved by using accelerating additives such as piperazine or piperidine or blending with other amines such as MEA or DEA (Abu-Zahra et al., 2009, Adeosun et al., 2013, Dubois et al., 2013).

Kohl et al. (1997) mentioned that blended solvents with/ without activating ingredients gain attention due to their high absorption and low regeneration energy requirement. For CO_2 absorption process using MEA, steam consumption is the major parameter as a result of high heat of reaction of MEA with CO_2. Therefore using amine blends with high concentrations such as 40-50% is recommended, given the fact the water present in the solution will be less and consequently less heat is needed to

vaporize the water regenerate the solvents. Moreover, mixed amine solvents can lead to lower circulation flow rate which means smaller equipment size and eventually less capital investments and operating costs required. A solution consisting of tertiary and primary amines or tertiary plus secondary amines such as MEA-MDEA or DEA-MDEA combine the high reactivity of primary or secondary amines with high capacity and low heat of absorption characteristic of tertiary amines; consequently, the heat requirement and absorber size will be decrease. The amine concentrations could be tuned to achieve the desired CO_2 removal percentage for a specific process configuration (Aroonwilas et al., 2004&2007, Lawal et al. 2005, Rodriguez et al., 2011).

Alternatively, other amine blends such as MEA-PZ and MDEA-PZ have suggested as solvents for chemical absorption process. Results show addition of PZ considerably accelerates CO_2 absorption rate and allows use of lower MEA concentrations that leads to lower thermal energy requirement for regeneration (Dang et al., 2003, Closmann, et al., 2009).

MEA solvent with concentration of 30 wt% is the most usual solvent for CO_2 removal as reported by Kohl et al. (1997) and in this thesis work is the solvent employed for chemical absorption processes.

2.2.3 Process modifications

The modifications to conventional system are numerous in the literature. There are various modifications that involve the absorber column, stripper column, heat integration between the columns and heat integration between absorption and compression plants. Cousins et al.(2011) reviewed a majority of process modifications that was found in the literature for chemical absorption CO_2 capture from exhaust gases of the power plants.

The attempt of changes to the conventional process described in section 2.2.2 is to decrease irreversibilities which are mainly large driving forces for the separation. This is employed by dividing the large driving forces into smaller portions, and distributes it evenly in the process to move toward more reversible processes.

Several of these process modifications have been explained in the following sections:

2.2.3.1 Absorber inter-stage cooling

In summary, the concept behind this configuration is to release the heat of absorption and reduce the solvent temperature at the absorber bottom. The driving force of the absorption process is defined as the difference between equilibrium and operating loading of CO_2 in the solvent. Inter-stage cooling causes a temperature reduction of the solvent, which is in favour of higher driving force for the absorption process and increases the absorption capacity of the solvent, i.e. solvent rich loading. Consequently, the solvent circulation rate and reboiler energy requirement is decreased.

As mentioned earlier, chemical absorption of CO_2 with 30% MEA solvent, achieves the highest rates of mass transfer in the range of 40-60°C (Aroonwilas et al., 2001). Because of the exothermic nature of absorption reaction, there is an overall increase in the temperature of the solvent in the absorber column; vaporization of water present in the solution has a slight effect on this temperature increase. This temperature increase leads to lower solvent viscosity and higher mass transfer coefficients, which favours the kinetics of the chemical absorption reaction. Reversely, this temperature increase due to the nature of the absorption reaction, impairs the thermodynamics of the absorption reaction by

decreasing its driving force (the difference between CO_2 equilibrium and operating loading) and decreasing the solvent absorption capacity i.e. CO_2 loading (Leites et al., 2003). These two counter-effects are competing in an absorber. To control the temperature in the conventional absorption process, the lean amine is cooled down before entering the top part of the column; also the flue gas temperature is cooled to around 40-45°C before entering the bottom part of the absorber column. However, there are in general no means of temperature control in the middle parts of the absorber column.

The aforementioned is the motivation for developing absorber inter-stage cooling configurations. Several authors such as Rochelle (2003), Chang et al. (2005) and Tobiesen et al. (2008) have investigated configurations with inter-stage coolers. Aroonwilas et al. (2007) patented a configuration with inter-stage cooling for the bottom part of the absorber to enhance the CO_2 loading and heating in the upper section of the column to improve the mass transfer rates. Due to the higher attainable rich loading and reduction in the solvent circulation rate, the stripper reboiler duty can be decreased.

Absorber inter-stage cooling has been assessed as one of the main process configurations in the current thesis. The process is based on cooling at the bottom part of the absorber where CO_2 loading in the solvent is high. The inter-stage cooling leads to lowering the equilibrium CO_2 partial pressure in the solvent and consequently increasing the driving force of the absorption of CO_2 to the solvent.

The modification to the conventional case as illustrated in Figure 2-7 is to extract semi-rich stream from the lower part of the absorber, cool via inter-stage cooler down to 25 °C and recycle it to the absorber column. All other process units and conditions are identical to the base case. The flow rate of side-draw stream to the cooler, the cooling temperature of the side-draw stream and the location of side-draw stream have been subject to optimization to approach the less reboiler duty compared to the base case.

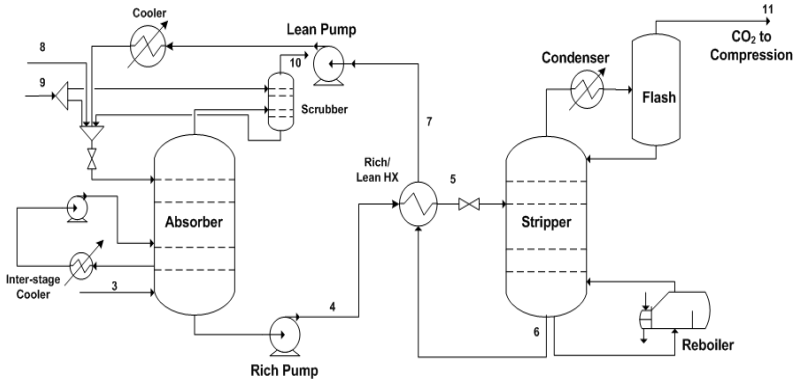

Figure 2-7: Process configuration of chemical absorption with inter-stage cooling

2.2.3.2 Split-flow

In summary in split-flow process assessed here, which is illustrated in Figure 2-8, rich amine leaving the absorption column is split into two streams. Here, the amount of rich amine which enters the bottom section of the stripper is reduced meaning less heat is required to remove CO_2 from solvent to reach same CO_2 lean loading as of conventional configuration. Recycling of a semi-lean amine from

stripper to the absorber via a cooler, acts as inter-cooling for the absorber column that increases the loading of solvent in the bottom of absorber. This semi-lean amine which enters the bottom half of the absorber column, is capable of reacting with majority of CO_2 while the rest of the flue gas is exposed to lean amine returned to the top of the absorber.

The split-flow configuration for chemical absorption processes (Figure 2-8), was first suggested by Shoeld (1934), developed by number of pioneers such as Thompson et al. (1987) and further analysed by Kohl et al. (1997) to reduce steam consumption of solvent regeneration. In the research paper by Aroonwilas et al. (2006), the authors pointed out 35% energy saving in reboiler duty for 95% CO_2 capture ratio. However, they pointed out the need of trade-off between the energy cost and the additional capital investment cost since the impact of complexity of the process on the investment cost should not be neglected.

In this configuration, which is analysed and studied in papers 2, 4 and 5, the rich amine leaving the absorber is split between two feed points to the stripper. One stream enters the top of the stripper and leaves it from the middle point and returns to the middle of the absorber. The other split stream enters the bottom of the stripper and leaves it towards the top of the absorber. Since less amount of rich amine enters the stripper bottom section, the solvent is stripped to the same CO_2 loading with lower energy consumption. Moreover, semi-rich amine enters the absorber column at 25 °C and cools the absorber column which is in favour of absorption process and was discussed more in Section 2.2.3.1.

The key parameters that are subject to optimization in order to achieve less reboiler duty are the split flow fraction, the feed tray of the second split to the stripper, the flow rate and the feed location of semi-rich amine that returns to the absorber, the CO_2 molar fraction in lean solution and the condenser temperature.

Comparing to the aforementioned split-flow configuration, there are suggested modifications suggested by different researchers. Tower et al. (1997) suggested modifications; first to control the composition of the side-stream including a second reboiler on the side draw which boils off enough water to maintain the concentration of solvent in this stream matching with the lean stream leaving the bottom of the stripper. The second modification is to design the stripper to create optimum conditions for regenerations; i.e. to return the condensate to the column a few stages above the rich stream feed to the stripper and then removing the condensate from the stripper to prevent it from flowing downwards. They claim this will reduce condenser duty and partially strips the condensate. With these modifications, they reached 70% less energy requirement for the stripper compared to conventional split-stream configuration. However it should be mentioned that their acid gas removal absorption/stripping process is performed for a high-pressure flue gas which has different nature than flue gases coming a NGCC (atmospheric pressure , $\approx$ 4% CO_2) .

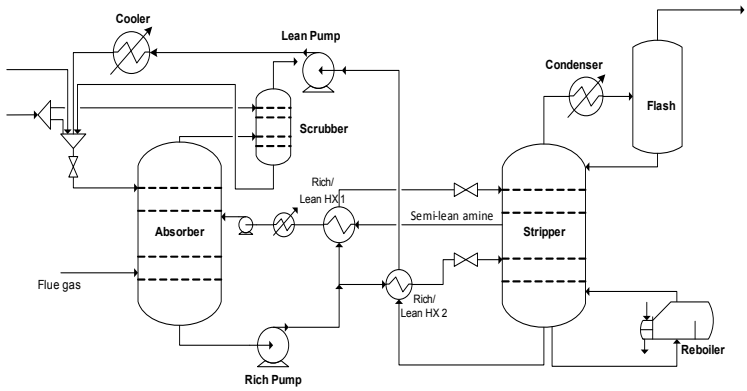

Figure 2-8: Conventional split-flow absorber-stripper arrangement

2.2.3.3 Lean vapour recompression (LVR) model

The principle for LVR is that by process modifications, it is possible to utilize a low temperature heat source in order to add exergy input in the form of steam to the stripper column and thus reduce the reboiler duty (Woodhouse et al., 2009). In summary, the steam will be extracted from the lean amine leaving the bottom of the stripper column, recompressed and reintroduced to provide surplus steam for stripping CO_2 from solvent. Alternatively, the recompressed steam could be condensed and the heat of condensation could be utilized as additional heat source to serve the reboiler.

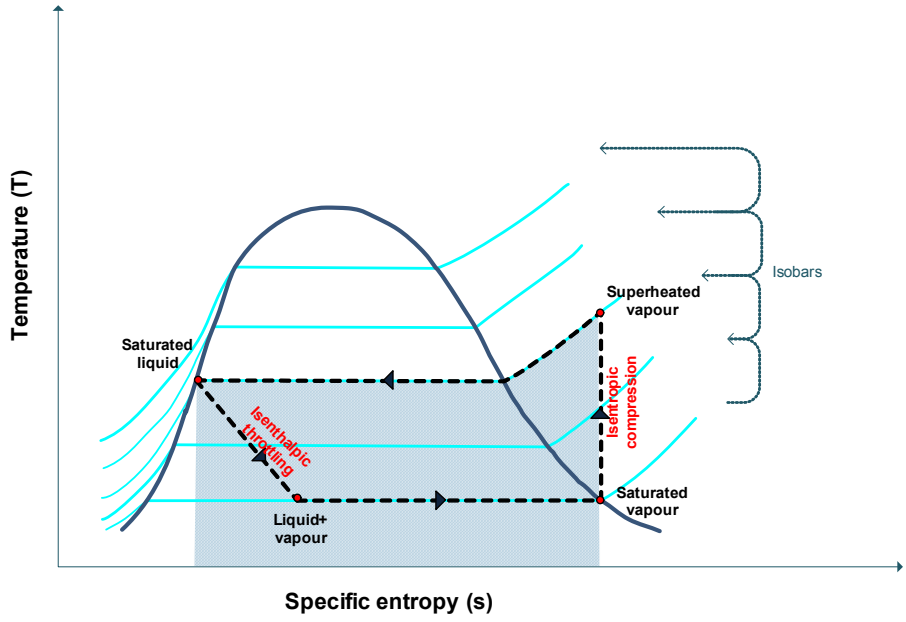

Figure 2-9: Thermodynamics of the LVR cycle. The shaded area represents the heat which steam releases through its phase change from superheated vapour to saturated liquid.

In the current thesis work, steam is extracted from the lean amine solution leaving the stripper. By this modification, the sensible heat of the hot lean amine at the bottom of the stripper is recovered in the form of latent heat of the steam. Here, the lean solvent is flashed over a flash valve and separated in a flash tank into a gaseous phase (comprising mainly of water and CO_2) and liquid which is the regenerated MEA. The produced vapour is compressed and injected at the bottom of the stripper column as the stripping media which is the steam at a low energy cost i.e. the compression work compared to the generation of the same amount of steam in the reboiler.

The thermodynamics of the LVR cycle is illustrated in Figure 2-9. The lean amine solution goes through flash evaporation. The saturated liquid stream undergoes a reduction in pressure by passing through a throttling valve which is located at the entry into a flash drum so that the flash evaporation occurs within the vessel. In throttling valve, the saturated liquid mixture goes through expansion while entering multi-phase region and getting cooled due to Joule Thompson effect. Through flash evaporation, water flashes immediately into vapour phase and the residual MEA is separated in the flash drum. Thereafter, water vapour at saturated conditions goes through isentropic compression resulting in a superheated steam which is sent to the stripper column. There, steam transfers both its sensible and latent heat to the solvent as mentioned before.

There are several models presented in the literature on how to do vapour recompression. As stated, the purpose of vapour recompression designs is to provide steam that is regained from the stripping process as heating media to the reboiler. One of the alternative designs of the vapour recompression model has been presented by Jassim and Rochelle (2006). In this design, the lean amine leaving the stripper bottom is used to intercool the gaseous stream in the multistage compressor (except the last two stages). The purpose of the design is to recover the heat of condensation of the overhead water vapour and the sensible heat of hot compressed CO_2 stream leaving each compression stage to re-boil the stripper. The results of this study show that the reboiler duty has been decreased by about 43%, but the total work demand of the process stayed at the same level regarding the increased amount of CO_2 compression work.

Another design, which was modelled and analysed in the paper 4 and 5, is a patent-based model outlined by Reddy et al. (2007). This lean vapour recompression design is based on flashing lean solution to generate the steam feed that is introduced to the stripper column via a compressor. The compressor type is a thermocompressor or mechanical vapour recompressor (Minton, P. E., 1986). The advantage of this design as claimed by Reddy et al. (2007) is that the water balance in the stripping column remains unaltered, which is one of the main concerns in other vapour recompression designs. A further modification to this model has been by presented by Woodhouse et al. (2009), which integrates the usage of low temperature heat for generation of steam in various locations of the stripper column

With vapour recompression as shown in Figure 2-10, the lean solution that is leaving the stripping column, decreases its pressure through a flash valve to 1 bar and flashes through a flash drum to produce a gaseous phase. This gaseous phase is composed mainly of water vapour, is recompressed to 2 bar and reintroduced to the stripping column. Similar to the base case, the liquid phase from the flash drum is cooled down by the rich solvent and returns to the absorber.

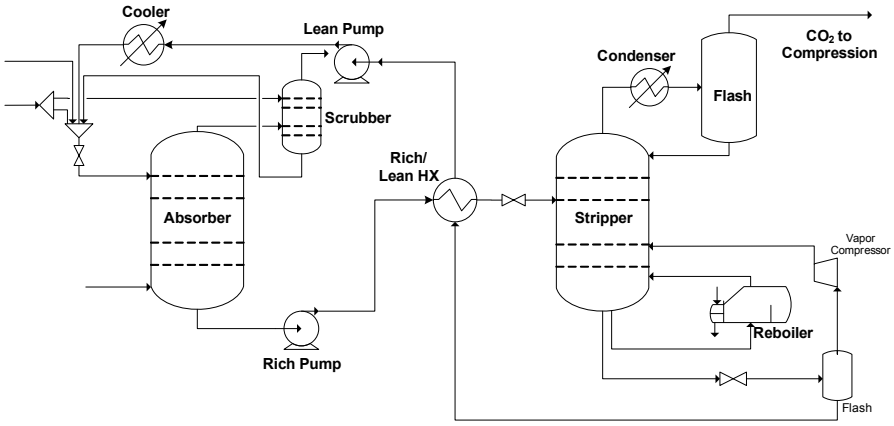

Figure 2-10: Vapour recompression arrangement

2.2.3.4 Stripper modifications

Advanced stripper modifications are focused on improving process reversibility. Each of these configurations applies heat and/or strips CO_2 in more steps using smaller heat and material driving forces (Leites et al., 2003). By operating several columns and vessels at several temperatures and pressures, stripping of CO_2 can be accomplished with much smaller driving forces, thus improving process reversibility (Rochelle, 2004).

There are many configurations found in literature such as 1 or 2 stage flash, multi-temperature/multi-pressure with/ without split feed, double matrix columns (Oyenekan, B.A. et al., 2007, Van Wagener, D. H., 2011).

Multi pressure (multi-flash) stripper design (Rochelle, 2004, Oyenekan, 2007) is an extension to vapor recompression process modification that has been discussed in 2.2.3.3, which attempts to reduce the regeneration energy requirement. The stripper column is divided into a few stages, each operating at different pressure. Vapour -as the stripping medium- from lower pressure stage is recompressed and send to an upper stage with higher pressure. The liquid solvent flashes as it moves to the lower pressure stages toward the bottom of the column. Since a good portion of the stripping medium is provided by various steam injections through different stages, the reboiler duty is decreased around 20% (Oyenekean et al., 2007). Another impact on the total work requirement is the reduced CO_2 compression work due to higher pressure CO_2 released from the stripper column. However, the drawback of this concept is the increased steam compression work along the various stages of the stripper column.

Inter-heated stripper column (integrated lean/ rich heat exchanger to striper column) was suggested by Leites et al. (2003) to reduce the solvent regeneration energy requirement. They state that since the equilibrium and operating condition are closer together along the length of the stripper, the exergy consumption will be decreased. The same concept was modelled by Oyenekan (2007) where he found the regeneration work requirement (including CO_2 compression) is reduced to 17% less than of a conventional stripper.

Fluor also acquired a number of patents on the implementation of advanced configurations, including a lean vapour recompression as described in 2.2.3.3 (Reddy et al., 2007).

The main process modifications that are analysed in this thesis are the absorber inter- cooling, the split flow, lean vapour recompression and combinations absorber inter-cooling with the two other modifications.

2.3 CO_2 compression plant

The CO_2 gas that is released from top of the stripper should be dehydrated and compressed to be ready for transportation and storage. The compression process consists of several stages with limited pressure ratios with heat exchangers to cool the CO_2 stream (intercooling). After each compression stage, the temperature of the compressed CO_2 is cooled using a heat exchanger (intercooler) in order to reduce the net work required by each stage.

The final delivery conditions (temperature and pressure) are based on the scenario that is chosen for CO_2 compression process. For pipeline transport, it is normally required that the pressure is over the critical point. This is due to the fact that the CO_2 specific volume at supercritical conditions is substantially smaller compared with values in the gas phase.[2] Furthermore, at supercritical pressure, the density of CO_2 stream is higher than that of gaseous CO_2 and a higher density is favourable when transporting liquid CO_2, as it is easier to move a dense liquid than a gas (Romeo et al., 2009 & Wong, 2005).

Drying is an important step due to pipeline corrosion and hydrate formation in the presence of liquid water in the stream. Some of the CO_2 compression plants include intercooling and dehydration units while some other suggest equipping every intercooler with a condensate trap to avoid the inlet of water droplets in the next compressor stage. Recent studies focus on integration of heat sources available from intercooling of the compression stages. This heat integration is either with the steam power cycle to provide energy for feedwater preheating (Romeo et al., 2009) or to provide low grade heat source to heat up the boiler condensate leaving the power cycle condenser (Lucquiaud et al., 2011). Furthermore, this heat integration is possible toward the stripper column; the latter concept considers lean amine leaving the bottom of the stripper column to intercool CO_2 compression stages. Here, most of the compressor work and the water vapor form the top of the stripper is converted to heat used by the reboiler (Rochelle, 2003).

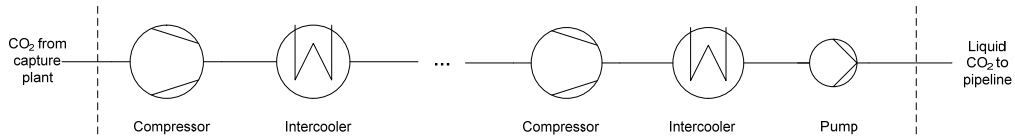

Figure 2-11: Schematic representing CO_2 compression plant with intercooling (Wilcox, 2012)

Typically, a 3-4 stage reciprocating compressor with individual cylinder for each stage is required with cooling between the stages. The compressor is used to compress the CO_2 to typically 90 bar, at

[2] Gaseous phase CO_2 Specific volume (1.013 bar and 25 °C): 0.5532 m^3/kg
CO_2 Specific volume at critical point (73.77 bar and 30.98 °C): 0.0021 m^3/kg

which it reaches supercritical liquid condition; further on CO_2 will be pumped to typical transport conditions of approximately 10-15 MPa (100-150 bar). A schematic representing a CO_2 compression plant is shown in Figure 2-11.

CO_2 compression work is dependent on compressor efficiency, pressure ratio, CO_2 inlet temperature and extent of compression intercooling. Another important factor in defining the required work of CO_2 compression is the initial pressure of CO_2 released from the stripper column . The higher this pressure is, the less work is required to compress the CO_2 to the final delivery pressure. This implies that increasing regeneration pressure in a CO_2 capture process reduces the efficiency penalty imposed by the CO_2 compression plant.

2.4 Efficiency of combined Cycle with CO_2 capture

When the chemical absorption CO_2 capture and compression plants are integrated into a power plant, there are several associated power losses at different points of the process which will affect the power plant efficiency. The net power plant efficiency for a power plant with capture system can be calculated based on the following expression (Bolland, O. & Undrum, H. 2003):

$$\eta_{pp} = \underbrace{\eta_{\text{Ref. NGCC}}}_{\text{a}} - \underbrace{\frac{E^{CO_2}_{rem,mech} C}{\text{LHV}}}_{\text{b}} - \underbrace{\frac{E^{CO_2}_{rem,heat} \alpha\, Cf}{\text{LHV}}}_{\text{c}} - \underbrace{\frac{E^{CO_2}_{comp} Cf}{\text{LHV}}}_{\text{d}}$$

Term a, shows the efficiency of natural-gas fired power plant without any CO_2 capture. Terms b, c and d are the efficiency penalties due to integration of CO_2 capture plant. These energy penalties are related to mechanical work demand of blower and several pumps/compressor in the capture plant (term b in net power plant efficiency formula), the steam turbine power reduction due to steam extraction to provide the reboiler steam-demand for the stripper column (term c) and the mechanical work demand of the compressors to compress captured CO_2 to a certain transport/injection pressure (term d). $E^{CO_2}_{rem,mech}$ (MJ/kg CO_2) is the mechanical energy for running the pumps and blower. Blower work is provided to cater for the pressure drop of the exhaust gases in the absorption column; volumetric flow rate of the exhaust gases also affect the blower work. Also, $E^{CO_2}_{rem,mech}$ includes the work consumption by few circulation pumps in CO_2 capture process; the pump work is totally dependent on the volumetric flow rates and the pressure drops in various process equipments. Here C is used as a mass conversion coefficient between 1 mole of combusted fuel and 1 mole of produced CO_2 which is 44m. $E^{CO_2}_{rem,heat}$ (MJ/kg CO_2) is the heat required for atmospheric stripping of CO_2 from the solvent which is as explained in 2.1.5 is the reboiler duty (Q_{Reboiler}). f defines the CO_2 capture ratio which is the fraction of CO_2 that is separated from the flue gas. $E^{CO_2}_{comp}$ (MJ/kg CO_2) nominates the power requirement for compression of CO_2 in efficiency expression.

References:

Aboudheir, A., El Moudir, W., 2009. Performance of formulated solvent in handling of enriched CO_2 flue gas stream. Energy Procedia, 1, 195-204.

Abu-Zahra, M.R.M., Schneiders, L.H.J., Niederer, J.P.M., 2007. CO_2 capture from power plants, Part I. A parametric study of the technical performance based on mono-ethanolamine. International Journal of Greenhouse Gas Control, 1(1), 37–46.

Abu-Zahra, M. R. M., Feron, P. H. M., Jansens, P. J., Goetheer, E. L. V., 2009. New process concepts for CO2 post-combustion capture process integrated with co-production of hydrogen. International Journal of Hydrogen Energy, 34**,** 3992-4004.

Adeosun, A., Abu-Zahra, M. R. M., 2013. Evaluation of amine-blend solvent systems for CO_2 post-combustion capture applications. Energy Procedia, 37**,** 211-218.

Aroonwilas, A., Veawab, A., 2004. Characterization and Comparison of the CO_2 Absorption Performance into Single and Blended Alkanolamines in a Packed Column. Industrial & Engineering Chemistry Research, 43**,** 2228-2237.

Aroonwilas, A., Veawab, A., 2006. Cost structure and performance of CO_2 capture unit using split-stream cycle. 8th International Conference on Greenhouse Gas Control Technologies, Trondheim, Norway.

Aroonwilas, A.; Veawab, A., 2007. Heat recovery gas absorption process. Patent No. WO 2007107004 A1, University of Regina

Bolland, O., 2009. Power Generation: CO_2 capture and Storage, Course material. Department of Energy and Process Engineering, NTNU.

Bonenfant, D., Mimeault, M.,Hausler, R., 2003. Determination of the Structural Features of Distinct Amines Important for the Absorption of CO_2 and Regeneration in Aqueous Solution. Industrial & Engineering Chemistry Research, 42**,** 3179-3184.

Cengel, Y. A. and Boles, MA., 2006. Thermodynamics: An Engineering Approach, 6th edition, McGraw-Hill.

Chang, H., Shih, C. M., 2005. Simulation and optimization for power plant flue gas CO_2 absorption-stripping systems. Separation Science and Technology.40(4), 877-909.

Closmann, F., Nguyen, T., Rochelle, G.T., 2009. MDEA/Piperazine as a solvent for CO_2 capture. Energy Procedia, 1**,** 1351-1357.

Cousins, A., Wardhaugh, L. T.,Feron, P. H. M., 2011. A survey of process flow sheet modifications for energy efficient CO2 capture from flue gases using chemical absorption. International Journal of Greenhouse Gas Control, 5, 605-619.

Dang, H., Rochelle, G.T., 2003. CO_2 Absorption Rate and Solubility in Monoethanolamine/Piperazine/Water. Separation Science and Technology, 38**,** 337-357.

Dubois, L., Thomas, D., 2013. Postcombustion CO_2 Capture by Chemical Absorption: Screening of Aqueous Amine(s)-based solvents. Energy Procedia, 37**,** 1648-1657.

Herzog, H., Meldon, J., Hatton, A., 2009.Advanced Post-Combustion CO_2 Capture, prepared for Clean Air Task Force. http://web.mit.edu/mitei/docs/reports/herzog-meldon-hatton.pdf

Hook, R. J., 1997. An Investigation of Some Sterically Hindered Amines as Potential Carbon Dioxide Scrubbing Compounds. Industrial & Engineering Chemistry Research, 36**,** 1779-1790.

Idem, R., Wilson, M., Tontiwachwuthikul, P., Chakma, A., Veawab, A., Aroonwilas, A.,Gelowitz, D., 2005. Pilot Plant Studies of the CO_2 Capture Performance of Aqueous MEA and Mixed MEA/MDEA Solvents at the University of Regina CO_2 Capture Technology Development Plant and the Boundary Dam CO_2 Capture Demonstration Plant. Industrial & Engineering Chemistry Research, 45**,** 2414-2420.

Jassim, M. S., Rochelle, G. T., 2005. Innovative absorber/stripper configurations for CO_2 capture by aqueous monoethanolamine. Industrial & Engineering Chemistry Research, 45(8), 2465-2472.

Jansen, D., ten Asbroek, N.A.M., van Loo, S., van Dorst, E., Geuzenbroek, F., Ploumen, P., Kamphuis, H., van Rijen, S., 2008. Integration of CO_2 Capture Technologies in Existing Plants in the Netherlands. EOS-CAPTECH. www.CO2-captech.nl/

Karimi, M., 2011 CO_2 capture and power production integration; optimization and conceptual design studies, PhD thesis, Norwegian University of Science and Technology.

Kehlhofer, R., Rukes, B., Hannemann, F., Stirnimann, F, 2009. Combined-Cycle Gas and Steam Turbine Power Plants; 3rd Edition; PennWell

Kohl, A., Nielsen R., 1997. Gas Purification, 5th edition, Texas: Gulf Publishing Company

Lawal, O., Bello, A., Idem, R., 2005. Pathways and reaction products for the oxidative degradation of CO_2 loaded and concentrated aqueous MEA and MEA/MDEA mixtures during CO2 absorption from flue gases. Greenhouse Gas Control Technologies 7. 2(1), 1159-1164.

Leites, I. L., Sama, D. A. , Lior, N., 2003. The theory and practice of energy saving in the chemical industry: some methods for reducing thermodynamic irreversibility in chemical technology processes. Energy, 28, 55-97.

Lucquiaud, M., Gibbins, J., 2011. On the integration of CO_2 capture with coal-fired power plants: A methodology to assess and optimise solvent-based post-combustion capture systems. *Chemical Engineering Research and Design,* 89**,** 1553-1571.

Mills, Stephen, 2012. http://newsletter.naseo.org/news/newsletter/documents/2012-11-30-Coal-fired-CCS-demonstration-plants-2012-by-Stephen-Mills.pdf

Oyenekan, B.A., Rochelle, G. T, 2007. Alternative stripper configurations for CO_2 capture by aqueous amines. AIChE Journal, 53, 3144-3154.

Oyenekan, B.A., 2007. Modeling of Strippers for CO_2 Capture by Aqueous Amines. PhD thesis ,The University of Texas at Austin

Reddy, S., Gilmartin, J., Francuz, V., 2007. Integrated compressor/stripper configurations and methods. Patent No. WO/2007/075466, Fluor Technologies Corporation Fluor Technologies Corporation .

Rochelle, G.T., 2003. Innovative Stripper Configurations to Reduce the Energy Cost of CO_2 Capture. Second Annual Carbon Sequestration Conference. Alexandria, VA

Rodríguez, N., Mussati, S.,Scenna, N., 2011. Optimization of post-combustion CO_2 process using DEA–MDEA mixtures. Chemical Engineering Research and Design, 89**,** 1763-1773.

Romeo, L. M., Bolea, I., Lara, Y., Escosa, J. M., 2009. Optimization of intercooling compression in CO_2 capture systems. Applied Thermal Engineering, 29**,** 1744-1751.

Saravanamutto, H.I.H., Rogers, G.F.C, Cohen, H., 2001. Gas turbine theory; fifth edition; Harlow: Prentice Hall

Sartori, G.,Savage, D. W., 1983. Sterically hindered amines for carbon dioxide removal from gases. Industrial & Engineering Chemistry Fundamentals, 22**,** 239-249.

Shoeld, M., 1934. Purification and Separation of Gaseous Mixtures, U.S. Patent 1,971,798.

Thompson, R.E., King, C.J., 1987. Energy conservation in regenerated chemical absorption processes. Chemical Engineering and Processing 21, 115–129.

Tobiesen, A.F., Dorao, C.A., 2008. A simulation study of alternative process configurations for CO_2 absorption plant using CO2SIM. Proceedings of 9th International Conference on Greenhouse Gas Control Technologies, GHGT-9

Tower, G.P., Shethna, H.K., 1997. Improved Absorber-Stripper Technology for Gas Sweetening to Ultra-Low H_2S Concentrations. Proceedings of the Seventy-Sixth GPA Annual Convention. 93-100

Undrum, H., Bolland, O., 2003. A novel methodology for comparing CO_2 capture options for natural gas-fired combined cycle plants. Advances in Environmental Research 7, 901–911.

Van Wagener, D. H., 2011. Modeling for CO_2 removal using monoethanolamine and piperazine solvents. PhD thesis ,The University of Texas at Austin

Woodhouse, S., Rushfeldt, P., Sanden, K., Haaland, A.H., 2009. Improved Method For Regeneration Of Absorbent. Patent No. WO/2009/035340 A1, Aker Clean Carbon.

Wong, S., 2005. CO_2 Compression and Transportation to Storage Reservoir. http://science.uwaterloo.ca/~mauriced/earth691-duss/CO2_Materials_From_ARC_APEC_Beijing_2006/CarSeq_Module4.pdf

3 Methodology

3.1 Simulation of MEA chemical absorption process

Many commercial softwares are used for simulation of post-combustion CO_2 capture plant, such as UniSim Design, Aspen HYSYS, Aspen Plus (RadFrac,Ratesep), Protreat, ProMax, CHEMCAD, CHEMASIM (Developed by BASF) and EBSILON Professional. For power plant simulations (design, off-design and part load) strong tools such as GT PRO/MASTER and STEAM PRO/MASTER, THERMOFLEX, PEACE, EBSILON Professional, IECM (developed by CMU and EPP for DOE/NETL) and ThermosysPro (developed by EDF R&D) are available. Other in-house simulators such as CO2SIM, is developed by SINTEF and NTNU. Some of these softwares, such as EBSILON Professional, can be used for both power plant and chemical absorption simulations, while most of others need either to be linked through interface managers such as ELINK, excel sheet or individual program codes to extract the data from one software (mostly power plant simulation software) and revert them to the main simulation worksheet (such as UniSim Design, Aspen HYSYS or Aspen Plus).

Different modelling tools are based on the variety of thermodynamic models, component and mixture properties and plant data packages. The aforementioned is also combined with different approaches in computational models. The extent of accuracy and complexity of each of these modelling tools are defined by the choice of abovementioned parameters. Also, transferring the results from one simulation tool to another, demands precise investigation of the similarity and accuracy of the thermodynamic model and component assumptions for both of the software. Moreover, while simulation tools offer generic solutions for specific problems, the importance of data validation affects the reliability of the simulation results.

3.1.1 Thermodynamic model;

The properties of components in solutions are dependent on temperature, pressure and component activities in the solution. These variables are themselves depending on molecular interactions taking place in multi-component solutions. Therefore, thermodynamic models are acquired to predict molecular interactions.

3.1.1.1 Phase equilibrium

The vapour-liquid equilibrium of CO_2/MEA solution in water can be expressed by empirical models as the function of concentrations of CO_2, amine and temperature at equilibrium conditions. There are available experimental vapour-liquid data for amine systems in literature such as the results from Jou et al. (1995). Empirical models also are developed to correlate relations for equilibrium solutions. Kent and Eisenberg (1976) predicts phase equilibrium data for CO_2 in MEA solution by using values for Henry's constants and equilibrium constants for water/carbonate/bicarbonate to fit with experimental data (Øi, 2012) . For phase equilibrium calculations, Henry's law constant has been used for prediction of CO_2 in aqueous phase. The fugacity coefficient of the molecular species of gas phase components was calculated by the Peng-Robinson equation of state (Peng and Robinson, 1976). The prediction of chemical equilibrium constants involve the simultaneous solution of a set of non-linear equations that describe the chemical and phase equilibrium and the electroneutrality (charge balance)

and mass balance of the electrolytes in the aqueous phase. A modified version of the Kent-Eisenberg model (Li et al., 1993) is used in Amine property package in Aspen HYSYS and UniSim Design. Other empirical model for vapour-liquid predictions of CO_2 in MEA solutions have been developed by Gabrielsen et al. (2005). Li-Mather (1994) developed a similar model by acquiring electrolyte-Margules model from Clegg and Pitzer (1992).

3.1.1.2 Activity-coefficient-based models

Excess Gibbs energy-based activity coefficient models provide thermodynamic framework to model thermodynamic properties of aqueous electrolyte systems, including aqueous alkanolamine systems for CO_2 capture. Based on the Debye-Huckel theory and the Guggenheim equation, Deshmukh et al. (1981) developed a model with activity and fugacity coefficients. Austgen et al. (1989 & 1991) and Posey (1996) developed a set of thermodynamic models based on the electrolyte-NRTL model by Chen et al. (1982 & 1986) to correlate CO_2 solubility in aqueous amine solution; these models assume the local composition around a molecule is influenced by the interactions of this molecule with its environment i.e. electrolyte solutions. They describe the VLE by utilizing Henry's law constants and different models using large number of parameters to fit with experimental data. Hoff et al. (2004) developed other semi-empirical model based on the Chen-Austgen model that determines activity coefficients as function of CO_2 concentration.

3.1.2 Mass transfer model;

Specifically, for chemical absorption with MEA there are two different approaches in simulating the process; equilibrium based models (Unisim Design, Aspen HYSYS) versus rigorous rate-based models (Aspen plus, Protreat) for the mass transfer phenomena.

3.1.2.1 Equilibrium model

This approach considers that the mass transfer through column occurs at successive equilibrium stages considering both vapour and liquid phases are individually well mixed. Taylor et. al (1993) defined MESH equations which includes material balances, equilibrium expressions, summation and heat balances to model the equilibrium stages. Chemical reactions can also be introduced on the stages for the reactive absorption by defining various ranges of Hatta number to determine effectivity of reactive absorption (Kenig et al., 2003).

On each stage, a perfect equilibrium is achieved, so that the liquid phase flowing to the lower stage is in equilibrium with the gas rising to the upper stage; the concept is simple and has been widely used in simulation softwares. However, it should be noted that thermodynamic equilibrium is rarely achieved and separation takes place due to the mass transfer between the vapour and liquid (Taylor et al., 2003). A simple way to improve the ideal stage calculation in a traditional process simulation program is to use Murphree efficiencies for a specific packing height. HETP (height equivalent to a theoretical plate) is used to adjust the number of real stage in tray or packed columns (Kenig et al., 2009). Since the mass and heat transfer limitations are neglected, the model is closer to ideality. Main characteristic of the softwares using these is the robustness in the convergence of the calculation (Øi, 2012).

3.1.2.2 Rate-based model

In this model, the reactive absorption is considered with mass and heat transfer limitations. To perform rate-based mass transfer calculations, it is required to solve the extended Maxwell-Stefan multi-component mass transfer equation to determine inter-phase transfer rates by estimation of mass and heat transfer coefficients and interfacial areas. ASPEN RateSep, the rate-based mode of RadFrac allows for the rate-based modelling of absorption and desorption columns. It acquires the two-film theory and allows for film discretization which is useful to get an accurate concentration profile in the film for fast reactions. It also combines the film equations with separate balance equations for the liquid and vapour phase, diffusion and reaction kinetics, electrolyte solution chemistry and thermodynamics (Kothandaraman, 2010).

3.1.3 Current work

In the current thesis work, CO_2 capture using MEA chemical absorption and CO_2 compression is modelled with UniSim Design software (Honeywell), which contains the Amines Property Package. This special property package has been designed to aid the modelling of alkanolamine treating units in which CO_2 is removed from gaseous streams. In this property package, a non-equilibrium stage model which is based on the stage efficiency concept is used to simulate the performance of absorber and stripping columns. This non-equilibrium stage model is a function of kinetic rate constants for the reactions between CO_2 and MEA, the physical and chemical properties of the amine solution, the pressure, temperature and the mechanical tray design variables. The modelling details and the basis of the simulations of UniSim Design are summarized in paper 4.

In this thesis work, which involves overall energy and exergy calculations and balance, it was chosen not to use rigorous rate-based mass transfer models to simulate the CO_2 capture plant due to the following reasons:

- Comparison between various process configurations; an extensive knowledge of design correlations (e.g. physical properties, kinetics, hydrodynamics and mass transfer) is necessary for simulation and design of a full-scale CO_2 capture plant using rate-based models. Therefore, the models are more complicated and their robustness is significantly affected by the accuracy of the required information in the model. Moreover, the choice of design parameters has a significant impact on the mass and energy balance in the CO_2 capture process (Razi, 2013). However, the nature of the current thesis work is to focus on simple and robust modelling for various process configurations and performing energy and exergy balances on a CO_2 capture system. The equilibrium-based approach is simpler and more robust, and allows for a much higher number of case calculations. The choice of equilibrium-based modelling does not affect the trends of the results for many cases compared in the current work.
- In the current thesis work, energy and exergy balance for CO_2 capture systems are made and the efficiencies are compared for various cases. The main input to the energy balance over a chemical absorption CO_2 capture process is the heat requirement for regeneration of MEA. According to the recent claims (Leonard, 2013), the equilibrium-based approach underestimates the heat requirement, however the deviations have not been quantified and verified compared to experimental results. It is not obvious whether an equilibrium-based or

rate-based calculation of CO_2 removal is most accurate method in terms of prediction of heat requirement for regeneration of MEA. As well as it is not demonstrated that differences in equilibrium models influence much on the parameter calculations (Øi, 2012). In fact, the strength of the rate-based calculation is depending on accessibility to a more accurate detailed description and design of the process. Karimi (2011) compared the simulation results of Unisim and ProTreat (which is a rate-based process simulation tool). His findings show less than 1% difference between the results of two different modelling approaches. A future incentive for the current work would be to validate the results of the current process simulations versus the experimental data and assess and document the potential deviations.

3.2 Exergy analysis

The exergy method of evaluating energy-intensive systems integrates the first and second laws of thermodynamics at the state of specific ambient conditions. Exergy analysis, with its specific method of process evaluation, has proven to be an efficient tool to define the second law performance of processes. It combines the principles of conservation of mass and energy together with the second law of thermodynamics to characterize the thermodynamic losses associated with each unit of a system. Hence, it enables to identify losses and to make improvements of energy consumption. This is an advantageous method to approach the goal of more efficient processes since it specifies the locations, types, and real magnitudes of irreversibilities, either being reduced or dissipated.

The exergy of a stream can be divided into physical exergy and chemical exergy. The physical exergy equals the maximum reversible amount of work obtainable when the stream of substance is brought from its actual state to the environmental state defined by P_0 and T_0 (Szargut et al., 1988) by physical processes involving only thermal and mechanical interaction with the environment. Assuming that potential and kinetic energy can be neglected, it is expressed as:

$$\varepsilon_{ph} = (h - h_0) - T_0(s - s_0) \tag{1}$$

where *h* and *s* are the specific enthalpy and entropy, respectively, and $h_0 = h\left(T_0, P_0\right)$ and $s_0 = s\left(T_0, P_0\right)$ for the flowing matter.

The chemical exergy of a substance is the minimum work requirement to deliver it in the environmental state $\left(T_0, P_0\right)$ from the environmental substances by means of processes involving heat transfer and exchange of substances only with the environment. The standard chemical exergies of various substances are given in the literature, e.g. Kotas (1995). The molar chemical exergy of an ideal mixture is expressed as:

$$\tilde{\varepsilon}_{0M} = \sum_i x_i \tilde{\varepsilon}_{0i} + \tilde{R}T_0 \sum_i x_i \ln x_i \tag{2}$$

where x_i and $\tilde{\varepsilon}_i$ are molar fraction and chemical exergy, respectively, of each component in the mixture and $\tilde{R}$ is the universal gas constant.

The exergy loss of each individual unit can be calculated by finding the difference between the exergy of input and output streams of a unit operation. To find irreversible losses in each unit operation, a steady-state exergy balance can be used;

$$\sum_{in} \dot{m}\varepsilon + \sum_{r} \dot{Q}_r (1 - \frac{T_0}{T_r}) = \sum_{out} \dot{m}\varepsilon + \dot{W}_x + \dot{I} \qquad (3)$$

Here, $\dot{m}$ denotes mass flow rate, $\dot{Q}_r$ denotes heat transfer rate, $\dot{W}_x$ denotes shaft work and $\dot{I}$ denotes irreversibility rate. On the left-hand side, the first term in Eq. 3 denotes the flow of exergy into the system and the second term denotes the flow of exergy associated with the inflow or outflow of the heat transfer. The first right-hand side term denotes the flow of exergy out of the system.

Exergy analysis can be done when composition and thermodynamic properties of all streams are available. For this purpose, UniSim simulation software was used to simulate the power plant and CO_2 capture and compression processes.

To calculate the chemical exergy of each stream, the chemical exergy of MEA in liquid phase was required. The value used in these calculations was estimated by the group contribution method (Szargut et al., 1988) to $1.536 \cdot 10^6$ kJ/kmol. This method considers the contribution of simple chemical groups in chemical enthalpy and exergy and it can be used when the chemical constitution of the substance is known. MEA with molecular formula of C_2H_7NO has the group constituents $-\overset{|}{C}H_2$, $-OH$ and $-NH_2$ and its chemical exergy was calculated accordingly. Furthermore, the reference environment for exergy calculations was assumed at $T_0 = 298.15$ K , $P_0 = 101.325$ kPa and the reference composition as defined by Kotas (1995).

The aforementioned method of exergy analysis has been employed in Papers 1, 2, 3 and 5.

3.2.1 Exergy Losses associated to temperature change

Temperature variations in a CO_2 capture process are the results of heating and cooling. Cooling process is the release of energy by the system whereas the heating process demands reception of energy by the process. In both of these processes, the changes would affect the physical exergy of streams. The irreversibility would be formulated as the following;

$$\dot{I} = T_0 (\sum_{out} \dot{m}_e s_e - \sum_{in} \dot{m}_i s_{i-} \sum_{r} \frac{\dot{Q}_r}{T_r})$$

3.2.2 Exergy Losses with Phase Change; premixing concept

The approach described here is according to premixing concept in which the separation process is decomposed into three sub-processes: premixing in the vapour phase, premixing in the liquid phase and the main process, where phase changes occurs. The great advantage of the premixing model is the possible extension to processes with several stages such as stripping process. In this connection each plate is described by a premixing model, where the output of the former plate represents the input of the subsequent plate. It is assumed that the phase change takes place under conditions far from the

feed streams and actually equal to that of the product streams (Ishida, et al., 1990). The gas inlet stream is assumed to be mixed with large amount of the excess outlet gas stream with same composition, temperature, and pressure as those of the outlet gas stream coming from the main process. This condition between the two process parts can be kept by assuming an exchange of heat between the two process parts. A similar premixing process is assumed for the liquid inlet stream, resulting in constant process temperature and pressure for the main process. Consequently, the two premixing processes for the vapour and liquid stream, respectively and the main process, where only phase change takes place, can be examined independently. With the premixing concept, the evaporation of light components and condensation of heavy components with different bubble/due points happen simultaneously, but can be separated so that exergy losses of each contribution are obtained. The current chapter theoretically reviews the exergy losses attributed by subcomponents in the premixing concept by rigorous equations.

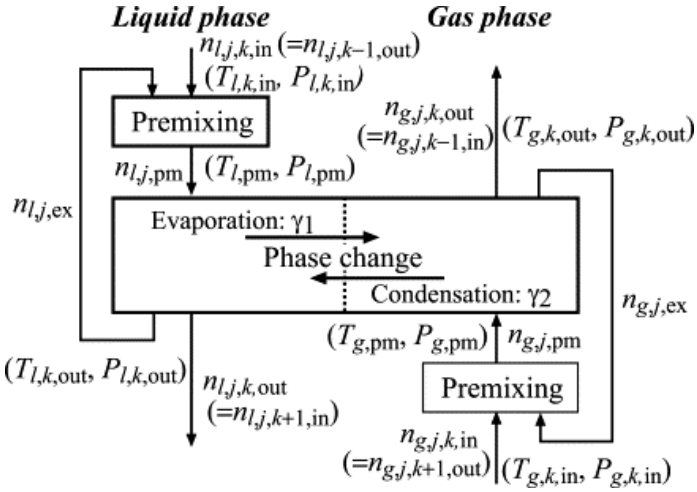

Figure 3-1: Premixing model for a plate (Budiman et al., 2004)

3.2.2.1 Mixing of the Liquid Phase

The following describes the approach to build the enthalpy and entropy balance around the Figure 3-1 for the premixing of the liquid phase (Taprap et al., 1992, Budiman et al., 2004);

Liquid coming in:

$$H_{L_{in}} = \sum_i n_{L_{in},i} \cdot h^o_{L_{in},i}$$

$$S_{L_{in}} = \sum_i n_{L_{in},i} \cdot (s^o_{L_{in},i} - R \cdot \ln x_{i,in})$$

Excess liquid stream fed back to the premixing process:

$$H_{L_{excess}} = \sum_i (n_{L_{excess},i} \cdot h^o_{L_{excess},i})$$

$$S_{L_{excess}} = \sum_i n_{L_{excess},i} \cdot (s^o_{L_{excess},i} - R \cdot \ln x_{i,excess})$$

Liquid stream out from the premixing process:

$$H_{L_{pm}} = \sum_i n_{L_{pm},i} \cdot h^o_{L_{pm},i}$$

$$S_{L_{pm}} = \sum_i n_{L_{pm},i} \cdot (s^o_{L_{pm},i} - R \cdot \ln x_{i,pm})$$

Enthalpy balance and entropy balance:

$$\Delta H_{L_{premixing}} = H_{L_{pm}} - (H_{L_{excess}} + H_{L_{in}})$$

$$\Delta S_{L_{premixing}} = S_{L_{pm}} - (S_{L_{excess}} + S_{L_{in}})$$

Changes in temperature and changes due to mixing of streams with varying parameters of temperature, pressure and composition, will contribute in exergy loss. Thus, individual expressions are defined to relate both of these contributions respectively;

$$\dot{I}_{L_{premixing}} = \dot{I}_T + \dot{I}_{mixing,x}$$

The first term of the above formula is the exergy loss due to changes in temperature and can be written as;

$$\dot{I}_{L,T} = Q \cdot \left[\left(1 - \frac{T_0}{T_{out}} \right) - \left(1 - \frac{T_0}{\left(\frac{T_{in} + T_{out}}{2} \right)} \right) \right]$$

The exergy loss caused by temperature changes in the premixing process for the liquid flow, is equivalent to the difference of Carnot efficiencies with regard to the inlet, outlet and ambient temperature. This efficiency indicates the fraction of maximum energy which can theoretically be converted to work.

$\dot{I}_{mixing,x}$ is the exergy loss caused by mixing in the liquid phase; (Kotas, 1995)

$$\dot{I}_{mixing,x} = RT_0 \sum_i n_{L_{in},i} \cdot \ln(\frac{x_{i,in}}{x_{i,out}})$$

3.2.2.2 Mixing of the Vapour Phase

The procedure applied to the premixing of the liquid phase can also be employed to the premixing of the vapour phase. Here $\dot{I}_{mixing,x}$ will be replaced by $\dot{I}_{mixing,p}$: (Taprap et al., 1992, Budiman et al., 2004)

$$\dot{I}_{mixing,p} = RT_0 \sum_i n_{G_{in},i} \cdot \ln(\frac{p_{i,in}}{p_{i,out}})$$

Where p_i is the partial pressure of the component. $\dot{I}_{mixing,p}$ can be decomposed to;

$$\dot{I}_{mixing,p} = \dot{I}_{mixing,P} + \dot{I}_{mixing,y}$$

$$\dot{I}_{mixing,P} = n_{G_{in}} RT_0 \sum_i \ln(\frac{P_{i,in}}{P_{i,out}})$$

$$\dot{I}_{mixing,y} = RT_0 \sum_i n_{G_{in},i} \ln(\frac{y_{i,in}}{y_{i,out}})$$

where $\dot{I}_{mixing,P}$ is the exergy loss due to decrease in the pressure.

3.2.2.3 Phase Change by Evaporation and Condensation

In general, exergy losses caused by phase changes may be taken as the deviation of the output state from the equilibrium and its analysis is carried out in the main process of the premixing concept, shown in Figure 3-1. Gas separation involving phase changes are classified into evaporation of the lighter components or condensation of the heavier components in a mixture with different freezing points. These processes take place at constant temperature and pressure.

Based on the changes of partial enthalpy and partial entropy during phase change of each component, the enthalpy balance for evaporation of one light component (i) is (Budiman et al., 2004);

$$\Delta H_{evaporation,i} = \gamma_{evaporation,i}(h^o_{G,i} - h^o_{L,i})$$

$$\Delta S_{evaporation,i} = \gamma_{evaporation,i}[(s^o_{i,G_{out}} - R\ln p_{i,out}) - (s^o_{i,L_{out}} - R\ln x_{i,out})]$$

To ensure a system going through phase change in premixing concept, the temperature is maintained constant which means (Budiman, et al., 2004):

$$\sum \Delta H = 0$$

To fulfil this, a heat source (for evaporation) or a heat sink (for condensation) is required, respectively. Then the exergy loss for the phase change by evaporation is given by (Budiman, et al., 2004);

$$\dot{I}_{evaporation,i} = -T_0(\Delta S_{evaporation,i} + \Delta S_T)$$

When equilibrium for the evaporation process holds, the Gibbs free energy is zero, yielding (Smith et al., 2005, Budiman, et al., 2004):

$$\Delta G_{evaporation,i} = \Delta H_{evaporation,i} - T\Delta S_{evaporation,i} = 0$$
$$(h^o_{G,i} - h^o_{L,i}) - T[(s^o_{i,G_{equilibrium}} - R\ln p_{i,equilibrium}) - (s^o_{i,L_{equilibrium}} - R\ln x_{i,equilibrium})] = 0$$

This relationship is then be used in order to obtain the final expression for the exergy loss by the evaporation process (Budiman, et al., 2004):

$$\dot{I}_{evaporation,i} = \gamma_{evaporation,i} RT_0 [\ln \frac{p_{i,equilibrium}}{x_{i,equilibrium}} - \ln \frac{p_{i,out}}{x_{i,out}}]$$

The evaporation process is accompanied by a decrease in the liquid phase and simultaneously an increase in the vapour phase. Therefore, the total pressure of the system will be higher after the process.

3.2.3 Exergy losses associated with Chemical Reactions

In systems involving chemical reactions, often large amounts of energy are converted. Therefore, information about concentration changes as well as exergy loss and gain contributions of each reaction provide key information for improving the system performance as a whole. A further criterion for improvement regarding chemical reactions is knowledge on the extent of deviation from chemical equilibrium.

In these systems, exergy losses can be attributed to contributions caused by a concentration difference and deviation from chemical equilibrium. That means, in the absence of driving forces, these specific terms are zero. Based on the general representation of a chemical reaction,

$$aA + bB \Leftrightarrow dD + eE$$

the equilibrium constant is defined as (Smith, J.M., et al., 2005):

$$K = \frac{[D]^d_{equilibrium}[E]^e_{equilibrium}}{[A]^a_{equilibrium}[B]^b_{equilibrium}}$$

[A], [B], [D] and [E] are concentrations of the chemical species in the system and the exponents, a, b, d and e, represent the stoichiometric coefficients for the reaction. In a similar manner the ratio of concentrations may be defined, which gives information about the extent of the chemical reaction and the distance from chemical equilibrium (Ishida et al., 2004);

$$K' = \frac{[D]^d[E]^e}{[A]^a[B]^b}$$

Again, these two values are equal when chemical equilibrium is reached. The enthalpy balance for the overall process involving chemical reactions can be simply expressed by the difference in partial molar enthalpies of the products and reactants. This quantity is dependent on the extent of reaction leading to the inclusion of a reaction extension variable (Ishida et al., 2004). Therefore, the enthalpy balance can be expressed as;

$$\Delta H_{reaction} = \gamma_{reaction}(dh^o_D + dh^o_E - (ah^o_a + bh^o_b))$$

with $\gamma_{reaction}$ as the extent of reaction. In combination with the stoichiometric coefficient, this parameter provides information on the moles of a specific component consumed in the chemical reaction under consideration.

The entropy change for the overall process including one chemical reaction is given by (Ishida et al., 2004):

$$\Delta S_{reaction} = \gamma_{reaction}(\Delta s^{o}_{i,reaction} - R\ln(K')) - \sum_{i} R \cdot N_{i,reaction_{in}} \cdot \ln(\frac{p_{i,out}}{p_{i,in}})$$

The exergy loss for a chemical reaction at constant temperature and pressure results in (Yamamoto et al., 2000a, 2000b, Yamamoto et al., 2002):

$$\dot{I} = -(\frac{T_0}{T})(\Delta H_{reaction} - T\Delta S_{reaction})$$

Similar to the main process in the premixing process the assumption of constant temperature and pressure is maintained by introducing a heat source and sink as required (Yamamoto et al., 2000a, 2000b, Yamamoto et al., 2002). Thus, the exergy loss for a chemical reaction is obtained by;

$$\dot{I} = -\sum_{i} n_{i,reaction_{in}} \cdot R \cdot T_0 \cdot \ln(\frac{p_{i,in}}{p_{i,out}}) + \gamma_{reaction} \cdot R \cdot T_0 \cdot \ln(\frac{K}{K'})$$

The exergy loss accompanied by a chemical reaction may be also interpreted using the Gibbs free energy relation. At chemical equilibrium the total Gibbs free energy reaches a minimum, and therefore, its differential at constant temperature and pressure is zero. Consequently, a deviation from chemical equilibrium can be equated with a work potential, which can theoretically be produced by the process. Consequently, the exergy loss by chemical reaction can also be expressed by (Ishida et al., 2004):

$$\dot{I}_{reaction} = -\Delta G_{reaction}$$

3.3 Minimum work requirement of separation processes

According to the second law of thermodynamics, the minimum work input required to accomplish a process equals the work input if that process undergoes reversibly; this is the net exergy change, in other words.

The work input for real irreversible processes is always higher than the work input of theoretical reversible processes. By definition a reversible process can be reversed without leaving a net effect on the surroundings. Therefore a work input during a reversible separation process must be equal to the work output during the reversible process of mixing given the fact that separation process is not a spontaneous process and it needs work to initiate. Therefore the work input to the separation process can be expressed as;

$$\dot{W}_{rev} = \Delta \dot{E}^{ch} = -RT_0 \sum_{i} \dot{n}_i \ln y_i = -\dot{n}_m RT_0 \sum_{i} y_i \ln y_i$$

The current formula is based on the approach chosen by Cengel et al. (2006); here $\dot{W}_{rev}$ is the $\dot{W}_{\min}$ (minimum work) required to completely separate a mixture of $\dot{n}_m$ kmole/s into its components. Thus

the minimum work requirement of an incomplete separation of mixtures into components (for example a case of 90% CO_2 capture with one pure stream of CO_2 and another stream with 10% CO_2 and the rest of the exhaust gas components) can be determined by calculating minimum work required for the separation process and minimum work output of mixing process of the rest of the components. Figure 3-2 shows the desired separated CO_2 stream C (n_C moles) separated from total n_A moles of inlet exhaust gas. The expression narrows down to;

$$\dot{W}_{rev}/\dot{n}_A = RT_0\left(\frac{\dot{n}_B}{\dot{n}_A}\sum_i y_{i,B}\ln y_{i,B} - \sum_i y_{i,A}\ln y_{i,A}\right) \quad (4)$$

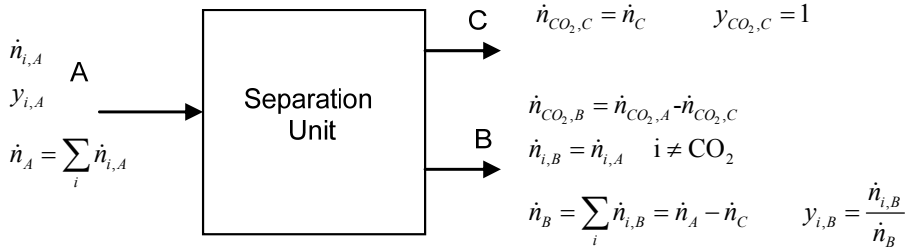

Figure 3-2: Schematic illustrating an ideal separation unit

The minimum work relations are independent of any hardware or process therefore these calculations are applicable for any kind of separation system including the subject of this thesis which is the separation of CO_2 from exhaust gases of a power plant.

For case of partial separation of CO_2 from other gas components it is worthy to introduce the capture ratio into the formulas.

$$\eta_{cap} = \dot{n}_{CO_2,C}/\dot{n}_{CO_2,A}$$

$$\rightarrow y_{CO_2,B} = \frac{y_{CO_2,A}(1-\eta_{cap})}{1 - y_{CO_2,A}.\eta_{cap}}$$

$$\& \; y_{i,B} = \frac{y_{i,A}}{1 - y_{CO_2,A}.\eta_{cap}} \qquad \text{i} \neq CO_2$$

These relations will reword Eq. 4 to a function based on exhaust gas molar flow rate, molar compositions and CO_2 capture rate. It would be beneficial to mention mostly the minimum work requirement is stated in the terms of MJ/kgCO_2. Figure 3-3 shows the graphs of minimum work requirement for CO_2 capture processes based on the incoming CO_2 molar composition in the exhaust gas.

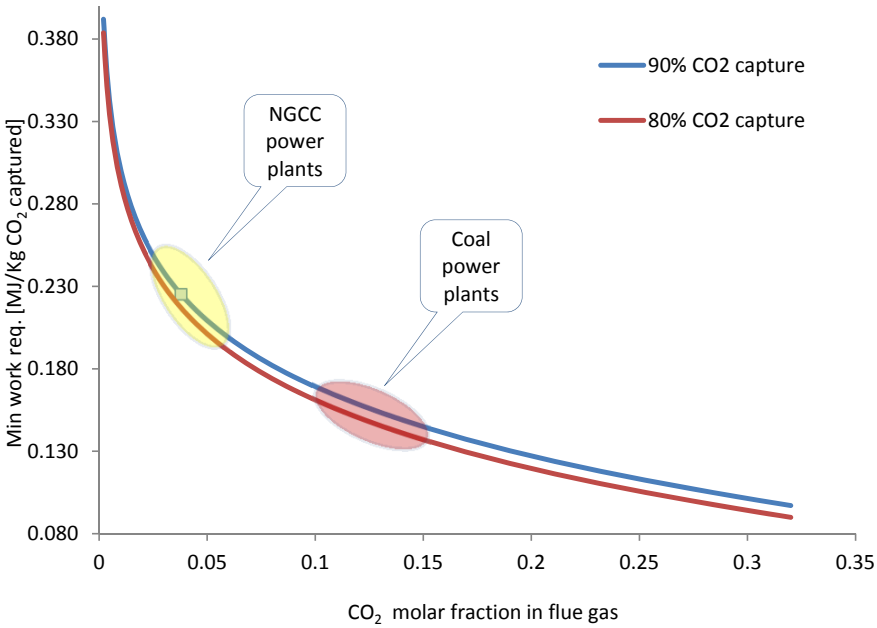

Figure 3-3: Minimum work required for separation of CO_2 from exhaust gases. Flue gas pressure is considered at 1 bara.

The graph shows, in case the CO_2 capture is performed thermodynamically perfect i.e reversible processes, the work required to separate 90% of CO_2 from the exhaust gases of a NGCC PP (with 3.8% CO_2 in exhaust) would be 0.225 MJ/kgCO_2.This would be approximately 34% less in case of 90% capture from the exhaust gases of a coal-fired PP (with ≈14% CO_2 in exhaust).

As stated before, all mixtures are assumed to be ideal. That means each gas component is unaffected by every other component in the mixture. However, for highly accurate calculations of actual gas separation applications, real gas behaviour may have to be taken into account, meaning that a separation process is accomplished by a change in its component properties. One way of including this real gas behaviour is to use more exact equations of state instead of applying the ideal gas law. This results in more complicated expressions for the minimum work requirement, where the deviation between ideal gas and real gas treatment at low temperatures and pressures often is negligible. Furthermore, the difference between the theoretical minimum work requirement and actual minimum work requirement, where additional exergy losses have to be taken into account, is larger than the gain by applying real gas behaviour instead of the ideal gas treatment. In fact, the minimum work requirement during an ideal reversible separation process is identical to the maximum work output during the ideal reverse mixing process. This is not valid for actual gas separation units. Therefore, it should be noted that the developed expressions for the minimum work requirement of gas separation units can be used for theoretical considerations and as a reasonable approximation.

3.4 Minimum work requirement of compression processes

As stated by Kotas (1995), the minimum work requirement of compression between two pressures corresponds to a frictionless isothermal process at environment temperature (T_0). Under conditions of full reversibility, internal and external, the work input equals to the ideal minimum work requirement. Therefore exergy balance is lead to;

$$\dot{W}_{rev} = \left[\dot{W}_C\right]_{\min} = E_2^{\Delta P} - E_1^{\Delta P} = RT_0 \ln(P_2 / P_1)$$

3.5 Total work requirement of CO_2 capture plant

The total work demand for a chemical absorption plant comprises of the electrical work demand of the pumps and blower to run the fluid through the process, the supply of shaft work to the compression plant and the work equivalent amount of reboiler heat supply. As mentioned in 2.1.5 and 2.1.6, the steam that is extracted from turbine with the purpose of MEA regeneration in the stripper could potentially produce work in the steam turbine. This power plant lost output work is less than the heat content of the steam because not all of the heat content of the steam could have been converted to power;

$$W_{eq} = P_{ppWO\text{-}extr} - P_{ppW\text{-}extr} = \alpha \cdot Q_{\text{Reboiler}}$$

The reboiler heat duty is comprised of a) the sensible heat supply to raise the temperature of the rich amine fed to the stripper to reboiler temperature, b) the heat of desorption equivalent to that of CO_2 absorption reaction to reverse the absorption reaction and c) heat of water vaporization to produce steam as the stripping media which maintains driving force for transfer of CO_2 from liquid phase to gas phase.

$$Q_{Reboiler} = Q_{sensible} + Q_{reaction} + Q_{vaporization}$$

$$Q_{Reboiler} = \frac{\dot{m}_{rich} \cdot C_{P,rich} \cdot (T_{rich} - T_{stripper})}{\dot{m}_{CO_2}} + \Delta H_{abs,CO_2} + \frac{\dot{m}_{wtr}}{\dot{m}_{CO_2}} . \Delta H_{vap,H_2O}$$

The base case of 90% CO_2 capture from NGCC combined cycle power plant that has been defined and analysed in detail in paper 1 and 4, is studied here to investigate the total work requirement. In order to determine the work requirement equivalent to regeneration heat supply, the steam extraction from power plant and the condensate from the reboiler have been determined at conditions defined in Section 2.1.4. At these conditions, the steam flow rate to be supplied to the reboiler is calculated by UniSim Design (Paper 1 and 4). The condition of steam and condensate as well as the mass flow rate of the steam is an input to GT PRO to evaluate the power plant output considering the steam extraction for solvent regeneration. The new power output i.e. $P_{ppW-extr}$ will be subtracted from $P_{ppWO-extr}$ and defines the work equivalent amount of reboiler heat supply. Figure 3-4 shows the reboiler heat duty and equivalent work based on the CO_2 content of the flue gas entering the chemical absorption plant. The design parameters of the process are elaborated in papers 1 and 4.

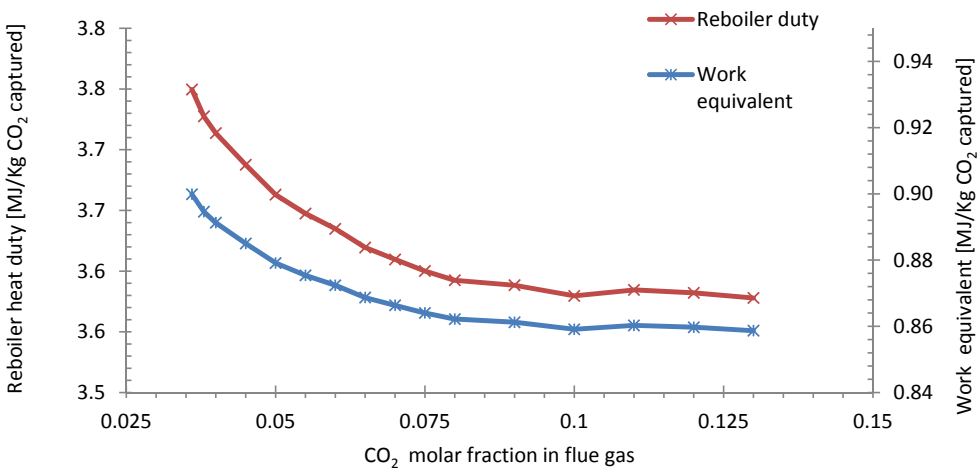

Figure 3-4: Primary vertical axis (left) indicates the reboiler duty for MEA regeneration. The secondary axis (right) shows the power plant output power loss due to heat supply to reboiler. Flue gas pressure is considered at 1 bara.

As Figure 3-4 shows, for higher CO_2 concentrations in the flue gas, the reboiler heat requirement per kilogram of CO_2 captured is less. As a matter of fact, the reboiler duty [kJ/hr] will be increased clearly since the solvent circulation rate increases to reach the same CO_2 capture percentage for each of the flue gas CO_2 fraction points. However, higher CO_2 content in the flue gas results in a higher driving force at the bottom of the absorber column, where the amine solution is the most loaded therefore the rich loading of MEA will increase for higher CO_2 concentrations in the flue gas (Kothandaraman, 2010). A higher rich loading leads to lower heat of vaporization $Q_{vaporization}$ since the equilibrium partial pressure of CO_2 increases with loading. On the other hand due to higher rate of MEA recirculation, the sensible heat $Q_{sensible}$ will increase substantially which dominates the reboiler duty [kJ/hr] for higher CO_2 concentrations in the flue gas.

Lean loading will be fairly constant due to the fixed CO_2 concentration in the lean amine. The results of the loadings and MEA circulation rate is presented in Figure 3-5 . It should be noted that for this analysis the CO_2 percentage in the inlet flue gas has been changed and the other parameters are fixed as referred to in Table 2 of paper 4.

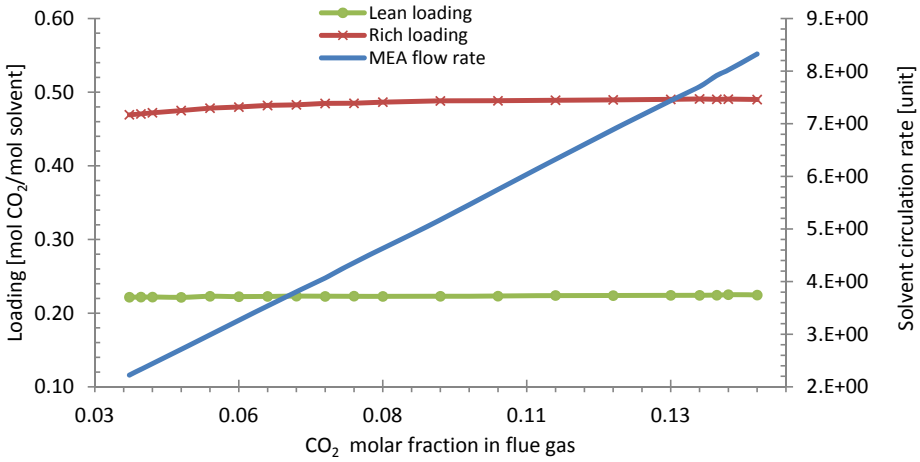

Figure 3-5: Primary vertical axis (left) indicates the loading of CO_2 in the solvent. The secondary axis (right) shows MEA circulation rate.

Due to the increase in the solvent circulation rate, total pump work demand will increase correspondingly. However, the work demand for blower and pumps per CO_2 separated will follow the same descending trend as the reboiler heat per separated CO_2. This is shown in Figure 3-6;

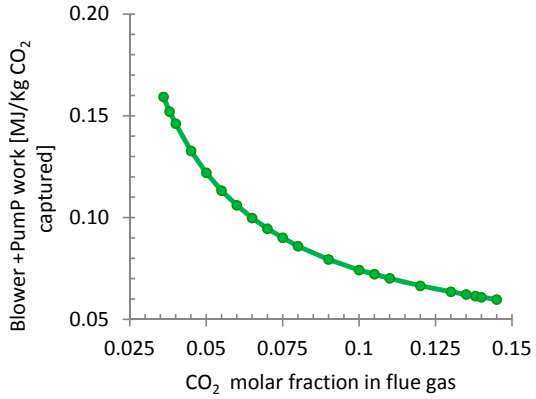

Figure 3-6: The blower and pump work demand correspondent to the system analysed in detail in paper 1 and 4

3.6 Thermodynamic efficiency (Exergy efficiency)

As discussed before, the actual work or "actual shaft work" is always higher than the theoretical reversible work. For CO_2 capture and compression plant, the actual total work demand will include the electrical power related to regeneration of solvent, pump and blower power requirements (the compressor in LVR configurations), and the CO_2 compression work demand.

Once the actual work demand is calculated, the thermodynamic efficiency can be calculated as the ratio of minimum, reversible work required to actual work required in the process;

$$\psi_{CC} = \frac{\dot{W}_{rev}}{\dot{W}_{act}}.$$

This efficiency is an identification of the ratio between the work requirement of the theoretical reversible process and the real irreversible process.

As presented in Figure 3-4, the trend of the changes of actual work demand along the x-axis is similar to what is observed in Figure 3-3 for minimum work requirement of separation of CO_2. However there is a gap between these two due to irreversible nature of actual process. The following graph (Figure 3-7) illustrates the thermodynamic efficiency of the Base case CO_2 capture plant (Paper 1 and 4).

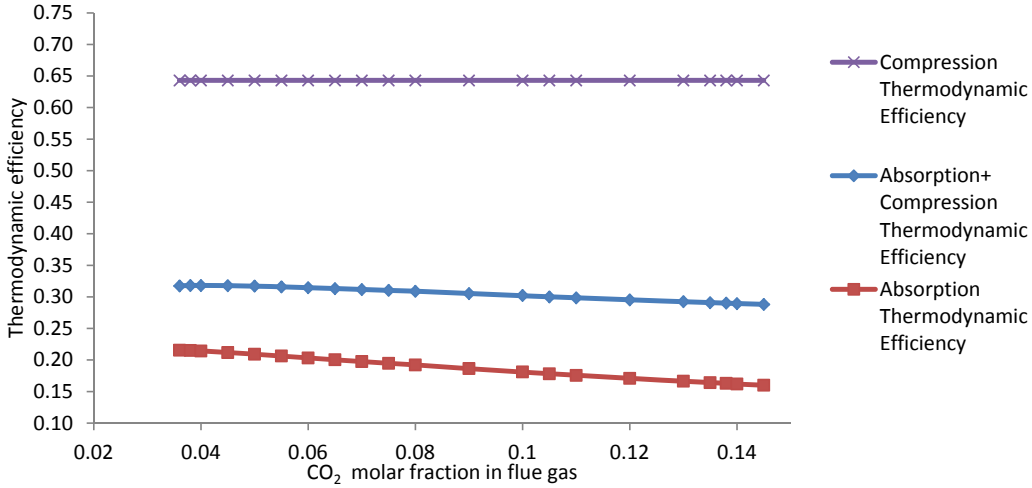

Figure 3-7: Thermodynamic efficiency of the CO_2 capture plant as a total and as breakdowns.

3.7 Rational efficiency

Another important value resulting from exergy analysis is rational efficiency, which is defined in various formulations for different processes. In a general formulation, named as the rational efficiency, it is expressed as the ratio of the useful exergy output to the total used exergy (Kotas, 1995). The exergy inputs and outputs are in different forms such as work, exergy associated with heat transfer, exergy transfer associated with the flow of matter into and out of the control region or change of exergy of a stream of matter passing through a control region such as heat exchangers.

$$\psi = \frac{\sum \Delta \dot{E}_{out}}{\sum \Delta \dot{E}_{in}}$$

The rational efficiency differentiates between the desired output exergy and any other kind of outflow from the system. This makes it a proper value to present the degree of thermodynamic perfection of a process. In the current thesis work, two desired exergy outputs from the system are identified; the net power output and the exergy of separated and compressed CO_2. On the other hand, any stream which is transferring physical and chemical exergy to the system, counts as exergy input stream. This is consisted of the fuel exergy, water and solvent make up exergy and the cooling water exergy in various parts of the process. The topic is elaborated in Paper 5.

References:

Austgen, D.M., Rochelle, G.T., Peng, X., Chen, C., 1989. Model of Vapor-Liquid Equilibria for Aqueous Acid Gas-Alkanolamine Systems Using the Electrolyte-NRTL Equation, *Industrial & Engineering Chemistry Research*, 28, 1060-1073.

Austgen, D. M., Rochelle, G. T.,Chen, C. C.,1991. Model of vapor-liquid equilibria for aqueous acid gas-alkanolamine systems. 2. Representation of hydrogen sulfide and carbon dioxide solubility in aqueous MDEA and carbon dioxide solubility in aqueous mixtures of MDEA with MEA or DEA. *Industrial & Engineering Chemistry Research,* 30**,** 543-555.

Budiman, A., Ishida, M., 2004. A new method for disclosing internal phenomena in a distillation column by use of material-utilization diagram; *Energy,* 29, 12-15, 2213-2223.

Cengel, Y. A. and Boles, MA. , 2006, Thermodynamics: An Engineering Approach, 6th edition, McGraw-Hill.

Chen, C.-C.,Evans, L.B. ,1982. Local Composition Model for Excess Gibbs Energy of Electrolyte Systems, *AIChE Journal,* 284, 588-596.

Chen, C.-C.,Evans, L. B.,1986. A local composition model for the excess Gibbs energy of aqueous electrolyte systems. *AIChE Journal,* 32**,** 444-454.

Deshmukh R., Mather A., 1981. A Mathematical Model for Equilibrium Solubility of Hydrogen Sulfide and Carbon Dioxide in Aqueous Alkanolamine Solutions. *Chemical Engineering Science,* 36, 355-362.

Gabrielsen J., Michelsen M., Stenby E., Kontogeorgis G., 2005. A Model for Estimating CO_2 Solubility in Aqueous Alkanolamines. *Industrial & Engineering Chemistry Research*, 44, 3348-3354.

GT PRO version 19, 2009, Thermoflow Inc

Hoff, K.A., 2003. Modeling and experimental study of carbon dioxide absorption in a membrane contactor, PhD Thesis, NTNU, Trondheim, Norway.

Ishida, M., Okuno, K., 2004. Systematic analysis of biochemical processes in cells by applying graphical diagrams; *Energy*, 29, 2461-2472.

Ishida, M., Taprap, R., 1996. Application of energy-utilization diagram for graphic exergy analysis of multicomponent distillation columns, *Journal of Chemical Engineering of Japan*, 25, 4, 396-402.

Jou, F., Mather, A.E., Otto, F.D., 1995. The Solubility of CO_2 in a 30 Mass Percent Monoethanolamine Solution, *The Canadian Journal of Chemical Engineering,* 73, 1, 140-147.

Karimi, M., 2011 CO_2 capture and power production integration; optimization and conceptual design studies, PhD thesis, Norwegian University of Science and Technology.

Kent, R. L. , Eisenberg, B., 1976. Better Data for Amine Treating. Hydrocarbon Processing, 55, 87-90

Kenig, E. Y. , Gorak, A. 2003. Rigorous Modeling of Reactive Absorption Processes. *Chemical Engineering & Technology*, 26, 631-646.

Kenig, E. Y. , Seferlis, P., 2009. Modeling Reactive Absorption. *Chemical Engineering Progress*, 105, 65-73.

Kothandaraman, A., 2010. carbon Dioxide Capture By Chemical Absorption: A Solvent Comparison Study. PhD Thesis, Massachusetts Institute Of Technology, USA

Léonard, G., 2013. Optimal design of a CO_2 capture unit with assessment of solvent degradation. PhD thesis. Universite de Liege, Belgium.

Li, M.H., Shen, K.P., 1993. Calculation of equilibrium solubility of carbon dioxide in aqueous mixtures of monoethanolamine with methyldiethanolamine, *Fluid Phase Equilib*. 85, 129-140.

Li, Y., Mather, A.E., 1994. Correlation and Prediction of the Solubility of Carbon Dioxide in a Mixed Alkanol Solution, *Industrial & Engineering Chemistry Research.,* 33, 2006-2015.

Peng, D. , Robinson, D. B. ,1976. New 2-Constant Equation of State. *Industrial & Engineering Chemistry Fundamentals*, 15, 59-64.

Posey, M. L. 1996. Thermodynamic Model for Acid Gas Loaded Aqueous Alkanolamine Solutions, Ph.D. Thesis, University of Texas at Austin, USA.

Smith, J.M., van Ness, H. C., Abbott, M. M., 2005. Introduction to chemical engineering thermodynamics, Boston: McGraw-Hill

Razi, N., 2013. Rate-based modeling of co_2 absorption in amine solutions, evaluation of mass transfer, kinetics and scale-up, PhD thesis, Norwegian University of Science and Technology.

Szargut J, Morris DR, Steward FR., 1988. Exergy analysis of thermal, chemical and metallurgical processes, New York: Hemisphere Publishing Corp.

Taprap, R., Ishida, M., 1996. Graphic exergy analysis of processes in distillation column by energy-utilization diagrams, *AIChE Journal*, 42, 6, 1633-1641.

Taylor, R., Krishna, R., 1993. Multicomponent Mass Transfer. John Wiley, New York

Taylor, R., Krishna, R., Kooijman, H., 2003. Real-World Modeling Of Distillation. *Chemical Engineering Progress*, 99, 28-39.

UniSim design user guide; Honeywell; 2008 R380 Release

Yamamoto, M., Ishida, M., 2000a. Analysis of behavior of individual components in extraction on material-utilization diagram, *Journal of Chemical Engineering of Japan,* 33, 3, 386-392.

Yamamoto, M., Ishida, M., 2000b. Application of material-utilization diagram to chemical reactions, *Journal of Chemical Engineering of Japan*, 33, 4, 638-644.

Yamamoto, M., Ishida, M., 2002. New graphical method for representing characteristic features of extraction, *Industrial & Engineering Chemistry Research,* 41, 277-284.

Øi L., 2012. Removal of CO_2 from exhaust gas. PhD thesis, Telemark University College, Norway.

4 Conclusions and further work

The results of this thesis work are presented in research papers (Appendix A). Particularly, the following breakdown refers to where the results could be found;

- Post-combustion CO_2 capture plant for NGCC: Various chemical absorption process configurations have been assessed and optimized to achieve lowest reboiler duty. Heat and work demand calculations and power plant efficiency results are presented in Papers 1, 2 and 4. The proposed process configurations were analysed and compared using exergy method. These findings, assisted in understating and insight to the irreversibilities in the chemical absorption process. Results and discussions presented in Papers 1, 2 and 5.
- Pre-combustion CO_2 capture plant for NGCC: Combination of power plant and exergy analysis have been used to investigate a pre-combustion reforming combined cycle (IRCC) process with chemical absorption CO_2 capture plant. The results are presented in Paper 3.

4.1 Conclusions and main contributions

In summary, this research work involves comparing various CO_2 capture chemical absorption process configurations. The following points summarize the main contributions of this thesis:

- **Quantification of minimum work requirement for CO_2 capture and compression processes**

As the first step, the work input during a theoretical reversible CO_2 capture process has been defined as the minimum work input required. Furthermore, the minimum work of compression of pure CO_2 has been defined. These set the basis values for measuring the distance of the actual work requirement for the real CO_2 capture plants and the theoretical ones. For the current thesis work, this minimum work required to separate 90% of CO_2 from the exhaust gases of a NGCC power plant (with 3.8% CO_2 in exhaust) would be 0.225 MJ/kgCO_2. The minimum reversible work of compression of pure CO_2 stream from 1.1 bar to 110 bar was calculated to 0.213 MJ/kg CO_2.

- **Review of various chemical absorption process configurations**

Several process configuration improvements have been chosen for a base case chemical absorption process for removal of acid gases; then elaborated in detail for the adaptation as a CO_2 capture plant for separation of CO_2 from exhaust gases of the power plant. Six chemical absorption process configurations for CO_2 capture were analysed, including base case chemical absorption with and without absorber inter-cooling, chemical absorption with split flow configuration and chemical absorption process with lean vapour recompression (LVR). These configurations have been all combined with absorber inter-cooling. Various process parameters for the chemical absorption process were chosen and optimized to fulfil the aim of lowering the reboiler duty and reduction of total work demand. The findings are as listed below:

- The inter-cooling of absorber column in the chemical absorption process, leads to increased solvent rich loading. Consequently, the solvent circulation rate and reboiler energy requirement is decreased.

- In split-flow configuration, due to splitting of the rich amine into two streams, the amount of rich amine which enters the bottom section of the stripper is reduced. Consequently, less reboiler energy is required to remove CO_2 from solvent to reach the same CO_2 lean loading as of conventional chemical absorption process.
- In configuration of chemical absorption with lean vapour recompression (LVR), low temperature heat source of the lean amine is utilized to add exergy input in the form of steam to the stripper column and thus reduce the reboiler duty.

- **Comprehensive breakdown of energy lost for various CO_2 absorption processes**

Various process configurations have been evaluated to optimize the overall efficiency of the NGCC power plant integrated with a post-combustion CO_2 capture and compression plant. The best optimized process with the lowest work demand was the configuration with absorber inter-cooling with stripper lean vapour recompression. Comparing this case (LVR + absorber inter-cooling) with the Base case, the power plant efficiency penalty decreased from 7%-points for the Base case to 6.2%-points. Table 4-1 summarises the power efficiency results for the studied cases.

Table 4-1 Summary of results for the NGCC with and without post-combustion CO_2 capture (natural gas LHV input (MW_{th}) = 681.421).

	Reference power plant without CO_2 capture	Ref. plant + Base Case	Ref. plant + Absorber inter-cooling	Ref. plant + Split flow	Ref. plant + Split-flow with absorber inter-cooling	Ref. plant + LVR	Ref. plant + LVR with absorber inter-cooling
Net power plant efficiency [% LHV]	56.40	49.35	49.53	49.67	49.96	50.06	50.16

- **Relating methods of first law and second law analysis, which is obtained by moving from first law to second law analysis**

Following the first law analysis, which identified the total work demand for each of the CO_2 capture chemical absorption configurations, exergy analysis was used to study and understand those results. Exergy analysis assisted to examine the irreversibilities in various parts of the process and understand how these attributed exergy losses led to differences in work demand for different process configurations. Furthermore, the exergy efficiency of the plant has been calculated to characterise the difference of the work input of theoretical reversible processes and the real irreversible processes.

Table 4-2 Exergy efficiency for different cases of CO_2 capture and compression plant.

	Base Case	Absorber inter-cooling	Split flow	Split-flow with absorber inter-cooling	LVR	LVR with absorber inter-cooling
Exergy efficiency of CO_2 capture process [%]	21.3	21.9	22.6	23.6	24.5	25.0
Exergy efficiency of compression process[%]	64.3	64.3	64.3	64.3	64.3	64.3
Exergy efficiency of CO_2 capture and compression plant[%]	31.6	32.3	33.0	34.1	35.1	35.6

Comparing the cases analysed in this work, the total work demand for the CO_2 capture and compression plant was decreased from 1.39 MJ/kg CO_2 for Base case to 1.23 MJ/kg CO_2 for the case of absorber inter-cooling with stripper lean vapour recompression. Considering the minimum work requirement of separation processes, the exergy efficiency of the capture and compression plants was increased from 31.6% for the Base case to 35.6% for the case of absorber inter-cooling with stripper lean vapour recompression. The breakdown of the results for various cases is presented in Table 4-2. The second law analysis confirmed the decreasing trend of irreversibility rates from 1.60 MJ/kg CO_2 for the Base case to 1.29 MJ/kg CO_2 for the case of LVR plus absorber inter-cooling. The breakdown of the irreversibility rates is presented in Table 4-3.

Table 4-3 Irreversibility [MJ/kg CO_2 separated] by unit sections for the CO_2 capture and compression plant.

	Base Case	Absorber inter-cooling	Split flow	Split-flow with absorber inter-cooling	LVR	LVR with absorber inter-cooling
Flue gas cooler [MJ/kg CO_2]	0.10	0.10	0.10	0.10	0.10	0.10
Blower [MJ/kg CO_2]	0.03	0.03	0.03	0.03	0.03	0.03
Absorption section [MJ/kg CO_2]	0.71	0.74	0.88	0.99	0.71	0.72
Rich/lean HE(s) [MJ/kg CO_2]	0.02	0.02	0.02	0.01	0.11	0.11
Stripper [MJ/kg CO_2]	0.60	0.54	0.38	0.24	0.26	0.19
Compression section [MJ/kg CO_2]	0.14	0.14	0.14	0.14	0.14	0.14
Total [MJ/kg CO_2]	1.60	1.57	1.54	1.51	1.35	1.29

- **Second law analysis for interpretation of irreversibilities in process configurations**

Through exergy balance for every CO_2 capture process configuration, the exchange of exergy content of material and energy streams was assessed and the following conclusions were made;

a) The inter-cooling process modification would increase the absorber irreversibilities but decreased the stripper irreversibilities. The absorber inter-cooling modification was combined with other modifications (split-flow and LVR) as an efficient method to decrease irreversibilities and the total work demand.
b) The split-flow process modification led to a significant increase of absorber irreversibilities and a major decrease in the stripper irreversibilities. Introducing cold semi-lean side-stream to the absorber caused a significant increase in the absorber irreversibility. However, the total irreversibility was reduced comparing the cases with split-flow to the Base case and inter-cooling case.
c) The LVR process modification decreased the irreversibility associated to the stripper substantially and did not increase the absorber irreversibility. The water vapour heat of condensation was made available in the stripper by compression of the steam to a sufficient pressure and temperature level.

Rational efficiency was used to present the degree of thermodynamic perfection by differentiating between the desired output exergy (exergy of pure compressed CO_2 stream and power plant net power

output) and any other kind of exergy outflow from the system. The results showed an increase in rational efficiency from 48.5% for the power plant integrated with the Base case chemical absorption process configuration to 49.5% for the modified chemical absorption process configuration of lean vapour recompression with absorber inter-cooling.

The latter capture process was the best process with the lowest power demand, lowest irreversibility and the highest exergy efficiency.

With performing exergy analysis on an IRCC pre-combustion CO_2 capture system, a rational efficiency of 43.8% has been achieved which indicates the percentage of input exergy utilised for work production by the power cycle in addition to the exergy of the pure compressed CO_2 stream. The highest amount of irreversibility is contributed by the GT and mainly by the combustor. The irreversibility which is inherent in the combustion process corresponds to a large fraction of original exergy of the fuel. A suggestion of improvement to decrease the combustor irreversibility is to increase the preheating of fuel supply to the combustor. With pre-heating the fuel up to 500 °C the GT irreversibility was decreased by 11 %. The ATR was observed as the second largest contributor to the cycle irreversibilities.

4.2 Future work

In the present study, exergy analysis was used to understand the effects of process configuration modifications leading to improved performance. However, several other modifications -as listed below- are triggered by the findings to further improve and optimize the current configurations.

a) As the inter-cooling individually and combination of inter-cooling with split-flow modification pointed out, the increased rich loading was in favour of CO_2 separation process by increasing the absorber driving forces. Thus increased rich loading led to higher absorber exergy losses, lower reboiler work demand, lower stripper exergy losses and higher CO_2 capture exergy efficiency. This, points towards process configuration modifications with several steps of inter-cooling along the lower stages of the absorber.
b) By adding several rich-stream splits to the stripper, the stripper exergy losses are expected to decrease since the temperature driving force will be distributed more gradually along the stripper. This is another process configuration for further analysis.
c) The combination of LVR and the split-flow configuration could be another interesting modification to be examined. The stage temperatures will be decreased at the top part of the stripper and gradually decreased along the stripper. Thus, the condensation exergy losses are reduced and more reduction in stripper exergy losses is expected.
d) Similar approach of combining first and second law analysis is suggested as future continuation of the current work for other process modifications such as high pressure and multi-pressure stripper configuration. The step-wise alteration of pressure as the driving force through stripper would be advantageous in terms of lowering the total exergy losses and work demand.

In the current thesis work, the process modifications have been assessed and compared according to lowest power demand and exergy losses. Yet, these modified process configurations would pay for energy savings with their higher investment costs. This will pinpoint the further work as a combination of overall economic and technical analysis (such as exergoeconomic analysis) for the power plant with capture and compression to avoid costly and non-operable designs.

Appendix

Paper 1

International Journal of Greenhouse Gas Control 5 (2011) 422–426

Contents lists available at ScienceDirect

International Journal of Greenhouse Gas Control

journal homepage: www.elsevier.com/locate/ijggc

Thermodynamic analysis on post-combustion CO_2 capture of natural-gas-fired power plant

Zeinab Amrollahi*, Ivar S. Ertesvåg, Olav Bolland

Department of Energy and Process Engineering, Norwegian University of Science and Technology, NO-7491 Trondheim, Norway

ARTICLE INFO

Article history:
Received 25 October 2009
Received in revised form
15 September 2010
Accepted 18 September 2010
Available online 22 October 2010

Keywords:
CO_2 capture
Chemical absorption
Exergy analysis

ABSTRACT

A chemical absorption, post-combustion CO_2 capture unit is simulated and an exergy analysis has been conducted, including irreversibility calculations for all process units. By pinpointing major irreversibilities, new proposals for efficient energy integrated chemical absorption process are suggested. Further, a natural-gas combined-cycle power plant with a CO_2 capture unit has been analyzed on an exergetic basis. By defining exergy balances and black-box models for plant units, investigation has been made to determine effect of each unit on the overall exergy efficiency. Simulation of the chemical absorption plant was done using UniSim Design software with Amines Property Package. For natural-gas combined-cycle design, GT PRO software (Thermoflow, Inc.) has been used. For exergy calculations, spreadsheets are created with Microsoft Excel by importing data from UniSim and GT PRO. Results show the exergy efficiency of 21.2% for the chemical absorption CO_2 capture unit and 67% for the CO_2 compression unit. The total exergy efficiency of CO_2 capture and compression unit is 31.6%.

1. Introduction

CO_2 capture from power plants is based on the separation of carbon either from the fuel or from the exhaust. The first process is called pre-combustion CO_2 capture while separation of carbon from exhaust gases is divided into two groups; if pure oxygen is the oxidant, it is called as Oxyfuel CO_2 capture combustion method and the post-combustion method, when ambient air is used as an oxidant.

There are several processes to recover CO_2, such as chemical absorption, adsorption, cryogenic separation and membranes. For post-combustion CO_2 capture from a natural-gas-fired power plant, chemical absorption using amine solutions is the most near-term technology according to the IEA report (IEA, 2008).

Techno-economic and thermodynamic analyses that evaluate natural-gas-fired combined-cycle (NGCC) power plant with CO_2 absorption unit have been done recently (Peeters et al., 2007; Hammond and Ondo Akwe, 2007). Abu-Zahra et al. (2007a,b) investigated the technical performance and economics of CO_2 capture with monoethanolamine (MEA) for a coal-fired power plant. In other studies done by Geuzebroek et al. (2004) and Yu et al. (2009), exergy analysis results of MEA based CO_2 capture processes have been presented.

The energy required by the capture process is provided by the power plant in the form of steam and electricity. So it is notable that CO_2 capture system causes a significant efficiency penalty on the power plant. The net electrical efficiency of NGCC based on state of the art gas turbines, ranges from 55% to 58% LHV-based. However, addition of a chemical absorption plant for CO_2 capture from exhaust gases leads to power production efficiency penalties of 8–10% points (Peeters et al., 2007; Göttlicher, 2004). Bolland and Undrum (2003) compared NGCC power plants with and without CO_2 capture and quantified the reduced efficiency related to CO_2 capture process.

Fig. 1 shows the flow sheet of the CO_2 capture process and the CO_2 compression unit. Flue gas containing CO_2 is flowing through an absorber while contacting with MEA solvent flowing counter-currently. The reaction between MEA solvent and the CO_2 is forming a water soluble salt. A CO_2-rich MEA stream is preheated in a heat exchanger and enters a stripper column to regenerate the solvent and reverse the reaction by means of heat supplied in a reboiler and release the CO_2 content as a stream leaving at the top of the column. The lean MEA-stream is recycled back to the absorption column while the CO_2 stream goes to the compression section.

Although it is a well-established separation method, the energy consumption and the associated costs of CO_2 capture are substantial and lead to consumption of more fossil fuel for a given power generation. This is a strong motivation to optimize the process and increase its energy efficiency. In the present work, exergy analysis was used as a tool for identification of exergy losses and irreversibilities. By comparing the magnitudes of irreversibility rates for different plant units, it was shown which of the process units that contributes the most to plant inefficiency.

* Corresponding author. Tel.: +47 73592768.
E-mail address: zeinab.amrollahi@ntnu.no (Z. Amrollahi).

1750-5836/$ – see front matter © 2010 Elsevier Ltd. All rights reserved.
doi:10.1016/j.ijggc.2010.09.004

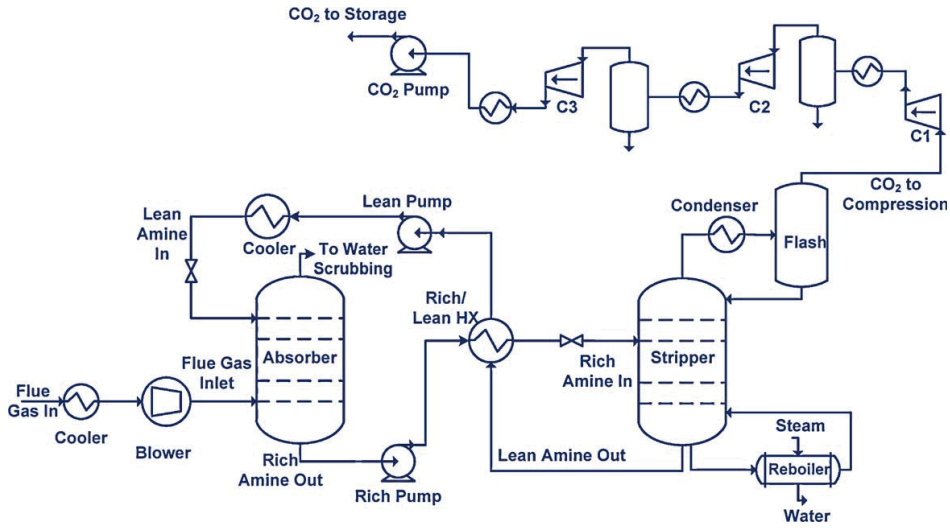

Fig. 1. Flow sheet of CO_2 capture and compression units.

2. Exergy analysis

The exergy method of evaluating energy-intensive systems integrates the first and second laws of thermodynamics at the state of particular environmental conditions. Exergy analysis with its certain methods of process evaluation has proven to be an efficient tool to define the second law efficiency of processes. It combines the principles of conservation of mass and energy together with the second law of thermodynamics to characterize the thermodynamic losses of each unit of a system, and it enables to identify losses and, consequently, to make improvements of energy consumption. This is an advantageous method to approach the goal of more efficient processes, since it specifies the locations, types, and real magnitudes of irreversibilities either to be reduced or to be dissipated.

The exergy of a stream can be divided into physical exergy and chemical exergy, assuming that potential and kinetic energy can be neglected. The physical exergy equals to maximum amount of work obtainable when the stream of substance is brought from its actual state to the environmental state defined by P_0 and T_0 (Szargut et al., 1988) by physical processes involving only thermal and mechanical interaction with the environment. It is expressed as:

$$\varepsilon_{\mathrm{ph}} = (h - h_0) - T_0(s - s_0) \tag{1}$$

where h and s are the specific enthalpy and entropy and $h_0 = h(T_0, P_0)$ and $s_0 = s(T_0, P_0)$ for the flowing matter.

The chemical exergy of a substance is the minimum work requirement to deliver it in the environmental state from the environmental substances by means of processes involving heat transfer and exchange of substances only with the environment. The standard chemical exergy of various substances is given in the literature, e.g. in Kotas (1995).

The molar chemical exergy of an ideal mixture is expressed as:

$$\tilde{\varepsilon}_{0M} = \sum_i x_i \tilde{\varepsilon}_{0i} + \tilde{R}T_0 \sum_i x_i \ln x_i \tag{2}$$

where x_i and $\tilde{\varepsilon}_i$ are molar fraction and chemical exergy, respectively, of each component in the mixture and R is the universal gas constant.

The exergy loss of each individual unit can be calculated by finding the difference between the exergy of input and output streams of a unit operation. To find irreversible losses in each unit operation, a steady state exergy balance can be used;

$$\underbrace{\sum_{\text{in}} \dot{m}_j \varepsilon_j}_{\text{Flow exergy into system}} + \underbrace{\sum_{l} \dot{Q}_l \left(1 - \frac{T_0}{T_l}\right)}_{\text{Exergy associated to heat exchange}} = \underbrace{\sum_{\text{out}} \dot{m}_k \varepsilon_k}_{\text{Flow exergy out of system}} + \underbrace{\dot{W}}_{\text{Work}} + \underbrace{\dot{I}}_{\text{Irreversibility}} \tag{3}$$

Here $\dot{m}$ denotes mass flow rate, $\dot{Q}_l$ denotes heat transfer rate, $\dot{W}$ denotes work rate and $\dot{I}$ denotes irreversibility rate.

Another important value resulted from exergy analysis is exergetic efficiency which is identified in various formulations for different processes. In one general definition, it is defined as the ratio of minimum, theoretical-reversible work required to actual work required in a process; i.e. $\eta_{\mathrm{ex}} = W_{\mathrm{rev}}/W_{\mathrm{act}}$. In other definition, named as rational efficiency, it is expressed as the ratio of the exergy output to the total used exergy (Kotas, 1995); i.e. $\psi = \sum \Delta\dot{E}^{\mathrm{out}} / \sum \Delta\dot{E}^{\mathrm{in}}$. The rational efficiency differentiates between the desired output exergy and any other kind of outflow from the system. This makes it a suitable value to present the degree of thermodynamic perfection of a process. For the current power cycle exergy analysis, rational efficiency is expressed as the ratio between of the exergy of product and the exergy of the fuel, i.e. $\psi = \dot{E}_{\mathrm{P}}/\dot{E}_{\mathrm{F}}$ or $\psi = 1 - (\dot{I}/\dot{E}_{\mathrm{F}})$ (Bejan et al., 1996).

Exergy analysis can be done when composition and thermodynamic properties of all streams are available. For this purpose, modeling software was used to simulate the power plant and CO_2 capture and compression processes.

To calculate the chemical exergy of each stream containing MEA component, chemical exergy of the MEA molecule in the liquid phase was required. The value used in these calculations was not found directly from literature but estimated by the group contribution method (Szargut et al., 1988) to 1.536×10^6 kJ/kmol.

3. Methodology

The plant subsystems that were analyzed included of gas turbine (GT), heat recovery steam generator (HRSG), steam turbine (ST), condenser, CO_2 absorption section, stripping section and compression section.

Particularly, the CO_2 capture plant was divided into control regions with exergy inputs and outputs associated with the inflow and outflow of matter, heat transfer and work transfer. The processes were approximated in steady state condition. Relevant thermodynamic data for the CO_2 capture plant was taken from UniSim Design software (Honeywell), which contains the Amines Property Package. This special property package has been designed to aid the modeling of alkanolamine treating units in which CO_2 is removed from gaseous streams. For simulation of other gaseous streams in the process, the Peng–Robinson equation of state was used.

Chemical and physical exergy of all streams were functioned in excel spreadsheets. Therefore, the amounts of exergy loss and irreversibility were calculated based on exergy balance in each control region.

Furthermore, the power plant design was done by GT PRO (Thermoflow, Inc.). The reference environment was assumed with ambient temperature $T_0 = 298.15$ K and pressure $P_0 = 101.325$ kPa.

4. Model description

The natural-gas-fired combined-cycle power plant was designed with power plant configuration of GT, HRSG and condensing reheat ST. The gas turbine was selected from GT PRO library as Siemens SGT5-4000F and the fuel selection to the combustor is natural gas without H_2S with 46.28 MJ/kg as lower heating value (at 25 °C). This equals to 681.4 MW as the fuel heat input to the GT. The flue gas flowing through the HRSG exits as exhaust gas with a flow rate of 651 kg/s and a molar composition of 3.8% CO_2, 12.4% O_2, 9% H_2O, 74.8% N_2 at atmospheric pressure and 95 °C. Table 1 shows power plant key data and the flow sheet of the designed combined cycle power plant is shown in Fig. 2.

As a base case, the CO_2 capture unit with chemical absorption model shown in Fig. 1 was simulated with a capture rate that was set to 90%. This capture rate was obtained by a MEA weight percentage of 30%, solvent circulation rate of 2230 t/h and a reboiler duty of 4.8×10^8 kJ/h. The reboiler energy consumption was 3.86 MJ/kg of separated CO_2, which was provided by the steam flow of 61.7 kg/s. The total mechanical work needed for the CO_2 capture and compression unit is given in Table 2. The CO_2 compression was done in three stages with inter-cooling where the CO_2 stream was compressed to 80 bara and then pumped to storage section at 110 bara. The adiabatic efficiencies of the three stages were, respectively, 85%, 85% and 80%.

The addition of the CO_2 capture unit to the power plant caused a power production efficiency penalty since the power plant provided the mechanical work for the CO_2 capture unit as well as the steam required for the regeneration of solvent. Table 3 shows the key data of the power plant with CO_2 capture unit.

Table 1
Power plant summary without CO_2 capture unit.

	Power output (MW)		Elect. eff. (LHV %)	
	Gross	Net	Gross	Net
Gas turbine	262.8		38.6	
Steam turbine	127.8			
Plant total	390.6	383.3	57.3	56.3

Table 2
Total mechanical work demand for the post-combustion CO_2 capture plant.

Work demand	MJ/kg CO_2 separated
Power production penalty	0.89
Compression work	0.30
Auxiliary power	0.17
Total	1.36

Table 3
Base case power plant summary.

	Power output (MW)		Elect. eff. (LHV %)	
	Gross	Net	Gross	Net
Gas turbine	262.8		38.6	
Steam turbine	95.0			
Plant total	357.8	335	52.5	49.2

5. Results

5.1. Natural-gas-fired combined-cycle power plant

The results of exergy calculation for the power plant are shown in Table 4.

To compare the rational efficiency of both plants, $\psi = \dot{E}_P/\dot{E}_F$, $\dot{E}_P$ is the net electric output of the system added to the exergy

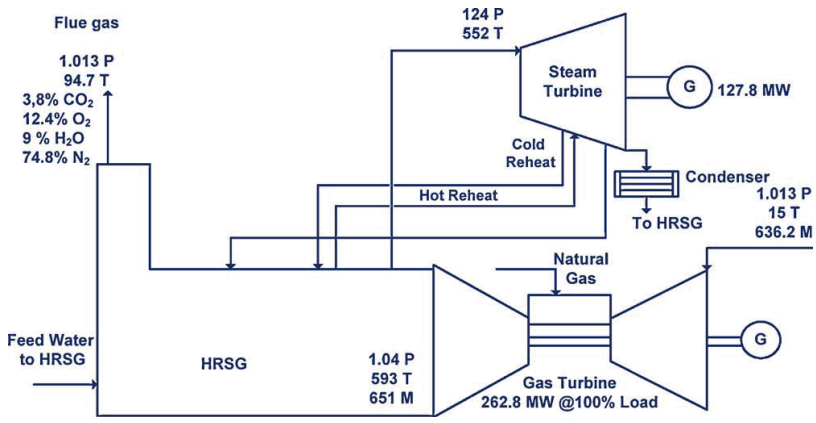

Fig. 2. Flow sheet of the designed power plant.

Table 4
Plant exergy analysis.

	Power plant without CO_2 capture unit (MW)	Power plant with CO_2 capture unit (MW)
Exergy in		
Fuel exergy	687.8	687.8
Exergy out		
Net electric output	383.3	335.0[a]
Pure compressed CO_2 stream	–	23.2
Irreversibility		
Exhaust exergy	18.0	7.6[b]
Gas turbine	239.0	239.0
HRSG	25.2	21.8
Steam turbine	16.4	10.1
Condenser	5.9	1.5
CO_2 capture and compression unit	–	49.8

[a] Work demand of CO_2 capture unit has been taken from the electric output of power plant.
[b] The outflow gaseous stream from the absorber.

of compressed CO_2 stream, while $\dot{E}_F$ is the fuel exergy. Therefore, the rational efficiency of the combined cycle power plant without CO_2 capture unit was 55.7% while the rational efficiency of the same power plant with CO_2 capture unit went down to 52.1%. The addition of CO_2 capture and compression units to the power plant increased the irreversibilities from 304.5 MW to 329.4 MW.

5.2. CO_2 capture and compression plant

The results showed that for the current chemical absorption unit, the minimum reversible separation work of CO_2 from the power plant exhaust stream, which was calculated based on the approach presented by Cengel and Boles (2006), was 0.225 MJ/kg CO_2. The minimum reversible work of compression of pure CO_2 stream from atmospheric pressure to 110 bara was 0.201 MJ/kg CO_2. Considering the actual work demand from Table 2, the exergy efficiency of the CO_2 capture unit was 21.2%, and the exergetic efficiency of compression unit was 67%. The total exergy efficiency of the CO_2 capture and compression plant was 31.6%.

Fig. 3a–c shows simplified block schemes for the illustration of control regions of the absorption, desorption and compression sections. Each block scheme shows the streams transferring exergy through each unit that are material and work streams.

In Fig. 3c, the *Ws* entering from the left side and exiting from the opposite, nominate the exergy content of cooling water streams that passes each of the intercoolers in the compression section, and *Ws* entering from the bottom side of block schemes are work streams for the pump and compressors.

In Table 5, physical streams' characteristics and relevant calculated exergy, which was used to find irreversibilities according to the exergy balance formula, are shown.

6. Discussion

As shown in Tables 1 and 3, the power plant with the CO_2 capture unit had a net electrical efficiency (LHV %) of 49.2% comparing to 56.3% for the power plant without CO_2 capture. This identifies 7.1% points of power production efficiency penalty for the CO_2 capture plant.

The results of the exergy analysis showed a rational exergy efficiency of the combined cycle power plant without CO_2 capture unit of 55.7%, while capture and compression of CO_2 from flue gases caused 3.6% points rational exergy efficiency reduction. The associated exergy losses took place in the GT section, the CO_2 capture unit and the HRSG.

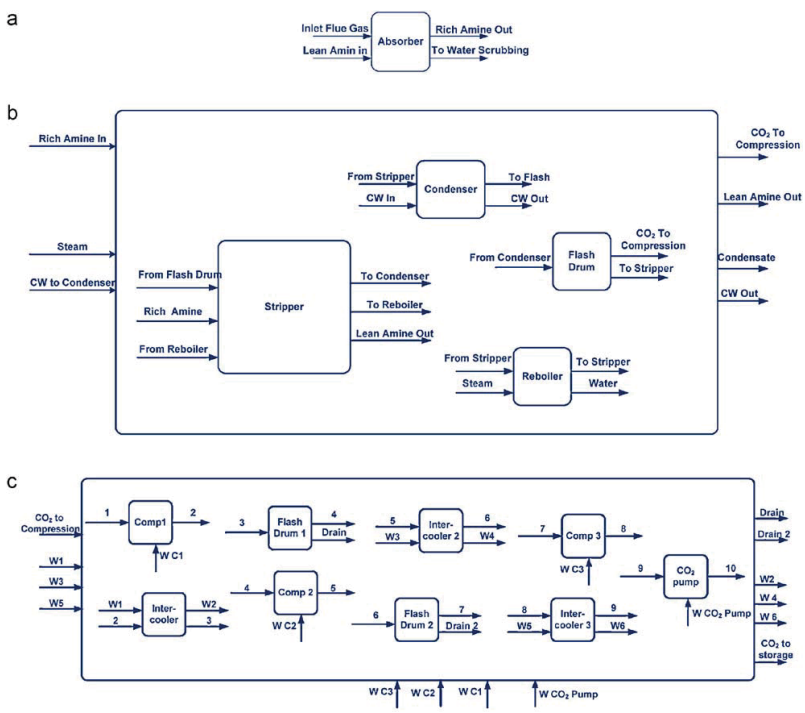

Fig. 3. (a) Block scheme for absorption section. (b) Block scheme for stripping section. (c) Block scheme for CO_2 compression section.

Table 5
Thermodynamical data and exergy of streams.

Stream	Temperature (°C)	Pressure (kPa)	Mass flow (kg/s)	Exergy (MJ/kg CO_2 separated)
CO_2 to storage	35.5	11,000.0	34.6	0.67
CO_2 to compression	28.0	167.2	34.9	0.49
Flue gas inlet	51.8	107.3	651	0.76
Flue gas in	95	101.3	651	0.77
To water scrubbing	53	101.3	631	0.75
Stripper overhead to condenser	100.4	172.4	55.9	0.89
Lean amine in	39.4	107.0	647	120.00
Lean amine out	119.4	186.2	632	123.10
Rich amine in	110.5	106.3	667	123.00
Rich amine out	46	106.3	667	120.2

Table 6
Irreversibility amounts by unit sections.

	Irreversibility (MJ/kg CO_2)
Flue gas cooler	0.12
Blower	0.03
Absorption section	0.67
Rich/lean heat exchanger	0.01
Stripping section	0.50
Compression section	0.11
Total	1.44

For the CO_2 capture and compression plant, the total exergy efficiency was 31.6%. As the exergy calculation results showed, Tables 5 and 6, the magnitude of irreversibilities in the absorption and stripping sections were larger than in the other units, which means that their thermodynamic perfection is low. The total amount of exergy losses in the chemical absorption process was 1.33 MJ/kg CO_2, which agreed with about 1.44 MJ/kg CO_2 for the similar CO_2 capture process observed in the literature (Geuzebroek et al., 2004).

Since the local driving forces are rather high and unevenly distributed along the absorber and stripper, their irreversibilities are high. In the stripper section, large amounts of heat exchange in the reboiler causes large driving forces at the bottom of the stripping column which is in favor of the process of stripping CO_2 from the MEA solvent, but reversely increases exergy losses in the stripper. An even distribution of driving forces over the unit operations would be the optimal solution for decreasing exergy losses. This motivated the design of similar processes with configuration changes, which deviates from stream splitting and recycling of streams to absorber column (Aroonwilas and Veawab, 2007) to inter-cooling of absorber and stripper vapor recompression models (Jassim and Rochelle, 2006).

Also recovering the heat of flue gas from flue gas cooler would reduce the steam consumption in the reboiler which would lead to decrease in the reboiler local driving forces and consequently decreases the stripper section exergy losses (Yu et al., 2009).

7. Concluding remarks

Adding a CO_2 capture and compression unit to a natural-gas-fired combined-cycle power plant, caused an energy efficiency penalty of 7.1% points and a rational exergy efficiency penalty of 3.6% points. The exergy efficiency of the CO_2 capture unit was 21.2%, the exergy efficiency of the compression unit was 67% and the total exergy efficiency of CO_2 capture and compression plant was 31.6%.

Although the exergy losses in the CO_2 capture and compression units are rather small comparing to those lost in gas turbine, HRSG and steam turbine, there are some points of potential improvements. The current study – as in Table 6 – shows that the absorber section and stripper section have the most irreversibilities, which motivates the further research on similar chemical absorption processes with optimized solutions for the stripper and lower exergy losses.

Acknowledgments

This publication forms a part of the BIGCO2 project, performed under the strategic Norwegian research program Climit. The authors acknowledge the partners: Statoil, GE Global Research, Statkraft, Aker Clean Carbon, Shell, TOTAL, ConocoPhillips, ALSTOM, the Research Council of Norway (178004/I30 and 176059/I30) and Gassnova (182070) for their support.

References

Abu-Zahra, M.R.M., Schneiders, L.H.J., Niederer, J.P.M., 2007a. CO_2 capture from power plants, Part I. A parametric study of the technical performance based on mono-ethanolamine. International Journal of Greenhouse Gas Control Technologies 1 (1), 37–46.

Abu-Zahra, M.R.M., Schneiders, L.H.J., Niederer, J.P.M., 2007b. CO_2 capture from power plants, Part II. A parametric study of the economical performance based on mono-ethanolamine. International Journal of Greenhouse Gas Control Technologies 1 (2), 135–142.

Aroonwilas, A., Veawab, A., 2007. Integration of CO_2 capture unit using single- and blended-amines into supercritical coal-fired power plants: implications for emission and energy management. International Journal of Greenhouse Gas Control Technologies 1 (2), 143–150.

Bejan, A., Tsatsaronis, G., Moran, M., 1996. Thermal Design and Optimization. Wiley, New York.

Bolland, O., Undrum, H., 2003. A novel methodology for comparing CO_2 capture options for natural gas-fired combined cycle plants. Advances in Environmental Research 7, 901–911.

Cengel, Y.A., Boles, M.A., 2006. Thermodynamics: An Engineering Approach, 6th edition. McGraw-Hill.

Göttlicher, G., 2004. The Energetics of Carbon Dioxide Capture in Power Plants. U.S. Department of Energy, National Energy Technology Laboratory.

Geuzebroek, F.H., Schneiders, L.H.J.M., Kraaijveld, G.J.C., Feron, P.H.M., 2004. Exergy analysis of alkanolamine-based CO_2 removal unit with Aspen Plus. Energy 29 (9–10), 1241–1248.

GT PRO, 2009. GT PRO version 19. Thermoflow, Inc.

Hammond, G.P., Ondo Akwe, S.S., 2007. Thermodynamic and related analysis of natural gas combined cycle power plants with and without carbon sequestration. International Journal of Energy Research 31 (12), 1180–1201.

IEA, 2008. Carbon Dioxide Carbon and Storage (a key carbon abatement option). OECD.

Jassim, M.S., Rochelle, G.T., 2006. Innovative absorber/stripper configuration for CO_2 capture by aqueous monoethanolamine. Industrial & Engineering Chemistry Research 45, 2465–2472.

Kotas, T.J., 1995. The exergy method of thermal plant analysis. Krieger Publishing Company, Malabar (FL).

Peeters, A.N.M., Faaij, A.P.C., Turkenburg, W.C., 2007. Techno-economic analysis of natural gas combined cycles with post-combustion CO_2 absorption, including a detailed evaluation of the development potential. International Journal of Greenhouse Gas Control Technologies 1 (4), 396–417.

Szargut, J., Morris, D.R., Steward, F.R., 1988. Exergy Analysis of Thermal, Chemical and Metallurgical Processes. Hemisphere Publishing Corp., New York.

UniSim, March 2008. UniSim design user guide. Honeywell, R380 Release.

Yu, Y.S., Li, Y., Li, Q., Jiang, J., Zhang, Z.X., 2009. An innovative process for simultaneous removal of CO_2 and SO_2 from flue gas of a power plant by energy integration. Energy Conversion and Management 50, 2885–2892.

Paper 2

Thermodynamic Analysis of a Post Combustion CO_2 Capture Process

Zeinab Amrollahi[a],[1] Ivar S. Ertesvåg[a] and Olav Bolland[a]
[a] *Department of Energy and Process Engineering, Norwegian University of Science and Technology, Trondheim, Norway*

Abstract: A chemical absorption, post-combustion CO2 capture unit is simulated and an exergy analysis was conducted, including irreversibity calculations for all process units. With pinpointing major irreversibilities, new proposals for efficient energy integrated chemical absorption process were suggested. Moving further to the whole natural gas combined cycle plant with a CO_2 capture unit, it has been analyzed on an exergetic basis. By defining exergy balances and black-box models for plant components, investigation has been made to determine effect of each component on overall exergy efficiency. Simulation of chemical absorption plant was done using UniSim Design software with Amine Property Package which maintains thermodynamic data. For overall power plant design, GT PRO software (Thermoflow, Inc.) was used for simulation of a natural gas combined cycle. For exergy calculations, spreadsheets were created with Microsoft Excel by importing data from UniSim and GT PRO. By pinpointing major irreversibilities, new proposal for energy-efficient integrated chemical absorption process is suggested. Results show that for current chemical absorption plant, the exergetic efficiency compared to the reversible separation work lies between 15% and 22%.

Keywords: CO_2 capture, Absorption, Exergy analysis

1.Introduction

For a natural gas-capture from flue gases, using chemical absorption with aqueous monoethanolamine (MEA) is one of the most near-term technologies.

Flue gas containing CO_2 is flowing through absorber while contacting with MEA solvent counter-currently. Meanwhile reaction is happening between MEA solvent and CO_2 forming a water soluble salt. A rich MEA stream which contains the chemically bound CO_2, preheated in a heat exchanger is entered to a stripper column to reverse the reaction by means of heat maintained by a reboiler and lose CO_2 content as a stream leaving at the top of the column. The lean MEA is recycled back to the absorption column while the CO_2 stream is going to compression section.

Although it is a well-established separation method, the energy consumption and the costs of CO_2 separation are substantially high and lead to consumption of more fossil fuel for the same power generation. In order to increase the energy efficiency and prevent forced extra costs and energy consumption, it is beneficial to optimize the process and evaluate the performance of the whole system by means of exergy analysis which identifies the energy consumption, potential improvements and thermodynamic irreversibilities. It should be noted that although the nature of exergy losses in power plants specially combustion chambers are higher than those of post combustion CO_2 capture plant, but because the capture plants are add-ons to existing power plants and their design and set-up is still under investigation and development, energy and exergy analysis, shows more potential of energetic and exergetic improvement in these processes.

2. Exergy analysis

The exergy method of evaluating energy-intensive systems integrates the first and second laws of thermodynamics at the state of particular environmental conditions. Exergy analysis with its own certain methods of process evaluation has proven to be an efficient method to define the second law efficiency of processes. It combines the principles of conservation of mass and conservation of energy together with the second law of thermodynamics to characterize the thermodynamic losses of each component of a

[1] Corresponding author. Email: zeinab.amrollahi@ntnu.no

system through the whole design and it enables to make possible improvements of work and energy consumption. This is an advantageous method to approach the goal of more efficient energy-resource use, since it specifies the locations, types, and real magnitudes of irreversibilities either to be recovered or inevitably lost.

In absence of potential and kinetic energy, exergy of stream is divided into physical exergy and chemical exergy. Physical exergy equals to maximum amount of work obtainable when the stream of substance is brought from its actual state to the environmental state defined by P_0 and T_0 [4] by physical processes involving only thermal interaction with the environment. It is depicted as:

$$\varepsilon_{ph} = (h - h_0) - T_0(s - s_0) \qquad (1)$$

Where h and s are the specific enthalpy and entropy and $h_0 = h(T_0, P_0)$ and $s_0 = s(T_0, P_0)$ for the flowing matter.

The chemical exergy of a substance is the minimum work requirement to deliver it in the environmental state from the environmental substances by means of processes involving heat transfer and exchange of substances only with the environment. There are tables of calculated standard chemical exergy of various substances in literature [1]. Molar chemical exergy of an ideal mixture is expressed as

$$\tilde{\varepsilon}_{0M} = \sum_i x_i \tilde{\varepsilon}_{0i} + \tilde{R}T_0 \sum_i x_i \ln x_i \qquad (2)$$

Exergy loss of each individual unit can be calculated by finding the difference between the exergy of input and output streams of a unit operation. To pinpoint irreversible losses in each unit operation, the exergy balance for steady state steady flow is used;

$$\sum_{in} \dot{m}_j \varepsilon_j + \sum_l \dot{Q}_l (1 - \frac{T_0}{T_l}) = \sum_{out} \dot{m}_k \varepsilon_k + \dot{W} + \dot{I} \qquad (3)$$

Flow exergy into system | Heat exchange | Flow exergy out of system | Work | Irreversibility

Exergy analysis can be done when composition and thermodynamic properties of all streams involving in capture process are available. For this purpose, a simulation software model is used to simulate the whole CO_2 capture process. By transferring stream physical properties and compositions to excel spreadsheets, exergy calculations are performed and reported.

To calculate the chemical exergy of each stream containing MEA component there is a need of chemical exergy of the MEA molecule in the liquid phase. The value which is used in these calculations is not found directly from literature but estimated. The value is $1.274 \cdot 10^6$ kJ/kmol.

3. Methodology

In the analysis, the mass, energy and exergy balances were applied to each unit (valve, pump, heat exchanger, etc.) of the plant. For presentation purposes, the plant was subdivided into sections comprising one or more units. These sections were the gas turbine, heat recovery steam generator (HRSG), steam turbine and condenser, CO_2 absorption column, main heat exchanger of CO_2 capture plant, stripping section, compression

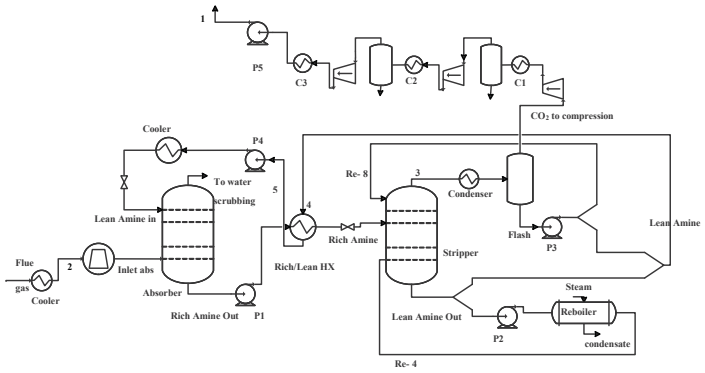

Figure 1: Flow sheet of CO_2 capture and compression units designed by UniSim Design

section. The irreversibility of a section was the sum of the irreversibilities of the contained units.

Chemical and physical exergy of all streams was functioned in excel spreadsheets. Furthermore, exergy analysis calculations for the designed power plant were derived from GTPro Thermoflow software calculation which will be depicted later. The reference environment is the local environment of the place where the natural gas fired power plant is located which it is assumed in here with ambient temperature T_0= 298.15 K and pressure P_0=101.325 kPa.

As mentioned before, this study is limited to the analysis of the physical exergy and chemical exergy. Other forms of exergy as kinetic and potential are insignificant in these processes so they are ignored. The degradation and consumption of the MEA solvent was neglected in CO_2 capture unit.

4. Base case model

As a base case, the CO_2 separation with MEA absorption model shown in Figure 1 is designed according to the capture rate that is set to 90.5%.

This capture rate for the base case was attained by MEA weight percentage of 30 and solvent circulation rate of 2500 t/h and reboiler duty of $5.12 \cdot 10^8$ kJ/h. Reboiler energy consumption is 3.86 (MJ/kg of separated CO_2) which is produced by the steam flow of 64.35 kg/s .Total mechanical work needed for the capture and compression unit is mentioned in Table 1. CO_2 compression was done in 3 stages with adiabatic efficiencies of 85%, 85% and 80% respectively with intermediate cooling after each stage. A pump further raised the pressure from 79.7 bara to 110 bara. The pump adiabatic efficiency was set to 75%.

Table 1: Total mechanical work demand for post combustion CO_2 capture plant

Work demand	MJ/kg CO_2 separated
Power production penalty	0.89
compression work	0.29
Auxiliary power	0.16
Total	1.34

Table 2: Power plant summary

	Power Output MW		Elect. Eff. LHV%	
	gross	net	gross	net
Gas Turbine	282.7		39.22	
Steam	92.7			
Plant Total	375.4	368.2	52.08	51.09

The virtual power plant that is connected to the CO_2 capture process provides mechanical work to cover the demand of the CO_2 capture unit as well as the steam demand of the regeneration reboiler. A complete schema of the designed combined cycle power plant is shown in Figure 2 with key stream information. The plant key data are shown in Table 2.

Figure 2: Flowsheet of the designed power plant

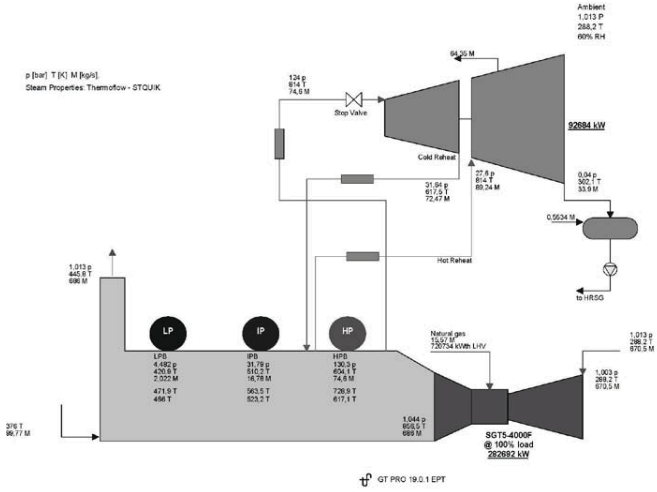

The fuel was considered as natural gas without H_2S with 722087 kW thermal as lower heating value and flow of stack gas is 686.4 kg/s with molar composition of 3.82% CO_2, 12.54% O_2, 8.24 % H_2O, 75.4% N_2 and temperature of 412.5 K which is going to be cooled in capture unit.

5. Results

5.1 Natural gas fired power plant

The results of exergy calculation for specified natural gas fired power plant designed by GTPro Thermoflow software are shown in Table 3.

Table 3: Plant exergy analysis

	kW	MJ/kg CO_2 separated
Exergy In	739008	19.96
Fuel exergy	727460	19.65
Ambient air exergy	0	0,00
Condenser cooling water in	6359	0.17
Process condensate return	5072	0.14
Makeup water	1.633	0.00
Exergy Out	435668	11.77
Net electric output	368193	9.94
Process steam exergy	45870	1.24
Condenser cooling water out	1391.5	0.04
Stack gas exergy	20214	0.55
Exergy Loss	303340	8.19
GT exergy loss	255216	6.89
HRSG exergy loss	22140	0.60
Steam turbine exergy loss	10584	0.29
Condenser exergy loss	5960	0.16
Non-heat balance related auxiliaries	2616	0.07
Transformer loss	1876.9	0.05
Miscellaneous exergy loss*	2369.9	0.06
Unaccounted exergy loss**	2577.6	0.07

* Includes piping loss, ST leakage to external sink, fuel compressor loss, condensate pump loss
** Includes losses from desuperheating, mixing, and throttling, small water streams, misc. aux. and heat rejection

5.2 Base case CO_2 capture plant

In Table 4, physical stream characteristics and relevant calculated exergy which is used to find irreversibility amounts according to exergy balance formula are shown. It should be noted here that for simulation of streams containing amine component, UniSim Design software [3] developed a specific property package which predicts behavior of systems containing MEA solvent. For simulation of other streams Peng-Robinson equation of state is used.

Table 4: Themodynamical data and exergy of streams for the base case model

Stream	Temperature (°C)	Pressure (kPa)	Mass Flow (kg/s)	Exergy (MJ/kg CO_2 separated)
1	24.66	11000.00	37	0.67
CO_2 to compression	28.00	167.20	37.3	0.486
2	43	101.30	686.4	0.6
Inlet abs	49.6	107.30	686.4	0.49
Flue gas	139.4	101.30	686.4	1
To water scrubbing	52	101.30	663.1	0.61
3	100.3	172.4	70.22	0.89
4	119.1	186.20	710.5	129.1
5	55.5	146.20	710.5	126.1
Lean Amine Out	119.5	186.20	809	143.2
Steam	177	400.00	64.35	2.4
Condensate	143	392.00	64.35	1.3
Lean Amine in	39.5	107.00	680.4	126.9
Rich Amine Out	46	106.30	748	125.9
Rich Amine	110.5	106.30	748	128.7

5.3 Improved model

Observing the exergy amounts of streams and process sections irreversibilities, a new model - see Figure 2- with lower energy consumption and irreversibility is investigated. The first configuration change is to split the *Rich Amine* stream which carries mainly the absorbed CO_2 and MEA amine and integrating those split streams with two streams returning from stripper; the first stream is *Lean Amine* which is also in the base case model, but the second stream is *Semi-Lean* stream which is a liquid side stream taken from the stripper. The concept behind these modifications is to divide the driving force along the stripper into smaller segments which makes the separation processes closer to its reversible situation and decreases the irreversibilities. The largest portion

of *Rich Amine* stream coming out of absorber is still passing through the *Rich/Lean heat exchanger 1* while its smaller portion is heated through *Rich/Lean heat exchanger 2* with the *Semi-Lean* stream that is taken from the stripper column and recycled back to the absorber. With these new changes, there is a chance of approaching exergy recovery and decreasing irreversibility amount of the whole system.

Table 5: Total mechanical work demand for new process configuration of CO_2 capture unit

Work demand	MJ/kg CO_2 separated
Power production penalty	0.88
compression work	0.29
Auxiliary power	0.17
Total	1.34

The CO_2 capture rate for this modified model which is shown in Figure 3 is 90.3% and the new reboiler duty is $5.1 \cdot 10^8$ kJ/h which is less than base case model. Reboiler energy consumption is 3.83 (MJ/kg of separated CO_2) which is produced by the steam flow of 63.71 kg/s .Total mechanical work needed for the capture and compression unit is given in Table 5.

Table 6: Themodynamical data and exergy of streams for new process configuration of CO_2 capture unit

Stream	Temperature (°C)	Pressure (kPa)	Mass Flow (kg/s)	Exergy (MJ/kg CO_2 separated)
1	24.88	11000.00	37	0.675
CO_2 to compression	28	167.20	37.3	0.49
2	43	101.30	686.4	0.6
Inlet abs	49.6	107.30	686.4	0.49
Flue gas	139.4	101.30	686.4	1
To water scrubbing	51.7	101.30	662.5	0.6
3	100.1	172.4	70	0.9
4	118.5	186.20	714.6	129.2
5	56.2	146.20	714.3	126.1
Lean Amine Out	118.6	186.20	809	143.1
Steam	176.9	400.00	63.7	2.37
Condensate	143	392.00	63.7	1.26
Lean Amine in	39.4	107.00	723.8	127.4
Rich Amine Out	50	106.30	881	148.3
Semi- Lean	114.5	184.1	130	22
RA 1	110.1	610	766.3	128.4
RA 2	114.4	650	136.6	23.6

Figure 3: Flow sheet of new configuration for CO_2 capture and compression units

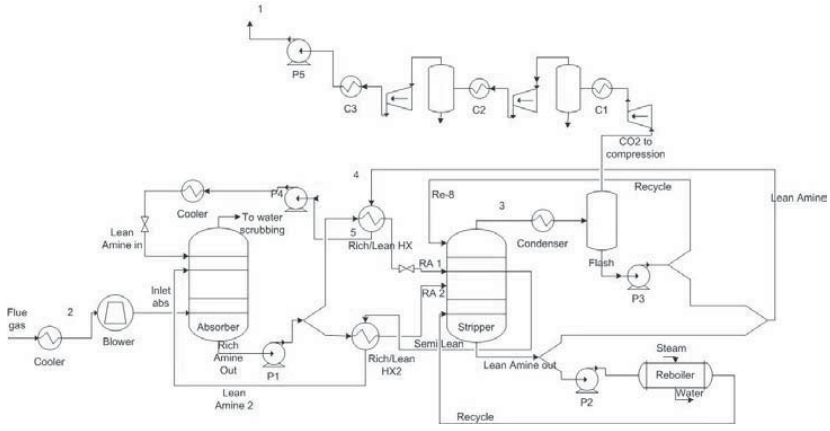

Table 7: Irreversibilities by process sections

Irreversibility [MJ/kg CO_2]	Base case	New design
Flue gas cooler	0.48	0.48
Blower	0.04	0.04
Absorption section	0.61	0.64
Rich /lean heat exchanger 1	0.01	0.0
Rich /lean heat exchanger 2	-	0.01
Stripping section	0.59	0.51
compression section	0.12	0.12
Total	**1.85**	**1.80**

5. Discussion

As the exergy calculation results show- Tables 6 and 7- the magnitude of irreversibilities which is currently happening in the absorption and stripping sections, motivates the design of similar process with configuration changes, which is mainly stream splitting and recycling of the streams. By taking out a side stream from stripper and recycling it through a heat exchanger to the absorber, the stream is taking out a considerable amount of irreversibility from stripper; but since this side stream is cooled before absorber, it affects the absorber irreversibilities less. Additionally, in the improved model, by splitting the feed stream before the absorber and feeding them into different trays, the driving forces are distributed more evenly along the column height which results in lower irreversibility. Furthermore, reboiler duty is decreased which will show its deduction in the stripper irreversibility amount.
More to add is since flue gas temperature entering chemical absorption plant is fairly the same in both models, the irreversibilities of flue gas cooler and blower for both of cases are equal.
Finally, from efficiency point of view, power plant with the modified model for CO_2 capture has slightly higher net electrical efficiency i.e 51.14% comparing to the power plant with base case model i.e. 51.09%. Since the steam demand in the reboiler in the improved model is decreased comparing to the reboiler duty of the base case, power plant's steam turbine has higher power output (93MW) and electrical efficiency (LHV%) increases. It should be mentioned that power plant efficiency (LHV%) without CO_2 capture is 56.34% that is higher than the efficiency of power plants with CO_2 capture .

6. Concluding remarks

Although the exergy loss in CO_2 capture and compression units are rather small comparing to those lost in Gas turbine, HRSG and steam turbine, there are points of potential improvements in CO_2 capture process. By process configuration changes and decreasing regeneration duty, improved CO_2 capture process with lower heat consumption and less irreversibility amount was designed.
Minimum reversible separation work for the flue gas stream coming to the CO_2 capture plant is 0.247 MJ/kgCO_2. When looking to the actual work demand Tables 1&5, it was calculated that for base case chemical absorption plant exergy efficiency was 18.36% and the modified case gave exergy efficiency of 18.37%.
Current study -as in Table 7- shows that by splitting the out-coming streams from the absorber and encountering them to various lean MEA recycles from the stripper, the irreversibility amounts through stripper decreases sensibly. Use of other solvents with lower binding energy is suggested to decrease the exergy loss of reboiler section. In order to minimize the exergy loss, it is important to have uniform exergy degradation along equipments, which can be an optimization idea for the regeneration column, flasher and reboiler. Furthermore in order to divide exergy losses through the absorption column and stripping column, process configuration changes such as stream splitting can be performed [5].

References:

[1] Kotas, TJ. , 1995, *The exergy method of thermal plant analysis*, Malabar (FL): Krieger Publishing Company.

[2] Cengel, Y. A. and Boles, MA. , 2006, *Thermodynamics: An Engineering Approach, 6th* edition, McGraw-Hill.

[3] UniSim design user guide; Honeywell; 2008 R380 Release

[4] Szargut J, Morris DR, Steward FR., 1988, *Exergy analysis of thermal, chemical and metallurgical processes*, New York: Hemisphere Publishing Corp.

[5] Adisorn Aroonwilas, 2005, Integration of CO_2 capture unit into supercritical coal-fired power plants: Implications for emission and energy management, International journal of Greenhouse Gas Control Technologies, 1(2), pp. 1841-1844.

Paper 3

GHGT-10 Conference Paper

Identifying areas for improvement and development in a pre-combustion CO_2 capture cycle

Zeinab Amrollahi*, Lars O. Nord, Ivar S. Ertesvåg, Olav Bolland

Department of Energy and Process Engineering, Norwegian University of Science and Technology, NO-7491 Trondheim, Norway

Abstract

This paper discusses the thermodynamic efficiency of an integrated reforming combined cycle (IRCC) process as one of the proposed pre-combustion CO_2 capture processes. By simulating an IRCC plant with CO_2 capture, for thermodynamic evaluation, exergy of streams and irreversibilities were calculated. The exergy analysis of the system, pinpoint major irreversibilities and exergy losses. Simulation of the IRCC plant with CO_2 capture was done using Aspen Plus software. For gas turbine and steam cycle design, GT PRO software (Thermoflow, Inc.) was used. For exergy calculations, ExerCom software (JACOBS consultancy) was used to calculate the exergy of streams and irreversibilities of each unit operation. To decrease the exergy losses in the gas turbine combustor, fuel pre-heating up to 500°C, would decrease the gas turbine irreversibility up to 11%. Additionally, preheating the inlet streams to the auto-thermal reformer would be beneficial in decreasing its exergy losses.

Keywords: CO_2 capture; Pre-combustion ; Exergy analysis

1. Introduction

Global warming is one of the most important environmental challenges of the 21st century. Therefore the power industry is increasingly facing regulations on the CO_2 emissions and this has been the motivation for the recent research and developments in CO_2 capture and storage processes from fossil fuelled power plants. One of the challenges for large-scale implementation of CO_2 capture is related to its high energy efficiency penalty. Consequently, power plants with integrated CO_2 capture have been proposed and discussed in the literature and various comparative performance analyses have been presented [1-3].

Among the technical solutions developed for CO_2 capture from natural gas power plants, Eide and Baily [4] described pre-combustion decarbonisation schemes which are based on different available reforming technologies as steam reforming, partial oxidation and auto-thermal reforming. Amann et al. [5] assessed the conversion and net electrical efficiency of a natural gas combined cycle power plant with auto-thermal reforming technology for CO_2 pre-combustion capture, while Lozza et al. [6] evaluated the thermodynamic efficiency based on exergy analysis and economic performance of steam methane reforming pre-combustion CO_2 capture. The exergy analysis of a similar process based on auto-thermal reforming technology for reforming pre-combustion CO_2 capture was presented by Ertesvåg et al. [7].
In a paper by Hoffman et al. [8], performance and cost analysis was carried out for an advanced natural gas fired gas turbine cycles with pre-combustion CO_2 capture. The pre-combustion process discussed by Hoffman et al. [8] was based on an advanced partial oxidation reformer.

2. Process description

The process described here has been titled as integrated reforming combined cycle (IRCC) with single-pressure heat recovery steam generator (HRSG). It reforms natural gas to a syngas as shown in Figure 1. Reforming of natural gas was modeled as a two-step process. In the pre-reformer higher hydrocarbons are converted to protect against coking in the auto-thermal reformer (ATR) according to endothermic reaction (1) and exothermic reactions (2) and (3).

$$C_X H_Y + xH_2O_{(g)} \rightleftharpoons xCO + (x + \frac{y}{2})H_2 \qquad -\Delta H^0_{298} < 0 \text{ kJ/mol} \tag{1}$$

$$CO + 3H_2 \rightleftharpoons CH_4 + H_2O_{(g)} \qquad -\Delta H^0_{298} = 206 \text{ kJ/mol} \tag{2}$$

$$CO + H_2O \rightleftharpoons CO_2 + H_2 \qquad -\Delta H^0_{298} = 41 \text{ kJ/mol} \tag{3}$$

The air-blown ATR is divided into a combustion zone, a thermal zone, and a catalytic zone. The heat generated in the combustion zone provides heat for the reforming in the thermal and catalytic zones. Substoichiometric methane combustion in the ATR can be represented as

$$CH_4 + \frac{3}{2}O_2 \rightarrow CO + 2H_2O_{(g)} \qquad -\Delta H^0_{298} = 519 \text{ kJ/mol} \tag{4}$$

In the thermal and catalytic zones, below the combustion zone, the main reactions are the water-gas shift reaction (3) and methane-steam reforming

$$CH_4 + H_2O_{(g)} \rightleftharpoons CO + 3H_2 \qquad -\Delta H^0_{298} = -206 \text{ kJ/mol} \tag{5}$$

In the high-temperature and low-temperature water-gas shift reactors (HTS and LTS) most of the remaining CO is converted to CO_2 according to reaction (3). Due to the temperature driving force in the HTS, the shift reactor equipment size can be kept smaller. However, the conversion would be too low if only using an HTS. Therefore, an LTS with a lower temperature and a more active catalyst is needed. Downstream of the shift reactors about 90% of the CO_2 is separated in the CO_2 capture subsystem. The hydrogen-rich fuel vented from the absorber is used for the gas turbine. As the ATR is air-blown there will be a significant portion of nitrogen in the gas. This nitrogen is used as fuel diluent for NO_x abatement in the gas turbine (GT) combustor. The air needed for the ATR is bled from the GT compressor discharge plenum and boosted up to system pressure with an air compressor. There are a number of heat exchangers in the system. The preheating of the reforming streams is handled in various zones in the HRSG. The syngas cooler, located after the ATR, acts as an evaporator for the high-pressure (HP) steam cycle. The other heat exchangers for the process streams either generate low-pressure (LP) steam for the reboiler in the capture subsystem or preheat fuel for the GT. The selected gas turbine is a GE 9FB. The bottoming steam cycle, including the HRSG and a steam turbine (ST), is a single-pressure system at approximately 85 bar. The CO_2 capture sub-system consists of a hot potassium carbonate chemical absorption process. The reboiler energy demand was

supplied (as heat) through steam exchange with the steam cycle and available heat exchangers in the IRCC system that would generate low-pressure steam. After the capture subsystem, the CO_2 is compressed to 150 bar in the CO_2 compression (four stages) and pump train.

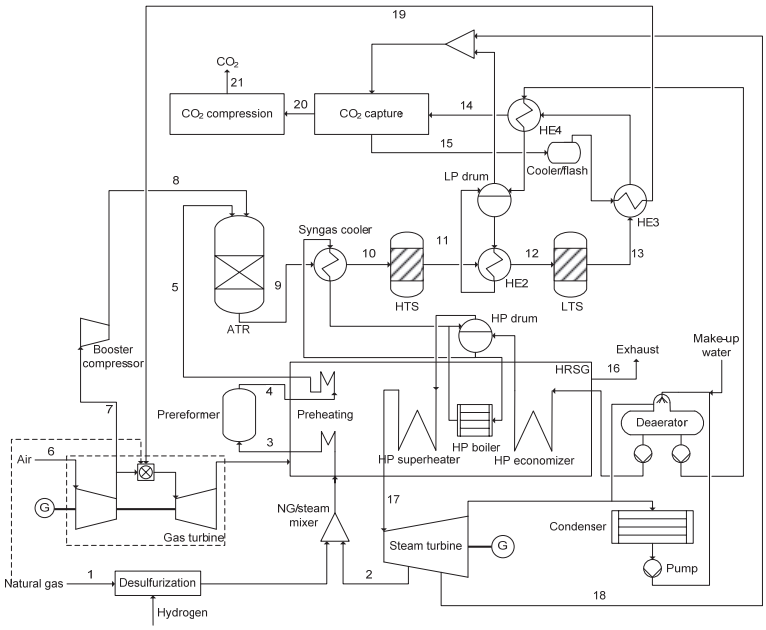

Figure 1. Process flow sheet of integrated reforming combined cycle

3. Methodology

The process shown in Figure 1 was modeled in GT PRO and in Aspen Plus with software linking approach described by Nord et al. [9,10].The models were linked by Aspen Simulation Workbook and the Thermoflow E-LINK. The flowsheet simulations provided mass and thermodynamic data for all of the streams. The power island was composed of GT, HRSG, ST and condenser. The downstream simulated units consisted of reforming, CO_2 capture and compression sections. The reforming model, as described in Section 2, consisted of natural gas and steam mixer, air booster compressor, process stream pre-heaters, pre-reformer, ATR, HTS and LTS and heat exchangers to utilize streams' available heat amounts for economizing, boiling and superheating in the water to steam cycle. Pre-reformer and ATR were modeled as adiabatic Gibbs reactors and HTS and LTS were modeled as adiabatic equilibrium reactors in Aspen Plus.

3.1 Exergy analysis

For thermodynamic efficiency evaluation of the system, exergy analysis has been chosen to identify the second law efficiency and irreversibility of each unit. This is an advantageous method to approach the goal of more efficient processes, since it specifies the locations, types, and real magnitudes of irreversibilities either to be recovered or inevitably lost. Exergy analysis could be performed by taking into account the composition and the physical properties of the investigated streams. In this paper, the exergy of streams was calculated with using ExerCom by

Jacobs Engineering, which is an add-on to Aspen Plus for calculations of the chemical, physical and mixing exergy for process gas and liquid streams.

The reference state is assumed the same as what defined by Szargut et al. [11], i.e. the reference temperature of T_0=298.15 K and pressure P_0=101.325 kPa. For chemical equilibrium as a reference state, the mean composition of the earth's atmosphere, the mean composition of seawater and the mean composition of the earth's crust are taken.

Exergy loss of each individual unit was calculated by finding the difference between the exergy of input and output streams of a unit operation. To find the irreversibility in each unit operation, a steady state exergy balance was used;

$$\sum_{in} \dot{m}_j \varepsilon_j + \sum_l \dot{Q}_l \left(1 - \frac{T_0}{T_l}\right) = \sum_{out} \dot{m}_k \varepsilon_k + \dot{W} + \dot{I} \qquad (6)$$

Flow exergy into system | Heat exchange | Flow exergy out of system | Work | Irreversibility

In order to use the same reference state for exergy calculation of power island streams , the reforming section, and CO_2 capture and compression units, the streams' physical properties as well as molar composition and flow rates were imported from GT PRO through Excel to Aspen Plus. Afterwards, by accessing ExerCom add-on, exergy of streams were calculated. Furthermore, to assess the performance of the whole system, a Grassmann diagram [12,13] was chosen to represent the exergy flows and losses apart from listing the irreversibilities of all process units.

3. Results and Discussion

The summary of results for the IRCC plant with single pressure HRSG in terms of power, efficiency and capture rate is presented in Table 1. The plant has a net electrical efficiency of 44.7% (LHV), with net power output of approximately 360 MW. Process data for the selected streams including their exergy rates are shown in Table 2.

Table 1: Summary of results for the IRCC with single-pressure HRSG [10]

Natural gas LHV input (MW)	838.5
Gross power output GT (MW)	256.8
Gross power output ST (MW)	154.8
Gross power output (MW)	411.7
Gross power output (% of LHV input)	49.1
Air compression (MW)	13.4
Air compression (% of LHV input)	1.6
CO_2 compression (MW)	15.3
CO_2 compression (% of LHV input)	1.8
CO_2 capture pumps (MW)	1.6
CO_2 capture pumps (% of LHV input)	0.2
Auxiliaries (MW)	6.2
Auxiliaries (% of LHV input)	0.7
Net Power output (MW)	357.2
Net plant efficiency (% of LHV input)	44.7
CO_2 emission (g CO_2/net kWh el.)	66.9
CO_2 capture rate (%)	85.9

For the pictorial presentation of exergy flows and losses, the Grassmann diagram is shown in Figure 2 and the irreversibilities for the whole process are given unit-wise in Table 3.

To evaluate the desired exergy change to the total used exergy, the exergy efficiency definition has been expressed as $\psi = \frac{\Delta \dot{E}^{desired}}{\Delta \dot{E}^{used}}$ [12]; the term $\Delta \dot{E}^{used}$ is equivalent to the exergy input to the system and $\Delta \dot{E}^{desired}$ is the Exergy output according to Table 3; therefore the exergy efficiency of 43.8% was calculated.

Table 2: Process streams data and corresponding calculated exergies

Point	Mass kg/s	P bar	T °C	Exergy MW	Ratio (To fuel exergy) %
1	18.4	37	10	873.9	
2	30.4	36	436.2	38.1	100.0
3	48.8	35.4	500	920.9	4.4
4	48.8	34.9	467.3	919.5	105.4
5	48.8	34.7	500	922.2	105.2
6	642.1	1.0	15	0	0
7	90.3	16.3	381.3	33.1	3.7
8	90.3	30	516.0	45.7	5.2
9	139.1	29.3	950	881.9	100.9
10	139.1	29	350	781.0	89.4
11	139.1	28.7	426.5	779.0	89.1
12	139.1	28.5	210.0	752.4	86.1
13	139.1	28.1	237.0	751.5	86.0
14	139.1	27.7	115.3	736.8	84.3
15	86.5	27.2	90.0	710.3	81.3
16	632.8	1.0	77.6	11.5	1.3
17	148.0	80.9	557	222.7	25.5
18	4.0	2.0	151.2	2.5	0.3
19	81.0	7.9	200	714.7	81.8
20	44.5	1.1	5	20.5	2.3
21	42.4	150.0	53.8	29.8	3.4

Table 3: Exergy analysis results and irreversibilities for the plant flowsheet of Figure 1.

	MW	Ratio (To fuel exergy) %
Exergy input		
Natural gas	873.89	100
Feed Water	7.1	0.8
Exergy output		
Net Power Production	375.2	42.9
Pure CO_2 exergy	29.8	3.4
Irreversibilities		
Gas Turbine (compression + combustion + expansion)	231.6	26.5
Heat Recovery steam generation (HRSG + deaerator)	19.6	2.2
Steam turbine	22.2	2.5
Condenser	6.5	0.7
Booster compressor	0.8	0.1
NG/steam mixer	7.2	0.8
Exhaust discharge*	10.5	1.2
ATR	85.9	9.8
Syngas cooler	30.3	3.5
HE2	14.3	1.6
HE3	3.3	0.4
HE4	0.5	0.1
Cooler/flash	1.1	0.1
CO_2 capture	24.2	2.8
CO_2 compression	5.7	0.7

* exergy in the exhaust outflow which has been lost

Table 4: Fuel supply temperature changes and irreversibility rates

Fuel temperature * °C	**200.0**	**300.0**	**400.0**	**500.0**
Air after GT compressor temp. °C	381.4	380.4	379.5	378.6
GT inlet temperature (TIT) °C	1327.4	1327.3	1327.5	1327.4
GT exhaust temperature °C	595.4	595.5	595.6	595.6
GT turbine inlet pressure bar	15.5	15.5	15.4	15.3
Air after GT compressor pressure bar	16.3	16.3	16.3	16.3
GT fuel flow * kg/s	81.0	78.6	76.9	75.1
Gas turbine exhaust mass flow kg/s	632.8	630.3	628.0	625.8
Turbine inlet mass flow kg/s	548.2	545.7	543.5	541.3
GT compressor discharge exergy MW	172.3	171.7	171.3	170.9
GT exhaust exergy MW	193.9	192.5	191.1	189.8
GT gross power MW	256.8	256.5	255.5	254.8
Fuel exergy * MW	714.7	700.3	688.7	677.8
Combustor outlet exergy MW	692.9	688.1	683.5	678.8
Combustor irreversibility MW	194.1	184.0	176.5	169.8
GT irreversibility MW	**231.6**	**221.7**	**214.4**	**207.6**

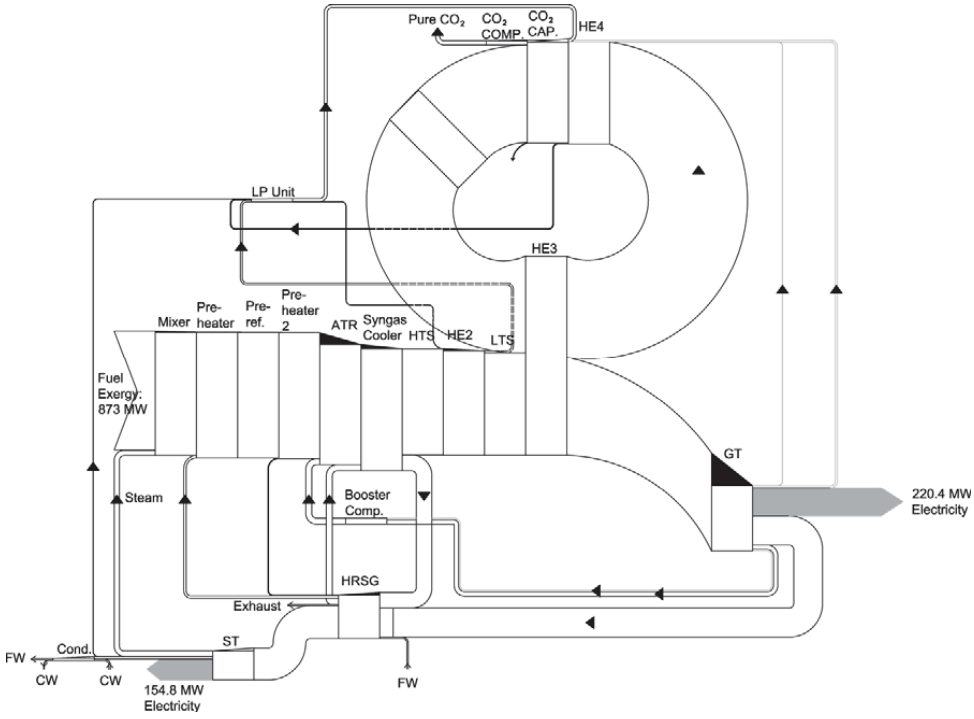

Figure 2. Grassman diagram for the integrated reforming combined cycle with single pressure HRSG. The figure presents the flow of exergy along the cycle; the black-colored areas are the irreversibility amounts in each unit.

From the results reported in Table 3 we can comment that:

- The pure pressurized CO_2 is a thermodynamic asset produced by the IRCC plant. Its exergy accounts for 3.4% of the fuel exergy input which equals to reversible work production by the isothermal expansion of pure pressurized CO_2 to CO_2 partial pressure in the environment.
- The largest irreversibility is contributed by the GT and mainly by the combustor section. The irreversibility, which is inherent in the combustion process, corresponds to a large fraction of the original exergy of the fuel. Reduction of irreversibility requires reduction in the rate of entropy production, which is associated with an increase in the maximum temperature of the combustion products. A suggestion of improvement to decrease the combustor irreversibility is to provide the preheating of fuel supply to the combustor. In the current analysis, parametric variations have been carried out for observation of irreversibility changes along the GT. Three different fuel supply temperatures to the combustor has been tested. The results in Table 4 show how variations of this temperature changed the total mass balance over the GT, exhaust gas composition, and exhaust temperature. It also affected the total work production of GT and the fuel flow to the combustor. It is shown that by these parametric changes, the irreversibility of combustor and consequently, the GT irreversibility have been decreased.
  The potential sources of this fuel preheating could be the ATR outlet stream and HTS outlet stream. The heat exchange with the ATR outlet stream which would lead to fuel preheating up to 500 °C, affected the total HP steam in HRSG and consequently would decrease the ST power generation. Utilizing the

available heat form HTS outlet stream would change the total amount of LP production which would lead to an increase in the steam demand as LP extraction from ST.

- The reforming unit in a natural gas-fired power plant is just required when pre-combustion CO_2 capture is being performed. Because of the need of high temperatures for steam reforming reaction of the fuel, a portion of the GT flue gas is used for reformer pre-heating. This leads to lower steam production in HRSG and lower IRCC net electrical efficiency. Thus, the exergy losses associated with steam reforming reaction, together with CO conversion, CO_2 separation and compression, are entirely attributable to CO_2 capture.
- In this process, 10 percent of the fuel exergy is lost by irreversibilities in the ATR. This is mainly due to the combustion process which is taking place in the reformer. Preheating the inlet streams to the ATR would be beneficial in decreasing the exergy losses of the ATR. This preheating can be rendered by a series of heat exchangers which cools the ATR exit stream and preheats the ATR inlet streams simultaneously.
- The syngas cooler contributes to 3.5 percent of the irreversibilities. Those losses occur during cooling of the synthesis gas prior to the CO shift reaction, due to the high temperature difference of flowing streams as well condensation of the excess steam component. However, part of the available enthalpy of vaporization is recovered via the syngas cooler to produce saturated high pressure steam and fed back to HRSG.
- To achieve a high CO_2 capture ratio, high CO or CH_4 conversion is required. It is achieved by introducing water higher than its stoichiometric amount for reaction but at the same time, the enthalpy of vaporization delivered with the excess steam contributes to the exergy losses in the CO shift reaction and reforming.
- The CO_2 capture plant contributes to 2.8 percent of the irreversibilities. This contributes mostly to steam consumption in the chemical absorption process for solvent regeneration. In the present simulation, a hot potassium carbonate system has been used as the capture process. However, MDEA would be an alternative to the current system. The reboiler duty would be lower for an activated MDEA system compared to hot potassium carbonate [14]. Alternative CO_2 capture configurations such as matrix stripper, split feed stripper and multi pressure stripper have been proposed in the literature [15]. Thus lowers the reboiler duty and decreases the irreversibility of the reboiler.

4. Conclusion and further research

With performing exergy analysis on an IRCC pre-combustion CO_2 capture system, the exergy efficiency of 43.8% has been calculated. This indicates the percentage of input exergy utilised for work production by the power cycle in addition to the exergy of the pure compressed CO_2 stream.

The highest amount of irreversibility is contributed by the GT and mainly by the combustor. The irreversibility which is inherent in the combustion process corresponds to a large fraction of original exergy of the fuel. A suggestion of improvement to decrease the combustor irreversibility is to increase the preheating of fuel supply to the combustor. With pre-heating the fuel up to 500 °C the GT irreversibility was decreased by 11 %. The ATR was observed as the second largest contributor to the cycle irreversibilities. A suggestion to decrease the ATR irreversibility is to preheat its inlet streams. This preheating can be rendered by a series of heat exchangers which cools the ATR outflow stream and preheats the ATR inflow streams simultaneously. These variations to the model are going to be done in the future simulations. A further goal to achieve is to identify the extent of avoidable and unavoidable exergy losses for the process units. This will gives us the idea of to what extent the exergy losses that occur in each unit could be avoided by process modifications. It also clarifies the amount of the unavoidable losses that adheres to the process itself.

Acknowledgements

This publication forms a part of the BIGCO2 project, performed under the strategic Norwegian research program Climit. The authors acknowledge the partners: Statoil, GE Global Research, Statkraft, Aker Clean Carbon, Shell, TOTAL, ConocoPhillips, ALSTOM, the Research Council of Norway (178004/I30 and 176059/I30) and Gassnova (182070) for their support.

References

[1] Kvamsdal H. M., Jordal K., Bolland O. (2007). "A quantitative comparison of gas turbine cycles with CO_2 capture." Energy 32(1): 10-24.
[2] Kanniche M., Gros-Bonnivard R., Jaud P., Valle-Marcos J., Amann J. M. and Bouallou C. (2010). "Pre-combustion, post-combustion and oxy-combustion in thermal power plant for CO_2 capture." Applied Thermal Engineering 30(1): 53-62.
[3] Bolland O. and Undrum H. (2003). "A novel methodology for comparing CO_2 captures options for natural gas-fired combined cycle plants." Advances in Environmental Research 7(4): 901-911.
[4] Eide L. I. and Bailey D. W. (2005). "Capture pre-combustion." Oil & Gas Science and Technology - Rev. IFP 60(3): 475-484.
[5] Amann J.-M., Kanniche M., Bouallou Ch. (2009). "Reforming natural gas for CO_2 pre-combustion capture in combined cycle power plant." Clean Technologies and Environmental Policy 11(1): 67-76.
[6] Lozza G. and Chiesa P. (2002). "Natural Gas Decarbonization to Reduce CO_2 Emission from Combined Cycles-Part II: Steam-Methane Reforming." Journal of Engineering for Gas Turbines and Power 124(1): 89-95.
[7] Ertesvåg I. S., Kvamsdal H. M. and Bolland O. (2005). "Exergy analysis of a gas-turbine combined-cycle power plant with pre-combustion CO_2 capture." Energy 30(1): 5-39.
[8] Hoffmann S., Bartlett M. , Finkenrath M. , Evulet A. , Ursin T.-P. (2009). "Performance and Cost Analysis of Advanced Gas Turbine Cycles With Pre-combustion CO_2 Capture." Journal of Engineering for Gas Turbines and Power-Transactions of the Asme 131(2).
[9] Nord L. O., Kothandaraman A., Herzog H., McRae G. and Bolland O. (2009). "A modeling software linking approach for the analysis of an integrated reforming combined cycle with hot potassium carbonate CO_2 capture." Energy Procedia 1(1): 741-748.
[10] Nord L.O., 2010. Pre-combustion CO_2 capture: Analysis of integrated reforming combined cycle. Ph.D. thesis, Department of Energy and Process Engineering, Norwegian University of Science and Technology, Trondheim, Norway. http://urn.kb.se/resolve?urn=urn:nbn:no:ntnu:diva-7917
[11] Szargut J, Morris DR, Steward FR., 1988, *Exergy analysis of thermal, chemical and metallurgical processes*. New York: Hemisphere Publishing Corp.
[12] Kotas TJ. , 1995, *The exergy method of thermal plant analysis*. Malabar (FL): Krieger Publishing Company
[13] Grassmann P. (1950). "Zur allgemeinen Definition des Wirkungsgrades." Chemie Ingenieur Technik 22(4): 77-80.
[14] Göttlicher G., 2004, *The Energetics of Carbon Dioxide Capture in Power Plants*, U.S. department of Energy, National energy Technology Laboratory.
[15] Oyenekan B. A. and Rochelle G. T. (2007). "Alternative stripper configurations for CO_2 capture by aqueous amines." Aiche Journal 53(12): 3144-3154.

Paper 4

International Journal of Greenhouse Gas Control 8 (2012) 1–11

Contents lists available at SciVerse ScienceDirect

International Journal of Greenhouse Gas Control

journal homepage: www.elsevier.com/locate/ijggc

Review

Optimized process configurations of post-combustion CO_2 capture for natural-gas-fired power plant – Power plant efficiency analysis

Zeinab Amrollahi*, Paul Andreas Marchioro Ystad, Ivar S. Ertesvåg, Olav Bolland

Department of Energy and Process Engineering, Norwegian University of Science and Technology, Trondheim, Norway

ARTICLE INFO

Article history:
Received 26 May 2011
Received in revised form
23 December 2011
Accepted 13 January 2012
Available online 24 February 2012

Keywords:
CO_2 capture
Chemical absorption
Process modification
Power plant efficiency
Natural-gas-fired power plant

ABSTRACT

Carbon dioxide was removed by chemical absorption processes from the flue gases of natural-gas-fired combined-cycle power plant. The main challenge of chemical absorption processes is reducing the energy requirement. This paper discusses the selection of most important parameters necessary to obtain 90% capture ratio and the lowest energy consumption for the CO_2 capture and compression plants. The integrated capture processes with power plant were evaluated by using the net power-plant efficiency. Several chemical absorption process configurations were analyzed and the design parameters were compared for the different cases. The findings show decreased reboiler energy consumption for the Base case chemical absorption process configuration with 3.74–2.71 MJ/kg CO_2 for the modified chemical absorption process configuration of lean vapor recompression with absorber inter-cooling. The net power plant efficiency with CO_2 capture and compression was increased from 49.4% (LHV) for the Base case chemical absorption process to 50.2% (LHV) for the chemical absorption process with absorber inter-cooling and lean vapor recompression. The power output reduction due to CO_2 capture and compression was decreased from 48 MW for the Base case chemical absorption process to 42.5 MW for the case with absorber inter-cooling and lean vapor recompression.

Contents

* Corresponding author. Tel.: +47 73592768.
E-mail address: zeinab.amrollahi@ntnu.no (Z. Amrollahi).

1750-5836/$ – see front matter © 2012 Elsevier Ltd. All rights reserved.
doi:10.1016/j.ijggc.2012.01.005

Nomenclature

C	ratio between formed CO_2 and fuel, 44 m
$E^{CO_2}_{rem,mech}$	mechanical work required for atmospheric stripping process (MJ/kg CO_2)
$E^{CO_2}_{rem,heat}$	heat required for atmospheric stripping of CO_2 from the solvent (MJ/kg CO_2)
$E^{CO_2}_{comp}$	power requirement for compression of CO_2 (MJ/kg CO_2)
f	CO_2 capture ratio
F_j	overall feed flow rate to stage j (kmol/s) (Fig. 1)
$h_{st,in}$	specific enthalpy of steam supplied to the stripper reboiler (kJ/kg)
$h_{cond,out}$	specific enthalpy of condensate leaving the stripper reboiler (kJ/kg)
H_j,h_j	vapor and liquid enthalpy flow rates from stage j (J/s) (Fig. 1)
$\Delta H_{reaction}^{\circ}$	standard enthalpy change (heat) of reaction (kJ/kmol)
K	equilibrium ratio (k-value)
K_{eq}	equilibrium constant of the reaction
LHV	lower heating value (kJ/kg)
L_j	overall liquid flow rate from stage j (kmol/s) (Fig. 1)
$\dot{m}$	mass flow (kg/s)
P	power (W)
Q_j	heat flow rate to stage j (kJ/s) (Fig. 1)
Q_{reb}	reboiler duty (kJ/s)
R	universal gas constant (kJ/kmol·K)
S_{V_j}, S_{L_j}	overall side stream from stage j in vapor and liquid, respectively (kmol/s) (Fig. 1)
T	temperature (K)
V_j	overall vapor flow rate from stage j (kmol/s) (Fig. 1)
$x_{i,j}$	mole fraction of component i in liquid phase from stage j (Fig. 1)
$y_{i,j}$	mole fraction of component i in vapor phase from stage j (Fig. 1)
$z_{i,j}$	mole fraction of component i in feed to stage j (Fig. 1)

Greek letters

α	ratio of incremental power reduction to incremental heat output ($MJ_{electrical}/MJ_{Heat}$)
η_{ij}	efficiency

Subscripts

cond	condensate
comp	compression
i	component number
j	stage number
mech	mechanical
pp	power plant
reb	reboiler
Ref	reference
st	steam
WO-extr	without steam extraction; reference power plant without CO_2 capture
W-extr	with steam extraction; power plant with CO_2 capture and compression

1. Introduction

CO_2 capture from power plants is based on separation of carbon either from the fuel or from the exhaust. Processes with carbon separation from fuel are called pre-combustion CO_2 capture. Carbon separation from exhaust gases is divided into two groups: oxyfuel or oxy-combustion CO_2 capture, where pure oxygen is the oxidizer, and post-combustion, where ambient air is the oxidizer.

There are several processes to remove CO_2, such as physical/chemical absorption, adsorption, cryogenic separation and membranes. For post-combustion CO_2 capture from a natural-gas-fired power plant, chemical absorption using amine solutions is the most near-term technology according to the IEA report (IEA, 2008). However the high energy consumption of CO_2 removal from the flue gases of natural gas fired power plants is a motivation to improve these processes. Several studies are found in the literature that discusses the two main paths, developing new solvents and optimization of the process configurations (Jassim and Rochelle, 2005; Oyenekan and Rochelle, 2007; Aroonwilas and Veawab, 2007; Schach et al., 2010).

Typically, the energy required in the capture process is provided by the power plant in the form of steam and electricity; steam is required at the reboiler and electricity is needed to run shafts of the blower, pumps and compressor. Therefore, the CO_2 removal process is carried out at the expense of the efficiency of thermo-electrical power plants and the power plant outputs of electricity and available heat are decreased. This shows the necessity of developing improved capture processes with lower energy requirements.

The net electrical efficiency of natural-gas-fired combined-cycle power plants (NGCC) based on state of the art gas turbines, range from 55% to 58% LHV-based. However, addition of a chemical absorption plant for CO_2 capture from exhaust gases leads to power production efficiency penalties of 8–10% points (Peeters et al., 2007; Göttlicher, 2004). Undrum and Bolland (2003) compared NGCC power plants with and without CO_2 capture and quantified the reduced efficiency related to the CO_2 capture process.

Techno-economic and thermodynamic analyses that evaluate NGCCs with CO_2 capture units have been done recently (Peeters et al., 2007; Hammond and Ondo Akwe, 2007; Schach et al., 2010). The literature includes various studies of energy analysis on coal-fired power plants with CO_2 capture units. For instance, Abu-Zahra et al. (2007) investigated the technical performance and economics of CO_2 capture with monoethanolamine (MEA) for a coal-fired power plant. Feron (2010) evaluated the potential improvements of the energy performance for coal fired power plants with CO_2 capture processes. Also heat integration suggestions have been made by Pfaff et al. (2010) to achieve optimized waste heat integration between the post combustion capture process and the power plant.

As mentioned, the high energy requirement of the conventional chemical absorption CO_2 removal with MEA is a motivation to develop different process configurations with lower energy expenditures. For the comparison and improvement of these process alternatives, proper evaluation methods should be developed and applied. The objective of the current study was to analyze, compare and improve various CO_2 capture process configurations in terms of their work demand. Consequently, net power plant efficiency was chosen to compare power plants with different CO_2 capture cases.

The remainder of this article is divided into Section 2, which describes the simulation methodologies for the MEA chemical absorption processes and power plant used in this study; Section 3, which includes the simulated models; Section 4, which shows and discusses the results and Section 5, which is devoted to concluding remarks.

2. Methodology

2.1. Simulation of MEA chemical absorption process

Fig. 3 shows the conventional process configuration for a gas treating system that uses aqueous alkanolamine solutions. The flue

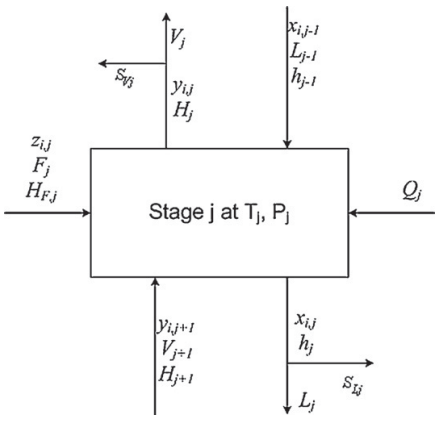

Fig. 1. Generalized stage model and nomenclature for the stage j. F_j = overall feed flow to stage j; z_{ij} = mole fraction of component i in feed to stage j; L_j, V_j = overall liquid and vapor flow from stage j; H_j, h_j = vapor and liquid enthalpy flows from stage j; Q_j = heat flow to stage j; S_{V_j}, S_{L_j} = overall vapor and liquid side-streams from stage j.

gas is contacted with MEA solution counter-currently in a packed absorber column. CO_2 is absorbed into the solvent, which is heated and fed to the top of the stripping column. Steam, which is provided by the column reboiler strips the CO_2 from the MEA solution as it passes down the column while the condenser provides reflux, and the CO_2 recovered overhead as a vapor product. The lean solution is cooled and recycled back to the absorber.

The CO_2 capture and compression units were modeled with UniSim Design software (Honeywell, 2008), which contains the Amines Property Package. This special property package has been designed to aid the modeling of alkanolamine treating units in which CO_2 is removed from gaseous streams. The following paragraphs are devoted to modeling details and the basis of the simulations of UniSim Design and are referred to, for further clarification.

In this property package, a non-equilibrium stage model which is based on the stage efficiency concept is used to simulate the performance of absorber and stripping columns. The generalized stage efficiency definition (η_{ij}) based on Fig. 1 is given (Standart, 1965) as:

$$\eta_{ij} = \frac{(V_j + S_{V_j})y_{i,j} - V_{j+1}y_{i,j+1}}{(V_j + S_{V_j})K_{ij}x_{i,j} - V_{j+1}y_{i,j+1}} \quad (1)$$

where indexes i and j denote, respectively, the component number and the stage number.

This stage efficiency is a function of the kinetic rate constants for the reactions between CO_2 and MEA, the physical and chemical properties of the amine solution, the pressure, temperature and the mechanical tray design variables. The non-equilibrium stage-model functions based in Fig. 1 are:

$$F_j + L_{j-1} + V_{j+1} - (L_j + S_{L_j}) - (V_j + S_{V_j}) = 0 \quad (2)$$

$$F_j z_{i,j} + L_{j-1}x_{i,j-1} + V_{j+1}y_{i,j+1} - (L_j + S_{L_j})x_{i,j} - (V_j + S_{V_j})y_{i,j} = 0 \quad (3)$$

$$F_j H_{F,j} + Q_j + L_{j-1}h_{j-1} + V_{j+1}H_{j+1} - (L_j + S_{L_j})h_j - (V_j + S_{V_j})H_j = 0 \quad (4)$$

$$\eta_{ij}K_{ij}x_{i,j}(V_j + S_{V_j}) - (V_j + S_{V_j})y_{i,j} + (1 - \eta_{ij})V_{j+1}y_{i,j+1} = 0 \quad (5)$$

$$\sum y_{i,j} = 1.0 \quad (6)$$

which are respectively, the overall mass balance, the component mass balance, the energy balance, the stage equilibrium relationship and the summation of mole fractions.

For correlation of the equilibrium solubility of CO_2 in the amine solutions, UniSim Design takes advantage of modified models based on the approach of Kent and Eisenberg (1976) and the study of Li and Mather (1994).

Kent and Eisenberg's (1976) model, which was based on defining the chemical reaction equilibrium in liquid phase, was modified by UniSim Design to extend the reliable range of loadings between 0.0001 and 1. Solubilities of inert components such as hydrocarbons are modeled using Henry's law constant adjusted for ionic strength effects. For phase equilibrium calculations, Henry's law constant has been used for prediction of CO_2 in aqueous phase. The fugacity coefficient of the molecular species of gas phase components was calculated by the Peng–Robinson equation of state (Peng and Robinson, 1976). The prediction of chemical equilibrium constants involves the simultaneous solution of a set of non-linear equations that describe the chemical and phase equilibrium and the electroneutrality (charge balance) and mass balance of the electrolytes in the aqueous phase.

Another simulation approach based on Li and Mather study (1994) uses Clegg and Pitzer's (1992) excess Gibbs energy equations to predict vapor–liquid equilibrium data for the MEA–CO_2–H_2O system using interaction parameters determined from experimental data. It shows a strong predictive capability over a wide range of temperatures, pressures, CO_2 loadings and amine concentration, and provides insights into concentrations of various ionic and molecular species in the liquid phase when CO_2 is dissolved into amine solutions. For phase equilibrium calculations, fugacity coefficients of the molecular species of gas phase components are calculated by the Peng–Robinson equation of state, and activity coefficients are calculated by the Clegg–Pitzer equations. The determination of the compositions of all molecular and ionic species in both vapor and liquid phases involves the simultaneous solution of a set of non-linear equations that describe the phase equilibrium and chemical equilibrium, the electroneutrality (charge balance) and mass balance of the electrolytes in the aqueous solution.

The principal reactions UniSim Design software takes as the basis of simulations are according to the study of Kent and Eisenberg (1976) that is presented below. In the following reactions, RNH_2 represents a primary amine.

Ionization of water:

$$H_2O \rightleftarrows H^+ + OH^- \quad (7)$$

Bicarbonate formation:

$$CO_2 + H_2O \rightleftarrows HCO_3^- + H^+ \quad (8)$$

Dissociation of the bicarbonate ion into the carbonate:

$$HCO_3^- \rightleftarrows CO_3^{2-} + H^+ \quad (9)$$

Carbamate formation:

$$RNH_2 + HCO_3^- \rightleftarrows RNHCOO^- + H_2O \quad (10)$$

Protonation of MEA:

$$RNH_2 + H^+ \rightleftarrows RNH_3^+ \quad (11)$$

For enthalpy calculations, vapor phase enthalpy is calculated by the Peng–Robinson equation of state, which integrates ideal gas heat capacity data from a reference temperature. The liquid phase enthalpy also includes the effects of latent heat of vaporization and heat of reaction. The absorption of CO_2 in an aqueous MEA solution involves heat exchange due to the chemical reaction. This heat effect is a function of concentration and CO_2 mole loadings. The heat

of solution of CO_2 is obtained by differentiating the experimental equilibrium solubility data using Van't Hoff's equation.

$$\left(\frac{\partial \ln K_{eq}}{\partial T}\right)_p = \frac{\Delta H_{reaction}^{\circ}}{RT^2} \quad (12)$$

The heat effect, which results from evaporation and condensation of amine and water in both the absorber and stripper, is accounted for through the latent heat term that appears in the calculation of liquid enthalpy calculation by UniSim design.

For simulation of the gaseous streams in the flue gas cooling section, the blower section and the compression section, the Peng–Robinson equation-of-state was used.

2.2. Power plant simulations

The power plant subsystems that were analyzed included gas turbine (GT), heat recovery steam generator (HRSG), steam turbine (ST) and condenser. The power plant design was done by GT PRO (Thermoflow Inc., 2009) and is described in Section 3.1.

The energy analysis of the power cycles integrated with CO_2 capture plant was expressed in terms of power production penalty, and the following equations were defined to quantify these power production penalties:

- α-Value, which is the ratio between the power reduction of the power plant due to steam extraction and the equivalent heat acquired from the extracted steam to provide the reboiler heat requirement;

$$\alpha = \frac{P_{pp\ \ WO\text{-}extr} - P_{pp\ \ W\text{-}extr}}{Q_{Reboiler}} \quad (13)$$

$$Q_{Reboiler} = \dot{m}_{st}(h_{st,in} - h_{cond,out}) \quad (14)$$

where $\dot{m}_{st}$ denotes the steam mass flow extracted from the steam turbine and supplied to the reboiler, $h_{st,in}$ is the enthalpy of steam to the reboiler and $h_{cond,out}$ the enthalpy of returning condensate.

Since the steam extracted from ST is superheated, it is saturated with water injection and supplied to the reboiler at the exact temperature and pressure that is required for the regeneration process.

- Net power plant efficiency:

$$\eta_{pp} = \underbrace{\eta_{Ref.\ \ NGCC}}_{a} - \underbrace{\frac{E_{rem,mech}^{CO_2} C}{LHV}}_{b} - \underbrace{\frac{E_{rem,heat}^{CO_2} \alpha\ Cf}{LHV}}_{c} - \underbrace{\frac{E_{comp}^{CO_2} Cf}{LHV}}_{d} \quad (15)$$

When the chemical absorption CO_2 capture and compression plants are integrated into a power plant, there are several associated power losses at different points of the process. These energy penalties are related to mechanical work demand of blower and several pumps/compressor in the capture plant (term *b* in Eq. (15)), the steam turbine power reduction due to steam extraction to provide the reboiler steam-need for the stripper column (term *c* in Eq. (15)), and the mechanical work demand of the compressors to compress captured CO_2 to a certain transport/injection pressure (term *d* in Eq. (15)) (Undrum and Bolland, 2003).

3. Model description

3.1. Reference NGCC without CO_2 capture

The natural-gas-fired combined-cycle power plant was designed with a power plant configuration of GT, HRSG and triple-pressure-condensing-reheat ST. The plant was designed for ambient conditions of 25 °C and 1.0132 bar. The GT was selected from the GT PRO library as Siemens SGT5-4000F, and the fuel selection to the combustor was natural gas without H_2S and with a lower heating value of 46.28 MJ/kg (at 25 °C). This corresponded to a rate of 681.4 MW fuel heat input to the GT. The flue gas flowing through the HRSG exits as exhaust gas with a flow rate of 650.9 kg/s at atmospheric pressure and 94 °C. The flow sheet of the designed combined cycle power plant is shown in Fig. 2. The power production was 384.4 MW, giving a net electric efficiency of 56.4% (LHV).

3.2. CO_2 capture scenarios

In the current study, six different CO_2 capture process configurations (Figs. 3–8) were simulated. After design, some of the main parameters affecting the capture processes were varied as an initial step toward the optimization of the processes. The optimization target was toward the reduction of reboiler energy consumption and the total work demand of the CO_2 capture plant.

The reboiler steam demand was supplied through extraction from ST. The extraction bleed from ST was superheated steam at 4.28 bar and 302.6 °C. This was mixed with desuperheating water. After the pipe losses, the process steam was delivered to the reboiler at 4 bar and 145 °C, which is 1.4 °C superheated. The thermodynamic conditions of steam extraction from ST were kept constant for all cases.

3.2.1. Base case model

As a Base case, the chemical absorption CO_2 capture and compression units shown in Fig. 3, were simulated with the capture ratio set to 90%. To summarize the process, the flue gas, which is flowing at atmospheric pressure, is cooled with a direct-contact water-cooler to 42 °C and is blown with a blower to the absorber to overcome the pressure drop caused by the absorber. After entering the absorber, it flows through the column while contacting with MEA solvent flowing counter-currently. The reaction between MEA solvent and the CO_2 is forming a water soluble salt. The amine stream that leaves the bottom of the absorber is referred to as *rich amine* stream since it is loaded with CO_2. The CO_2-rich MEA solution is preheated in a heat exchanger and enters a stripper column to regenerate the solvent and reverse the reaction by means of heat supplied in a reboiler and release the CO_2 content as a stream leaving at the top of the column. The amine stream that leaves the bottom of the stripper is referred to as *lean amine* stream since it is stripped of CO_2. The lean MEA solution is recycled back to the absorption column while the CO_2 stream goes to the compression section. The CO_2 compression was done in three stages with inter-cooling to 30 °C, where the CO_2 stream was compressed to 80 bar and then pumped to storage section at 110 bar. The adiabatic efficiency of the three stages was set to 85%.

Table 1 shows the flue gas specifications and design parameters for the chemical absorption and compression units, which were held constant from the Base case to the other process configurations. The absorber performance was controlled by adjusting the solvent circulation rate to meet 90% CO_2 capture ratio.

The lean solution CO_2 molar fraction and the condenser temperature were specified as the stripper specification. Particularly, the CO_2 molar fraction of the lean solution was twigged to reach the lowest reboiler duty in the Base case and the other cases. The stripper pressure was set at 1.86 bar with the condenser pressure set at 1.1 bar. According to Abu-Zahra et al. (2007), the increased operating pressure of the stripper from 1.5 to 2.1 bar led to a 8.5% reduction in the thermal energy requirement of the stripping process. However, higher degradation rates and corrosion problem should be expected.

CO_2 loading is one of the optimized parameters that specifies the amount of CO_2 absorbed in molecular form by the solution. In

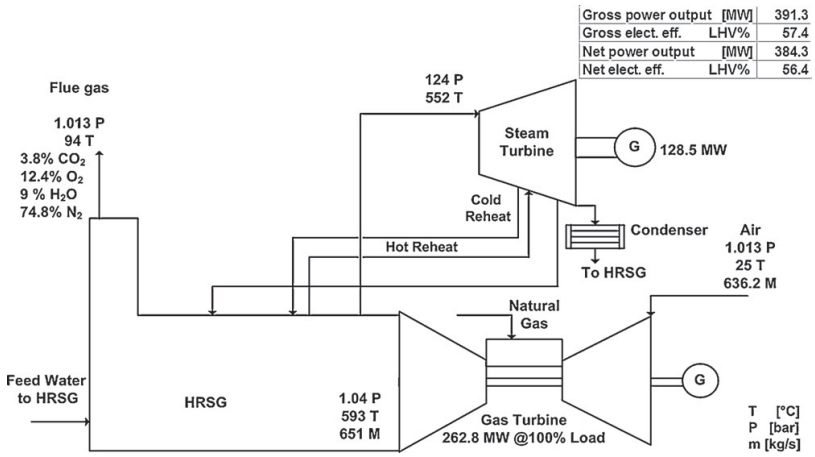

Fig. 2. Flowsheet of the reference power plant.

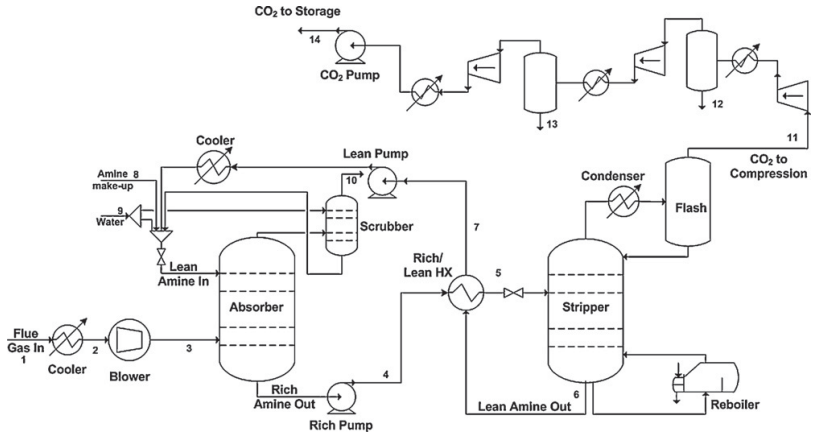

Fig. 3. Flow sheet of the Base case CO_2 capture and compression units.

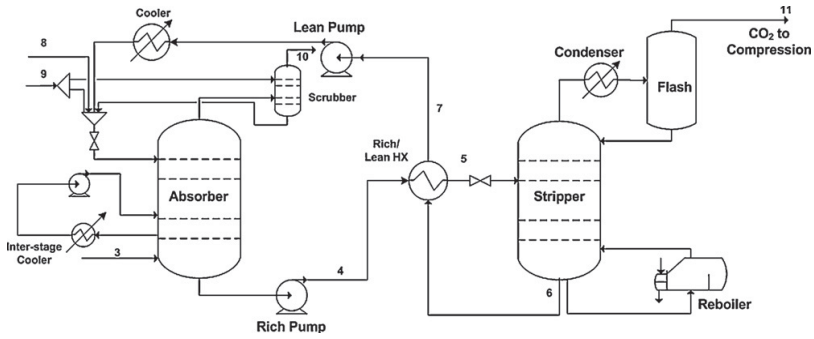

Fig. 4. Process flowsheet of absorber inter-cooling (Case 1).

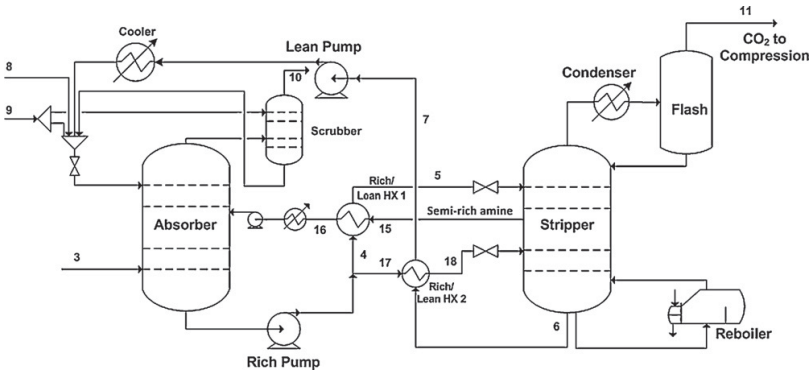

Fig. 5. Process flowsheet with split-flow to stripper (Case 2).

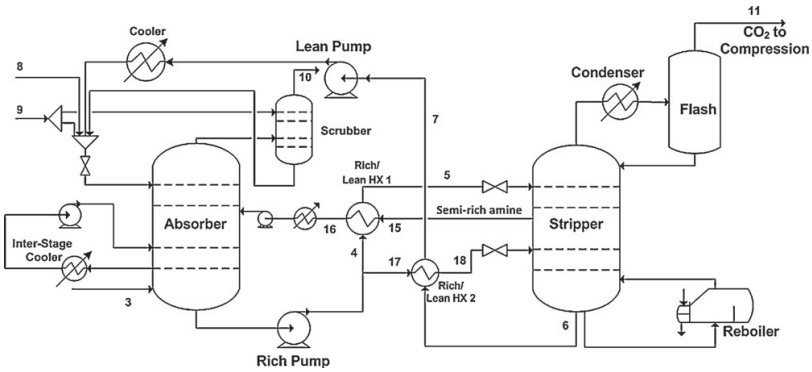

Fig. 6. Process flowsheet of absorber inter-cooling with split-flow feed to stripper (Case 3).

the current study it was defined as the ratio of CO_2 mole fraction and MEA mole fraction in the solution:

$$\text{Loading} = \frac{x_{CO_2}}{x_{MEA}} \tag{16}$$

The optimized CO_2 molar fraction at the bottom of the stripper, rich and lean loading, and solvent circulation rate is shown in Table 2.

3.2.2. Absorber inter-cooling model (Case 1)

The concept behind inter-cooling is to remove the heat generated by the exothermic absorption reaction and reduce the liquid temperature at the absorber bottom. Because of the exothermic nature of absorption reaction, there is an overall temperature increase in the absorber. Inter-cooling causes temperature reduction, which is in favor of higher driving force for the absorption process and increases the absorption capacity of the solvent, i.e. solvent rich loading. Higher rich loadings lead to reduced solvent

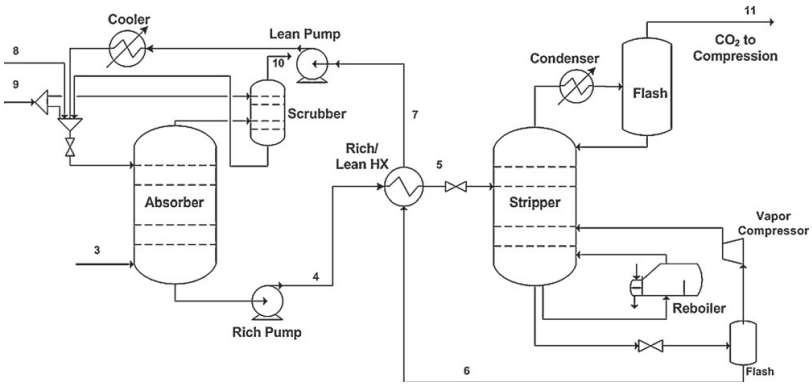

Fig. 7. Process flowsheet of stripping with lean vapor recompression (Case 4).

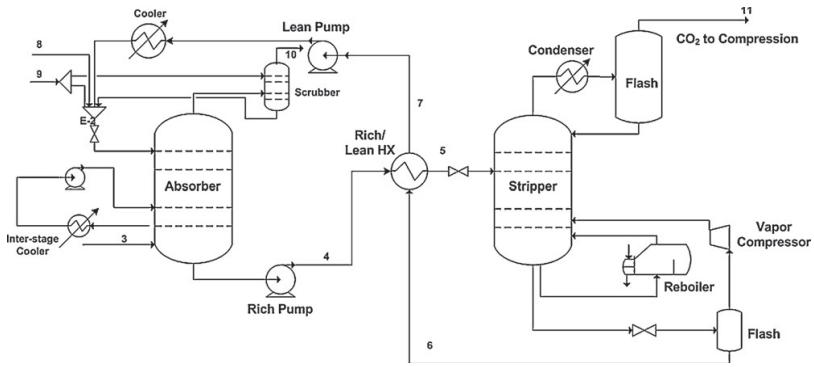

Fig. 8. Process flowsheet of absorber inter-cooling with lean vapor recompression stripping (Case 5).

Table 1
Design parameters for all process configurations.

Solvent	30	wt. % MEA
CO_2 capture ratio[a]	90	%
Flue gas mass flow	650.9	kg/s
Flue gas composition		
CO_2	3.80	vol %
O_2	12.42	vol %
N_2	74.76	vol %
H_2O	9.02	vol %
Rich/lean HX minimum approach temperature	8.5	°C
CO_2 compression final pressure	110	bar
Absorber		
No. of stages	13	
Absorber pressure	1.1	bar
Pressure drop	50	mbar
Lean solvent inlet temperature	40	°C
Cooled flue gas inlet temperature	50.3	°C
Stripper		
No. of stages	36	
Condenser temperature	30	°C
Reboiler pressure	1.86	bar
Cooling water temperature	8	°C
Cooling water ΔT	10	K
Steam to reboiler		
Temperature	145	°C
Pressure	4	bar
Condensate		
Temperature	130	°C
Pressure	3.92	bar

[a] CO_2 capture ratio is defined as the fraction of CO_2 that is separated from the flue gas.

circulation rates and lower regeneration energy requirements. The modification to the Base case as illustrated in Fig. 4 is to extract semi-rich stream from the lower part of the absorber, cool via inter-stage cooler down to 25 °C and recycle it to the absorber column. All other process units and conditions are identical to the Base case. The flow rate of side-draw stream to the cooler, the cooling temperature of the side-draw stream and the location of side-draw stream have been subject to optimization to approach the less reboiler duty compared to the Base case. Due to the higher attainable rich loading and reduction in the solvent circulation rate, the stripper reboiler duty has been decreased. The results of optimization showed the side-stream draw point at near bottom of the column and returns at one upper stage. Table 2 shows the lean solution CO_2 molar fraction at the bottom of the stripper, which was subject to optimization, and the rich and lean loading and the solvent circulation rate for this process configuration. Several authors such as Tobiesen and Dorao (2008) and Chang and Shih (2005) have investigated configurations with inter-stage coolers.

3.2.3. Split-flow model (Case 2)

The split-flow configuration for chemical absorption processes, which is illustrated in Fig. 5, was developed and suggested by Thompson and King (1987) and further analyzed by Kohl and Nielsen (1997) to reduce steam consumption of solvent regeneration. In the article by Aroonwilas and Veawab (2006), the authors pointed out 35% energy saving in reboiler duty for 95% CO_2 capture ratio. However, they pointed out the need of trade-off between the energy cost and the additional capital investment cost since the impact of complexity of the process on the investment cost should not be neglected.

In this configuration, the rich amine leaving the absorber is split between two feed points to the stripper. One stream enters the top of the stripper and leaves it from the middle point and returns to the middle of the absorber. The other split enters the bottom of the stripper and leaves it toward the top of the absorber. Since less amount of rich amine enters the stripper bottom section, the solvent would be stripped to the same CO_2 loading with lower energy input. Moreover, *semi-rich amine* enters the absorber column at 25 °C and cools the absorber column which favors the absorption process as discussed in Section 3.2.2.

The split flow fraction, the feed tray of the second split to the stripper, the flow rate and the feed location of *semi-rich amine* that returns to the absorber were subject to optimization in this configuration. Furthermore, as in all the other configurations, the CO_2 molar fraction in lean solution and the condenser temperature were subject to optimization that is presented in Table 2.

Table 2
Optimized design parameters for various process cases.

	Base case	Case 1	Case 2	Case 3	Case 4	Case 5
CO_2 mole fraction in lean solution	2.51×10^{-2}	2.47×10^{-2}	2.45×10^{-2}	2.47×10^{-2}	2.5×10^{-2}	2.48×10^{-2}
Lean loading	0.22	0.22	0.22	0.23	0.23	0.23
Rich loading	0.47	0.48	0.47	0.49	0.47	0.48
Solvent circulation rate (kg/s)	649.4	613.8	550.3	529.3	641.2	611.1

Case 1: absorber inter-cooling; Case 2: split-flow; Case 3: absorber inter-cooling + split-flow; Case 4: lean vapor recompression; Case 5: absorber inter-cooling + LVR.

3.2.4. Absorber inter-cooling combined with split-flow model (Case 3)

This process configuration illustrated in Fig. 6 combines the effect of inter-cooling of absorber column and the split-flow configuration. The parameters that were subject to optimization include the flow-rate of inter-cooled stream, the split flow fraction and the flow rate of *semi-rich amine* from the stripper. The mole fraction of CO_2 at the bottom of the absorber, the rich and lean loadings and the solvent circulation rate are shown in Table 2.

3.2.5. Lean vapor recompression (LVR) model (Case 4)

There are several designs presented in the literature as the vapor recompression models. The purpose of vapor recompression designs is to provide steam that is regained from the stripping process as the heating media to the reboiler. One of the alternative designs of the vapor recompression model has been presented by Jassim and Rochelle (2005). In this design, the stripper bottom is used to intercool the gaseous stream in the multistage compressor. The purpose of the design is to recover the heat of condensation of the overhead water vapor and the heat of compression to re-boil the stripper. For the aforementioned design, the number of compression stages has been doubled. The results of this study show that the reboiler duty has been decreased by 43%, but the total work demand of the process stayed at the same level regarding the increased amount of CO_2 compression work.

Another design, which was modeled and analyzed in the current study, is a patent-based model outlined by Reddy et al. (2007). This lean vapor recompression design is based on flashing lean solution to generate the steam feed that is introduced to the stripper column via a compressor. The compressor type is a thermocompressor or mechanical vapor recompressor (Minton, 1986). The advantage of this design as claimed by Reddy et al. (2007) is that the water balance in the stripping column remains unaltered, which is one of the main concerns in other vapor recompression designs. A further modification to this model has been presented by Woodhouse et al. (2009), which integrates the usage of low temperature heat for generation of steam in various stripping process locations.

With vapor recompression as shown in Fig. 7, the lean solution that is leaving the stripping column, decreases its pressure through a flash valve to 1 bar and flashes through a flash drum to produce the gaseous phase. This gaseous phase composed mainly of water vapor, is recompressed to 2 bar and reintroduced to the stripping column. Similar to the Base case, the liquid phase is cooled down by the rich solvent and returns to the absorber. The optimized mole fraction of CO_2 at the bottom of the absorber and rich and lean CO_2 loading is shown in Table 2.

3.2.6. LVR combined with absorber inter-cooling model (Case 5)

This process configuration illustrated in Fig. 8 combines the effect of inter-cooling of absorber column and the configuration of lean vapor recompression. The parameters that were subject to optimization include the flow-rate of inter-cooled stream, the optimized molar composition fraction of CO_2 component at the bottom of the absorber, rich and lean loading and solvent circulation rate, as shown in Table 2.

Table 3
Reboiler energy consumption and power/heat factor for the optimized process configurations (steam and condensate specifications are given in Table 2).

	Base case	Case 1	Case 2	Case 3	Case 4	Case 5
α (power/heat factor)	0.24	0.24	0.24	0.24	0.24	0.24
Duty reboiler (MJ/kg CO_2)	3.74	3.62	3.48	3.30	2.77	2.71

4. Results and discussion

In this section, several sets of results are presented and discussed. Section 4.1 shows the results of work demand for all five process configurations. The data for each stream from the simulations of each of the various cases are reported in Appendix A. The work demand amounts that are presented in Section 4.1 are the basis of net electrical efficiency calculations, which are shown in Section 4.2. This subsection includes the results of the integrated NGCC with various CO_2 capture scenarios and compares the energy efficiency of the reference NGCC integrated with CO_2 capture and compression plant.

4.1. Total work demand of chemical absorption process configurations

As mentioned earlier, the process configurations that were described in Section 3.2 were optimized regarding lower energy consumption. By addressing the definition from Eq. (13), the α value was calculated for each case. It was expected that since the thermodynamic conditions of the steam supply to the reboiler and condensate return to the power plant was kept constant for all simulated cases, the α calculation would result in the approximately same amount that is shown in Table 3.

As Table 4 lists, the total work demand of the capture and compression processes consisted of power penalty due to regeneration of solvent, power requirement for the pumps and the blower and the compressor in LVR configurations, and the CO_2 compression work demand.

Obviously, as the reboiler duty was decreased from the Base case to the last case, the total work demand for each case was decreased. It should be mentioned that for Lean vapor recompression (LVR) model (Case 4) and LVR combined with absorber inter-cooling model (Case 5), the compressor work needed for lean vapor recompression increased the work amount that was covered under the *Other work* term. Nevertheless, the major reduction of energy requirement of the reboiler, led to overall work demand reduction for Cases 4 and 5.

The compression work demand remained approximately constant since the capture ratio was set at 90% of the CO_2 content from flue gas.

4.2. Natural gas fired power plant with CO_2 capture and compression plant

Based on the definitions clarified in Section 2.2, the comparison analysis has been done on the integration of each of the cases with the reference power plant and the results of net power plant efficiency (%LHV) have been demonstrated in Table 5. As the total work demand of the CO_2 capture and compression plants was decreased

Table 4
Total work demand for the optimized process configurations.

	Base case	Case 1	Case 2	Case 3	Case 4	Case 5
Power production penalty for solvent regeneration (MJ/kg CO_2)	0.90	0.88	0.84	0.80	0.66	0.65
CO_2 compression work (MJ/kg CO_2)	0.33	0.33	0.33	0.33	0.33	0.33
Other work-pumps, blower (MJ/kg CO_2)	0.15	0.15	0.16	0.16	0.25	0.25
Total work (MJ/kg CO_2)	1.39	1.36	1.33	1.29	1.25	1.23

Table 5
Summary of results for the NGCC with and without post-combustion CO_2 capture (natural gas LHV input (MW_{th}) = 681.421).

	Reference plant without capture	Ref. plant + Base case capture	Ref. plant + Case 1	Ref. plant + Case 2	Ref. plant + Case 3	Ref. plant + Case 4	Ref. plant + Case 5
Net power plant efficiency (%LHV)	56.40	49.35	49.53	49.67	49.96	50.06	50.16
Net power output (MW)	384.31	336.30	337.49	338.44	340.42	341.10	341.78

along the cases, the power plant efficiency penalty was decreased from 7.0 percentage points for the Base case to 6.2 percentage points for Case 5.

The choice of the best option from the current energy analysis has supported by an exergy analysis of the same processes that would be presented in the second part of the paper (Amrollahi et al., 2011). By means of exergy analysis, the minimum work requirement of the each process was calculated and the rate of irreversibility changes in the process sections for different process configuration was demonstrated.

This study was based on MEA solvent; though the effect of process modifications on minimizing the total work demand could be coupled with choice of other types of solvents with lower binding energies.

The main limitation of the improvements is the increase of complexity of such processes which would lead to higher costs of design and operation. This necessitates the combination of overall economical and technical analysis for the power plant with capture and compression to avoid costly and non-operable designs.

5. Concluding remarks

The process configuration modifications were selected in this study to optimize the overall efficiency of the NGCC power plant integrated with a post combustion capture CO_2 capture and compression plant. Six chemical absorption plants for CO_2 capture were analyzed and compared according to their total work demand. These cases comprised the typical chemical absorption process as the Base case, Case 1 as the chemical absorption process with absorber inter-cooling, Case 2 as the chemical absorption process with split flow configuration, Case 3 as the chemical absorption process with absorber inter-cooling and split flow configuration, Case 4 as the chemical absorption process with lean vapor recompression (LVR) and Case 5 as the chemical absorption process with absorber inter-cooling and LVR. Various process parameters for the chemical absorption process were chosen and optimized to fulfil the aim of lowering the reboiler duty and reduction of total work demand. The best optimized process with lowest work demand was the fifth case i.e. the absorber inter-cooling with stripper lean vapor recompression.

From the Base case to the fifth case, reboiler heat consumption decreased from 3.74 MJ/kg CO_2 to 2.71 MJ/kg CO_2. For the fourth and fifth cases, the addition of vapor compressor increased the *Other work* which is defined in Section 4.1, but the total work demand of the capture and compression plants decreased from the fourth to the fifth case.

Along the reduction of total work demand for the CO_2 capture and compression plant from the Base case to the fifth case, the power plant efficiency penalty decreased from 7% points for the Base case to 6.2% points for Case 5.

Acknowledgments

This publication forms a part of the BIGCO2 project, performed under the strategic Norwegian research program Climit. The authors acknowledge the partners: Statoil, GE Global Research, Statkraft, Aker Clean Carbon, Shell, TOTAL, ConocoPhillips, ALSTOM, the Research Council of Norway (178004/I30 and 176059/I30) and Gassnova (182070) for their support.

Appendix A.

The details of the streams resulting from the simulations for each of the cases are reported here in Tables 6–11. The points that are selected to show in the tables consist of, but are not limited to, flue gas entering the chemical absorption process, the exhaust gas that is leaving from the top of the scrubber, rich amine from the absorber and lean solution from the stripper, amine and water make-up streams, stream of captured CO_2 and stream of compressed CO_2.

Table 6
List of streams with their thermodynamic data, streams' compositions, and molar enthalpy for Base case. Selected positions according to Fig. 3.

Stream no.	Temperature (°C)	Pressure (bar)	Mass flow (kg/s)	Molar enthalpy (kJ/kmol)	Mole fraction				
					CO_2	N_2	O_2	H_2O	MEA
1	94.0	1.0	650.9	10,847.1	0.038	0.748	0.124	0.090	0.000
2	42.0	1.0	646.7	9290.1	0.038	0.755	0.125	0.081	0.000
3	48.4	1.1	646.7	9479.3	0.038	0.755	0.125	0.081	0.000
4	46.0	6.8	699.2	−27,991.6	0.052	0.000	0.000	0.838	0.110
5	110.3	6.4	699.2	−22,253.9	0.052	0.000	0.000	0.838	0.110
6	119.0	1.9	663.6	−20,433.3	0.025	0.000	0.000	0.862	0.113
7	54.5	1.5	663.6	−26,340.1	0.025	0.000	0.000	0.862	0.113
8	25.0	4.0	0.1	21,546.5	0.000	0.000	0.000	0.000	1.000
9	25.0	4.0	16.9	−34,106.1	0.000	0.000	0.000	1.000	0.000
10	49.4	1.0	628.1	9528.9	0.004	0.752	0.125	0.120	0.000
11	30.1	1.1	35.4	9576.2	0.961	0.000	0.000	0.039	0.000
12	20.0	4.3	0.5	−286,862.1	0.002	0.000	0.000	0.998	0.000
13	20.0	18.9	0.1	−287,683.7	0.010	0.000	0.000	0.990	0.000
14	24.9	11.0	34.8	−404,508.8	0.998	0.000	0.000	0.002	0.000

Table 7
List of streams with their thermodynamic data, streams' compositions and molar enthalpy for Case 1. Selected positions according to Fig. 4.

Stream no.	Temperature (°C)	Pressure (bar)	Mass flow (kg/s)	Molar enthalpy (kJ/kmol)	Mole fraction				
					CO_2	N_2	O_2	H_2O	MEA
1	94.0	1.0	650.9	10,847.1	0.038	0.748	0.124	0.090	0.000
2	42.0	1.0	646.7	9290.1	0.038	0.755	0.125	0.081	0.000
3	48.4	1.1	646.7	9479.3	0.038	0.755	0.125	0.081	0.000
4	41.4	6.8	671.5	−28,506.0	0.052	0.000	0.000	0.840	0.108
5	110.2	6.4	671.5	−22,397.7	0.052	0.000	0.000	0.840	0.108
6	119.0	1.9	636.1	−20,563.5	0.025	0.000	0.000	0.864	0.111
7	49.9	1.5	636.1	−26,856.7	0.025	0.000	0.000	0.864	0.111
8	25.0	4.0	6.0	21,546.5	0.000	0.000	0.000	0.000	1.000
9	25.0	4.0	7.0	−34,106.1	0.000	0.000	0.000	1.000	0.000
10	45.6	1.0	618.4	9388.0	0.004	0.770	0.128	0.099	0.000
11	30.1	1.1	35.3	9577.2	0.961	0.000	0.000	0.039	0.000
12	20.0	4.3	0.5	−286,862.1	0.002	0.000	0.000	0.998	0.000
13	20.0	18.9	0.1	−287,683.7	0.010	0.000	0.000	0.990	0.000
14	24.9	11.0	34.8	−404,508.8	0.998	0.000	0.000	0.002	0.000

Table 8
List of streams with their thermodynamic data, streams' compositions and molar enthalpy for Case 2. Selected positions according to Fig. 5.

Stream no.	Temperature (°C)	Pressure (bar)	Mass flow (kg/s)	Molar enthalpy (kJ/kmol)	Mole fraction				
					CO_2	N_2	O_2	H_2O	MEA
1	94.0	1.0	650.9	10,847.1	0.038	0.748	0.124	0.090	0.000
2	42.0	1.0	646.7	9290.1	0.038	0.755	0.125	0.081	0.000
3	48.4	1.1	646.7	9479.3	0.038	0.755	0.125	0.081	0.000
4	43.5	6.5	400.8	−28,447.7	0.049	0.000	0.000	0.846	0.104
5	98.2	6.1	400.8	−23,635.0	0.049	0.000	0.000	0.846	0.104
6	119.1	1.9	566.1	−20,477.8	0.025	0.000	0.000	0.864	0.112
7	52.0	1.5	566.1	−26,606.6	0.025	0.000	0.000	0.864	0.112
8	25.0	4.0	0.2	21,546.5	0.000	0.000	0.000	0.000	1.000
9	25.0	4.0	10.1	−34,106.1	0.000	0.000	0.000	1.000	0.000
10	46.7	1.0	621.1	9428.1	0.004	0.765	0.127	0.105	0.000
11	30.1	1.1	35.4	9576.5	0.961	0.000	0.000	0.039	0.000
12	20.0	4.3	0.5	−286,862.1	0.002	0.000	0.000	0.998	0.000
13	20.0	18.9	0.1	−287,683.7	0.010	0.000	0.000	0.990	0.000
14	24.9	110	34.8	−404,508.8	0.998	0.000	0.000	0.002	0.000
15	106.7	1.8	400.0	−22,978.2	0.040	0.000	0.000	0.861	0.098
16	53.7	1.4	400.0	−27,702.7	0.040	0.000	0.000	0.861	0.098
17	43.5	6.5	601.2	−28,447.7	0.049	0.000	0.000	0.846	0.104
18	109.5	6.1	601.2	−22,600.2	0.049	0.000	0.000	0.846	0.104

Table 9
List of streams with their thermodynamic data, streams' compositions and molar enthalpy for Case 3. Selected positions according to Fig. 6.

Stream no.	Temperature (°C)	Pressure (bar)	Mass flow (kg/s)	Molar enthalpy (kJ/kmol)	Mole fraction				
					CO_2	N_2	O_2	H_2O	MEA
1	94.0	1.0	650.9	10,847.1	0.038	0.748	0.124	0.090	0.000
2	42.0	1.0	646.7	9290.1	0.038	0.755	0.125	0.081	0.000
3	48.4	1.1	646.7	9479.3	0.038	0.755	0.125	0.081	0.000
4	37.0	6.5	397.5	−29,091.0	0.050	0.000	0.000	0.847	0.102
5	96.0	6.1	397.5	−23,938.5	0.050	0.000	0.000	0.847	0.102
6	118.9	1.9	553.5	−20,661.1	0.025	0.000	0.000	0.866	0.110
7	45.5	1.5	553.5	−27,315.6	0.025	0.000	0.000	0.866	0.110
8	25.0	4.0	0.3	21,546.5	0.000	0.000	0.000	0.000	1.000
9	25.0	4.0	1.2	−34,106.1	0.000	0.000	0.000	1.000	0.000
10	43.5	1.0	614.1	9313.9	0.004	0.778	0.129	0.089	0.000
11	30.1	1.1	35.0	9577.3	0.960	0.000	0.000	0.039	0.000
12	20.0	4.3	0.5	−286,862.1	0.002	0.000	0.000	0.998	0.000
13	20.0	18.9	0.1	−287,683.7	0.010	0.000	0.000	0.990	0.000
14	24.9	110	34.8	−404,508.8	0.998	0.000	0.000	0.002	0.000
15	104.5	1.8	405.1	−23,191.0	0.042	0.000	0.000	0.860	0.098
16	49.2	1.4	405.1	−28,158.5	0.042	0.000	0.000	0.860	0.098
17	37.0	6.5	596.3	−29,091.0	0.050	0.000	0.000	0.847	0.102
18	108.3	6.1	596.3	−22,820.4	0.050	0.000	0.000	0.847	0.102

Table 10
List of streams with their thermodynamic data, streams' compositions and molar enthalpy for Case 4. Selected positions according to Fig. 7.

Stream no.	Temperature (°C)	Pressure (bar)	Mass flow (kg/s)	Molar enthalpy (kJ/kmol)	Mole fraction				
					CO_2	N_2	O_2	H_2O	MEA
1	94.0	1.0	650.9	10,847.1	0.038	0.748	0.124	0.090	0.000
2	42.0	1.0	646.7	9290.1	0.038	0.755	0.125	0.081	0.000
3	48.4	1.1	646.7	9479.3	0.038	0.755	0.125	0.081	0.000
4	45.9	6.8	689.9	−28,001.3	0.052	0.000	0.000	0.838	0.110
5	93.1	6.4	689.9	−23,829.4	0.052	0.000	0.000	0.838	0.110
6	101.8	1.0	654.5	−22,039.7	0.025	0.000	0.000	0.862	0.113
7	54.4	0.6	654.5	−26,335.1	0.025	0.000	0.000	0.862	0.113
8	25.0	4.0	0.0	21,546.5	0.000	0.000	0.000	0.000	1.000
9	25.0	4.0	17.0	−34,106.1	0.000	0.000	0.000	1.000	0.000
10	49.5	1.0	628.4	9532.9	0.004	0.751	0.125	0.120	0.000
11	30.2	1.1	35.4	9578.1	0.961	0.000	0.000	0.039	0.000
12	20.0	4.3	0.5	−286,862.1	0.002	0.000	0.000	0.998	0.000
13	20.0	18.9	0.1	−287,683.7	0.010	0.000	0.000	0.990	0.000
14	24.9	110	34.8	−404,508.8	0.998	0.000	0.000	0.002	0.000

Table 11
List of streams with their thermodynamic data, streams' compositions, and molar enthalpy for Case 5. Selected positions according to Fig. 8.

Stream no.	Temperature (°C)	Pressure (bar)	Mass flow (kg/s)	Molar enthalpy (kJ/kmol)	Mole fraction				
					CO_2	N_2	O_2	H_2O	MEA
1	94.0	1.0	650.9	10,847.1	0.038	0.748	0.124	0.090	0.000
2	42.0	1.0	646.7	9290.1	0.038	0.755	0.125	0.081	0.000
3	48.4	1.1	646.7	9479.3	0.038	0.755	0.125	0.081	0.000
4	41.8	6.8	667.9	−28,459.8	0.052	0.000	0.000	0.840	0.108
5	93.0	6.4	667.9	−23,955.7	0.052	0.000	0.000	0.840	0.108
6	101.7	1.0	632.4	−22,152.3	0.024	0.000	0.000	0.864	0.111
7	50.3	0.6	632.4	−26,794.2	0.024	0.000	0.000	0.864	0.111
8	25.0	4.0	0.1	21,546.5	0.000	0.000	0.000	0.000	1.000
9	25.0	4.0	7.6	−34,106.1	0.000	0.000	0.000	1.000	0.000
10	45.8	1.0	618.9	9393.6	0.004	0.769	0.128	0.100	0.000
11	30.1	1.1	35.5	9576.4	0.961	0.000	0.000	0.039	0.000
12	20.0	4.3	0.5	−286,862.1	0.002	0.000	0.000	0.998	0.000
13	20.0	18.9	0.1	−287,683.7	0.010	0.000	0.000	0.990	0.000
14	24.9	110	34.8	−404,508.8	0.998	0.000	0.000	0.002	0.000

References

Abu-Zahra, M.R.M., Schneiders, L.H.J., Niederer, J.P.M., 2007. CO_2 capture from power plants. Part I. A parametric study of the technical performance based on monoethanolamine. International Journal of Greenhouse Gas Control 1 (1), 37–46.

Amrollahi, Z., Ertesvåg, I.S., Bolland, O., 2011. Optimized process configurations of post-combustion CO_2 capture for natural-gas-fired power plant—Exergy analysis. International Journal of Greenhouse Gas Control 5 (6), 1393–1405.

Aroonwilas, A., Veawab, A., 2007. Integration of CO_2 capture unit using single- and blended-amines into supercritical coal-fired power plants: implications for emission and energy management. International Journal of Greenhouse Gas Control 1 (2), 143–150.

Aroonwilas, A., Veawab, A., 2006. Cost structure and performance of CO_2 capture unit using split-stream cycle. In: 8th International Conference on Greenhouse Gas Control Technologies, Trondheim, Norway.

Chang, H., Shih, C.M., 2005. Simulation and optimization for power plant flue gas CO_2 absorption–stripping systems. Separation Science and Technology. 40 (4), 877–909.

Clegg, S.L., Pitzer, K.S., 1992. Thermodynamics of multicomponent, miscible, ionic solutions: generalized equations for symmetrical electrolytes. The Journal of Physical Chemistry 96, 3513–3520.

Feron, P.H.M., 2010. Exploring the potential for improvement of the energy performance of coal fired power plants with post-combustion capture of carbon dioxide. International Journal of Greenhouse Gas Control 4, 152–160.

Göttlicher, G., 2004. The Energetics of Carbon Dioxide Capture in Power Plants. U.S. Department of Energy, National energy Technology Laboratory.

GT PRO version 19, 2009, Thermoflow Inc.

Hammond, G.P., Ondo Akwe, S.S., 2007. Thermodynamic and related analysis of natural gas combined cycle power plants with and without carbon sequestration. International Journal of Energy Research 31 (12), 1180–1201.

IEA, 2008, Carbon Dioxide Carbon and Storage (a key carbon abatement option). OECD.

Jassim, M.S., Rochelle, G.T., 2005. Innovative absorber/stripper configurations for CO_2 capture by aqueous monoethanolamine. Industrial & Engineering Chemistry Research 45 (8), 2465–2472.

Kent, R.L., Eisenberg, B., 1976. Better data for amine treating. Hydrocarbon Processing 55, 87–90.

Kohl, A., Nielsen, R., 1997. Gas Purification, fifth ed. Gulf Publishing Company, Texas.

Li, Y.G., Mather, A.E., 1994. Correlation and Prediction of the Solubility of Carbon-Dioxide in a Mixed Alkanolamine Solution. Industrial & Engineering Chemistry Research 33, 2006–2015.

Minton, P.E., 1986. Handbook of Evaporation Technology. Noyes Publications, Park Ridge, N.J., U.S.A.

Oyenekan, B.A., Rochelle, G.T., 2007. Alternative stripper configurations for CO_2 capture by aqueous amines. AIChE Journal 53 (12), 3144–3154.

Peeters, A.N.M., Faaij, A.P.C., Turkenburg, W.C., 2007. Techno-economic analysis of natural gas combined cycles with post-combustion CO_2 absorption, including a detailed evaluation of the development potential. International Journal of Greenhouse Gas Control 1 (4), 396–417.

Peng, D., Robinson, D.B., 1976. New 2-constant equation of state. Industrial & Engineering Chemistry Fundamentals 15, 59–64.

Pfaff, I., Oexmann, J., Kather, A., 2010. Optimised integration of post-combustion CO_2 capture process in greenfield power plants. Energy 35, 4030–4041.

Reddy, S., Gilmartin, J., Francuz, V., 2007. Integrated compressor/stripper configurations and methods. Patent No. WO/2007/075466, Fluor Technologies Corporation Fluor Technologies Corporation.

Schach, M.O., Schneider, R., Schramm, H., Repke, J.U., 2010. Techno-economic analysis of post-combustion processes for the capture of carbon dioxide from power plant flue gas. Industrial & Engineering Chemistry Research 49 (5), 2363–2370.

Standart, G., 1965. Studies on distillation. V. Generalized definition of a theoretical plate or stage of contacting equipment. Chemical Engineering Science 20, 611–622.

Thompson, R.E., King, C.J., 1987. Energy conservation in regenerated chemical absorption processes. Chemical Engineering and Processing 21, 115–129.

Tobiesen, A.F., Dorao, C.A., 2008. A simulation study of alternative process configurations for CO_2 absorption plant using CO2SIM. Proceedings of 9th International Conference on Greenhouse Gas Control Technologies, GHGT-9.

UniSim design user guide; Honeywell, 2008 R380 Release.

Undrum, H., Bolland, O., 2003. A novel methodology for comparing CO_2 capture options for natural gas-fired combined cycle plants. Advances in Environmental Research 7, 901–911.

Woodhouse, S., Rushfeldt, P., Sanden, K., Haaland, A.H., 2009. Improved method for regeneration of absorbent. Patent No. WO/2009/035340 A1, Aker Clean Carbon.

Paper 5

International Journal of Greenhouse Gas Control 5 (2011) 1393–1405

Contents lists available at SciVerse ScienceDirect

International Journal of Greenhouse Gas Control

journal homepage: www.elsevier.com/locate/ijggc

Review

Optimized process configurations of post-combustion CO_2 capture for natural-gas-fired power plant—Exergy analysis

Zeinab Amrollahi*, Ivar S. Ertesvåg, Olav Bolland

Department of Energy and Process Engineering, Norwegian University of Science and Technology, Trondheim, Norway

ARTICLE INFO

Article history:
Received 26 May 2011
Received in revised form 25 August 2011
Accepted 26 September 2011
Available online 22 October 2011

Keywords:
CO_2 capture
Chemical absorption
Process modification
Exergy analysis

ABSTRACT

Several chemical absorption CO_2 capture process configurations were analyzed and compared according to their associated exergy losses. The total work demand was decreased from 1.39 MJ/kg CO_2 for the Base case chemical absorption process configuration to 1.23 MJ/kg CO_2 for the modified chemical absorption process configuration of lean vapor recompression with absorber inter-cooling (best case). Considering the minimum work requirement of separation processes, the exergy efficiency of capture and compression plants was increased from 31.6% for the Base case chemical absorption process to 35.6% for the best case. Respectively, irreversibilities were reduced from the 1.60 MJ/kg CO_2 for the Base case to 1.29 MJ/kg CO_2 for the case with absorber inter-cooling and lean vapor recompression. The rational efficiency for the natural-gas-fired combined cycle power plant with CO_2 capture and compression shows an increase from 48.5% for the Base case chemical absorption process configuration to 49.5% for the best case.

Contents

* Corresponding author. Tel.: +47 48356625.
E-mail address: zeinab.amrollahi@ntnu.no (Z. Amrollahi).

1750-5836/$ – see front matter © 2011 Elsevier Ltd. All rights reserved.
doi:10.1016/j.ijggc.2011.09.004

Nomenclature

h	specific enthalpy (J/kg)
LHV	lower heating value (J/kg)
m	mass flow rate (kg/s)
P	pressure (bar)
O	heat transfer flow rate (J/s)
$\tilde{R}$	Universal gas constant (J/(mol K))
s	specific entropy (J/kg)
T	temperature (K)
$\dot{W}_x$	shaft work rate (J/s)
x	mole fraction

Greek letters

E, ε	exergy, specific exergy, J (J/kg)
$\tilde{\varepsilon}$	specific molar exergy (J/mol)
ψ	rational efficiency

Subscripts

0	environmental state
i	i-th component of a mixture
r	r-th thermal energy reservoir
act	actual
CC	CO_2 capture and compression
in	input
ph	physical
out	output
rev	reversible

1. Introduction

Carbon dioxide capture is considered as an option to reduce the emissions of greenhouse gases and large efforts are devoted to research and development. The main barrier for deployment of industrial-scale CO_2 capture systems for power generation is that these processes comes at the expense of the efficiency of thermo-electrical power plants, and the plant power output and available heat are also decreased. This necessitates the development of improved capture processes with minimized parasitic efficiency and power losses.

There are several processes to remove CO_2, such as physical/chemical absorption, adsorption, cryogenic separation and membranes. For post-combustion CO_2 capture from a natural-gas-fired power plant, chemical absorption using amine solvents is the most near-term technology according to the IEA report (IEA, 2008). The main challenge of these processes is to develop energy integrated processes with high capture ratio and low energy requirement. Several studies are found in the literature that discusses the two main paths; developing new solvents and optimization of the process configuration (Jassim and Rochelle, 2005; Oyenekan and Rochelle, 2007; Aroonwilas and Veawab, 2007; Tobiesen and Dorao, 2008; Reddy et al., 2007).

Techno-economic and thermodynamic analyses that evaluate natural-gas-fired combined-cycle (NGCC) power plants with CO_2 capture units have been done recently (Peeters et al., 2007; Hammond and Ondo Akwe, 2007; Schach et al., 2010). The thermodynamic analyses consisting of energy and exergy analyses have been performed by various researchers recently to evaluate the performance of the power production cycles with CO_2 capture (Lozza and Chiesa, 2002; Ertesvåg et al., 2005; Zhang and Lior, 2008; Romeo et al., 2010; Amrollahi et al., 2011). In studies done by Geuzebroek et al. (2004), Yu et al. (2009) and Valenti et al. (2009), exergy analysis results of MEA and chilled ammonia based CO_2 capture processes have been presented. Heat integration suggestions have been made by Pfaff et al. (2010) to achieve optimized heat integration between the post combustion capture process and the power plant.

This study was based on the several chemical absorption process configurations that were analyzed and comparison of various cases by Amrollahi et al. (submitted for publication). The approach was the evaluation of net power plant efficiency (%LHV) for the reference power plant and the integrated post-combustion capture processes.

In the current paper, the second law of thermodynamics is used as a tool to quantify the reduction of exergy penalty associated with CO_2 capture for the proposed process modifications. These processes were analyzed and compared according to their work demand. Consequently, exergy analysis has been applied to detect and demonstrate the changes of irreversibility rates in the main process sections for various process configurations. Furthermore, overall exergy analysis was performed to identify the irreversibilities associated with the integration of power plant with various CO_2 capture and compression processes.

The remainder of this article is divided into Section 2, which describes the methodologies used for simulation of MEA chemical absorption process and power plant and the fundamentals of exergy analysis, Section 3, which includes the simulated models, Section 4 that shows and discusses the results and Section 5 with concluding remarks.

2. Methodology

2.1. Simulation of MEA chemical absorption process

The conventional process configuration for a gas treating system with aqueous alkanolamine solution was simulated. The flue gas was contacted with MEA solution counter-currently in a packed absorber column. CO_2 was absorbed into the solvent which was then heated and fed to the top of the stripping column. Steam, which was provided by the column reboiler, stripped the CO_2 from the MEA solution as it passed down the column, while the condenser provided reflux and the CO_2 recovered overhead as a vapor product. The lean amine solution was cooled and recycled back to the absorber.

The CO_2 capture and compression units were modeled with UniSim Design software (Honeywell), which contains the Amines Property Package. This special property package has been designed to aid the modeling of alkanolamine treating units in which CO_2 is removed from gaseous streams. The modeling details and the basis of the simulations of UniSim Design have been presented by Amrollahi et al. (submitted for publication).

For simulation of the gaseous streams in the flue gas cooling section, blower section and compression section, the UniSim (2008) enhanced Peng–Robinson equation of state was used, which is applicable over the range of the current simulations.

2.2. Power plant simulations

The power plant subsystems included gas turbine (GT), heat recovery steam generator (HRSG), steam turbine (ST) and condenser. The power plant simulations were done by GT PRO (Thermoflow, Inc.), which is described in Section 3.1.

The energy analysis of the power cycles integrated with CO_2 capture plant, which is expressed in terms of power production penalty and net power plant efficiency, has been thoroughly documented by Amrollahi et al. (submitted for publication).

2.3. Exergy analysis

The exergy method of evaluating energy-intensive systems integrates the first and second laws of thermodynamics at the state of

specific environmental conditions. Exergy analysis, with its certain methods of process evaluation, has proven to be an efficient tool to define the second law performance of processes. It combines the principles of conservation of mass and energy together with the second law of thermodynamics to characterize the thermodynamic losses associated with each unit of a system. Hence, it enables to identify losses and to make improvements of energy consumption. This is an advantageous method to approach the goal of more efficient processes since it specifies the locations, types, and real magnitudes of irreversibilities, either being reduced or dissipated.

The exergy of a stream can be divided into physical exergy and chemical exergy. The physical exergy equals to the maximum reversible amount of work obtainable when the stream of substance is brought from its actual state to the environmental state defined by P_0 and T_0 (Szargut et al., 1988) by physical processes involving only thermal and mechanical interaction with the environment. Assuming that potential and kinetic energy can be neglected, it is expressed as:

$$\varepsilon = (h - h_0) - T_0(s - s_0) \tag{1}$$

where h and s are the specific enthalpy and entropy, respectively, and $h_0 = h(T_0, P_0)$ and $s_0 = s(T_0, P_0)$ for the flowing matter.

The chemical exergy of a substance is the minimum work requirement to deliver it in the environmental state (T_0, P_0) from the environmental substances by means of processes involving heat transfer and exchange of substances only with the environment. The standard chemical exergies of various substances are given in the literature, e.g. Kotas (1995). The molar chemical exergy of an ideal mixture is expressed as:

$$\widetilde{\varepsilon} = \sum_i x_i \widetilde{\varepsilon} + RT_0 \sum_i x_i \ln x_i \tag{2}$$

where x_i and $\tilde{\varepsilon}_i$ are molar fraction and chemical exergy, respectively, of each component in the mixture and $\tilde{R}$ is the universal gas constant.

The exergy loss of each individual unit can be calculated by finding the difference between the exergy of input and output streams of a unit operation. To find irreversible losses in each unit operation, a steady-state exergy balance can be used;

$$\sum_{in} \dot{m}\varepsilon + \sum_r \dot{Q}_r \left(1 - \frac{T_0}{T_r}\right) = \sum_{out} \dot{m}\varepsilon + \dot{W}_x + \dot{I} \tag{3}$$

Here, $\dot{m}$ denotes mass flow rate, $\dot{Q}_r$ denotes heat transfer rate, $\dot{W}_x$ denotes shaft work and $\dot{I}$ denotes irreversibility rate. On the left-hand side, the first term in Eq. (3) denotes the flow of exergy into the system and the second term denotes the flow of exergy associated with the inflow or outflow of the heat transfer. The first right-hand side term denotes the flow of exergy out of the system.

Another important value resulting from exergy analysis is exergy efficiency, which is defined in various formulations for different processes. In a general formulation, named as the rational efficiency, it is expressed as the ratio of the useful exergy output to the total used exergy (Kotas, 1995).

$$\psi = \frac{\sum \Delta \dot{E}_{out}}{\sum \Delta \dot{E}_{in}} \tag{4}$$

The rational efficiency differentiates between the desired output exergy and any other kind of outflow from the system. This makes it a proper value to present the degree of thermodynamic perfection of a process.

Exergy analysis can be done when composition and thermodynamic properties of all streams are available. For this purpose, modeling software was used to simulate the power plant and CO_2 capture and compression processes.

To calculate the chemical exergy of each stream, the chemical exergy of MEA in liquid phase was required. The value used in these calculations was estimated by the group contribution method (Szargut et al., 1988) to 1.536×10^6 kJ/kmol. This method considers the contribution of simple chemical groups in chemical enthalpy and exergy and it can be used when the chemical constitution of the substance is known. MEA with molecular formula of C_2H_7NO has the group constituents $-\overset{|}{C}H_2$, –OH and $-NH_2$ and its chemical exergy was calculated accordingly. Furthermore, the reference environment for exergy calculations was assumed at $T_0 = 298.15$ K, $P_0 = 101.325$ kPa and the reference composition as defined by Kotas (1995).

For exergy calculations, the chemical and physical exergy of all streams were tabulated in excel spreadsheets with the data input from Unisim simulations. Hence, the amounts of exergy loss and irreversibility were calculated and formed exergy balance for each control region. For the power plant, the results were based on the GTRPO exergy calculations.

3. Model description

3.1. Reference NGCC without CO_2 capture

The natural-gas-fired combined-cycle power plant was designed with power plant configuration of GT, HRSG and triple-pressure-condensing-reheat ST at an ambient-air condition of 25 °C and atmospheric pressure. The gas turbine Siemens SGT5-4000F was selected from the GT PRO library. The fuel was natural gas without H_2S with 46.3 MJ/kg as lower heating value (at 25 °C), which equaled to 681.4 MW as the fuel heat input to the GT and the chemical exergy of 48.5 MJ/kg. The flue gas flowing through the HRSG exited as exhaust gas with a flow rate of 650.9 kg/s at atmospheric pressure and 94 °C. The flow sheet of the designed combined cycle power plant is shown in Fig. 1.

3.2. CO_2 capture scenarios

In the current study, six different CO_2 capture process configurations (Figs. 2–4) were simulated. After an initial design, some of the main parameters affecting the capture processes were varied towards the optimization of the processes. The optimization target was the reduction of reboiler energy consumption and the total work demand of the CO_2 capture plant. Here, the cases will be described briefly, yet the thorough process information was included in the first paper (Amrollahi et al., submitted for publication).

3.2.1. Base case model

As a Base case, the chemical absorption CO_2 capture and compression units shown in Fig. 2 were simulated with the capture ratio set at 90%. Table 1 shows the flue gas specifications and design parameters for the chemical absorption and compression units, which were held constant for all cases. The absorber performance was controlled by adjusting the solvent circulation rate to meet 90% CO_2 capture ratio.

The lean solution CO_2 molar fraction and the condenser temperature were specified as the stripper specification. The former parameter was optimized to reach the lowest reboiler duty in the Base case and the other cases. Additionally the rich and lean loading and solvent circulation rate were among the optimized parameters for each case. The figures of the optimized parameters are shown in Table 2 for the Base case and the other cases as well.

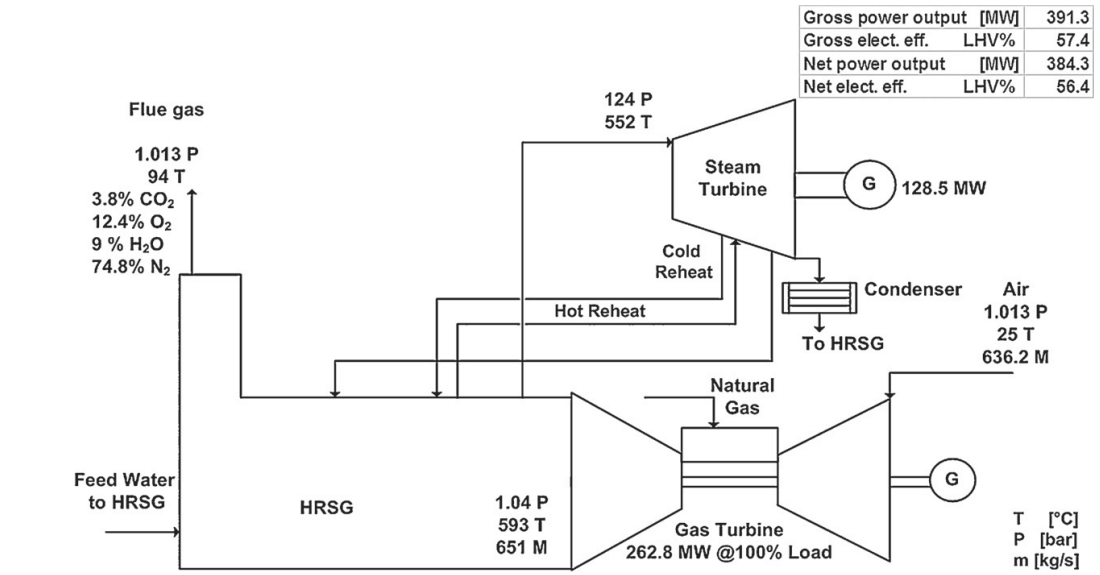

Fig. 1. Flowsheet of the reference power plant.

3.2.2. Absorber inter-cooling model (Case 1)

By inter-cooling the absorber, heat of absorption was released and the liquid temperature at the absorber bottom was reduced. The absorber temperature reduction was in favor of higher driving forces for the absorption process and increased the absorption capacity of the solvent, i.e. solvent rich loading. The modification to the Base case as illustrated in Fig. 2, was to extract a semi-rich stream from the lower part of the absorber, cool in an inter-stage cooler down to 25 °C and recycle it to the absorber column. All other process units were identical to the Base case. The flow rate and the location of the side-stream which was sent to the inter-stage cooler, were subject to optimization to achieve lower reboiler duty compared to the Base case. Due to the higher attainable rich loading and reduction in the solvent circulation rate, the stripper reboiler duty

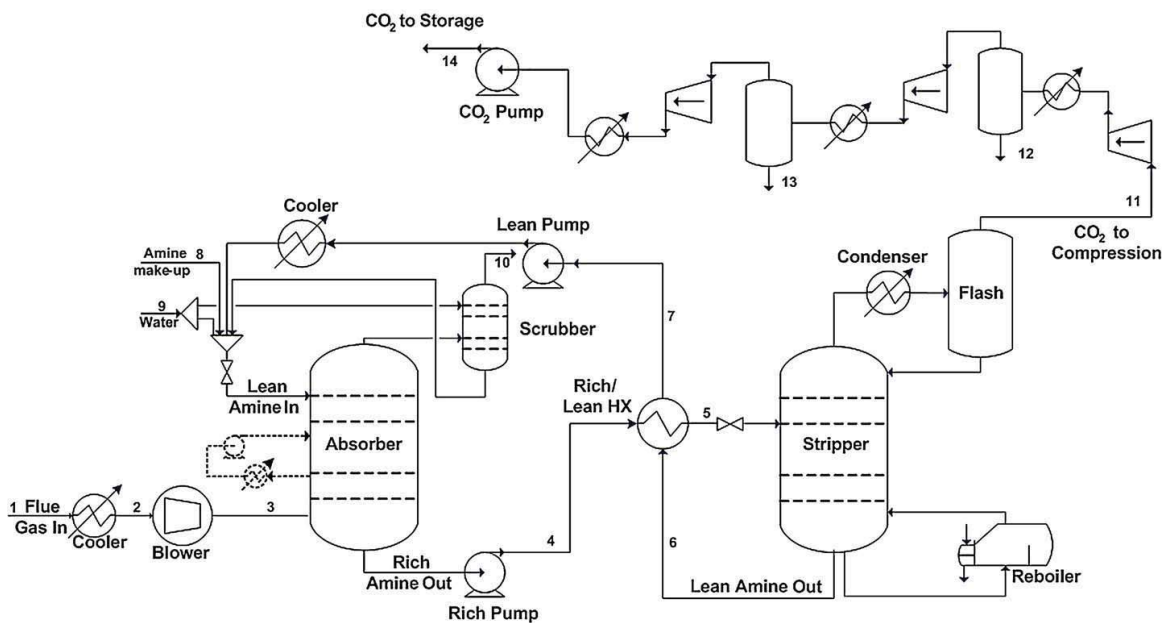

Fig. 2. Flow sheet of the chemical absorption CO_2 capture and compression unit without (Base case) and with (Case 1) absorber inter-cooling. Here the dashed part added to the Base case flow sheet demonstrates the absorber inter-cooling model (Case 1).

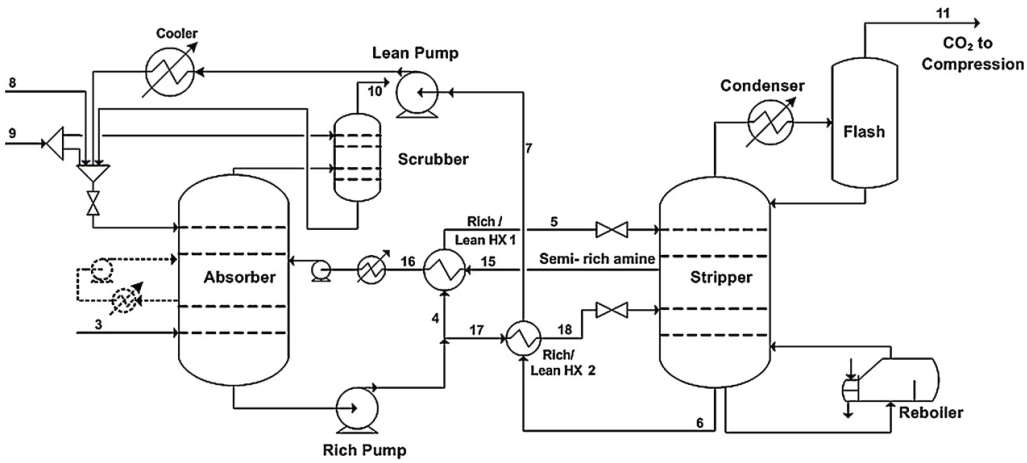

Fig. 3. Flow sheet of the chemical absorption with split-flow feed to stripper without (Case 2) and with (Case 3) absorber inter-cooling. Here the dashed part added to Case 2 flow sheet demonstrates the absorber inter-cooling model (Case 3).

Table 1
Design parameters for all process configurations.

Solvent	30	wt.% MEA
CO_2 capture ratio[a]	90	%
Flue gas mass flow	650.9	kg/s
Flue gas composition		
CO_2	3.80	vol%
O_2	12.42	vol%
N_2	74.76	vol%
H_2O	9.02	vol%
Rich/lean HX minimum approach temperature	8.5	°C
CO_2 compression final pressure	110	bar
Absorber		
No. of stages	13	
Pressure drop	50	mbar
Inlet lean temperature	40	°C
Cooled flue gas inlet temperature	50.3	°C
Stripper		
No. of stages	36	
Condenser temperature	30	°C
Reboiler pressure	1.86	bar
Cooling water temperature	8	°C
Cooling water ΔT	10	K
Steam to reboiler		
Temperature	145	°C
Pressure	4	bar
Condensate		
Temperature	130	°C
Pressure	3.92	bar

[a] CO_2 capture ratio is defined as the fraction of CO_2 that is separated from the flue gas.

was decreased. Table 2 shows the lean solution CO_2 molar fraction at the bottom of the stripper which was subject to optimization and the rich and lean loading and the solvent circulation rate for this process configuration.

3.2.3. Split-flow model (Case 2)

The split-flow configuration for chemical absorption processes was designed according to the concept of thermodynamic optimization based on the reduction of driving forces to reduce steam consumption of solvent regeneration. In general the changes in flowsheets that make driving forces more uniform can simultaneously reduce both exergy losses and capital investments (Leites et al., 2003). In this configuration, instead of single rich amine feed stream to the stripper column, there are split-flows fed to the column. The idea is to approach the theoretical level of adding and removing all flow streams which causes more evenly distribution of component concentration driving forces (mass transfer core) through the vapor and liquid phase.

In this flowsheet, the rich amine leaving the absorber was split between two feed points to the stripper; one stream entered the top of the stripper and left it from the middle point and returned to the middle of the absorber. The other split entered the bottom of the stripper and left it towards the top of the absorber. Since less amount of rich amine enters the stripper bottom section, the solvent was stripped to the same CO_2 loading with lower energy input. Moreover, since *semi-rich amine* entered the absorber column at 25 °C, the split-flow behaved as an intercooler for the absorber column with some of the effects discussed in Section 3.2.2. The split flow fraction, the feed tray of the second split to the stripper, the flow rate and the feed location of *semi-rich amine* that returns to the absorber were subject to optimization in this configuration.

3.2.4. Absorber inter-cooling combined with split-flow model (Case 3)

This process configuration illustrated in Fig. 3 combined the effect of inter-cooling of absorber column and the split-flow configuration. The parameters which were subject to optimization

Table 2
Optimized design parameters for various process cases.

	Base case	Case 1	Case 2	Case 3	Case 4	Case 5
CO_2 mole fraction in lean solution	2.51×10^{-2}	2.47×10^{-2}	2.45×10^{-2}	2.47×10^{-2}	2.5×10^{-2}	2.48×10^{-2}
Lean loading	0.22	0.22	0.22	0.23	0.23	0.23
Rich loading	0.47	0.48	0.47	0.49	0.47	0.48
Solvent circulation rate [kg/s]	649.4	613.8	550.3	529.3	641.2	611.1

CO_2 loading is defined as the ratio of CO_2 mole fraction to MEA mole fraction in the solution.

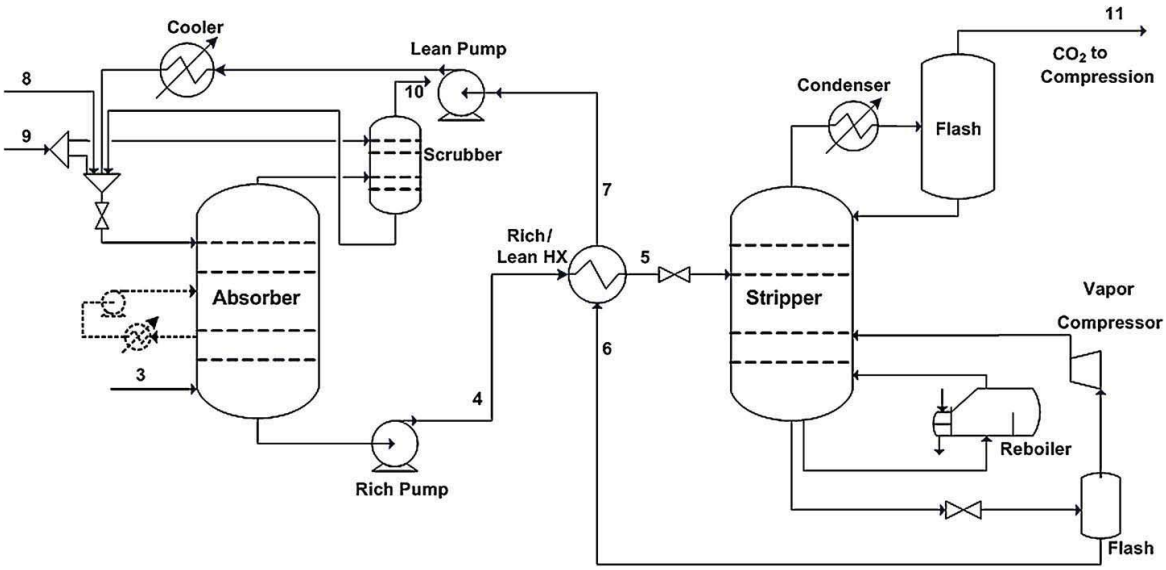

Fig. 4. Flow sheet of the chemical absorption with lean vapor recompression stripping without (Case 4) and with (Case 5) absorber inter-cooling. Here the dashed part added to Case 4 flow sheet demonstrates the absorber inter-cooling model (Case 5).

include the flow-rate of inter-cooled stream, the split flow fraction and the flow rate of *semi-rich amine* from the stripper.

3.2.5. Lean vapor recompression (LVR) model (Case 4)

The purpose of the vapor recompression concept was to provide steam that is regained from the stripping process as the heating media to the reboiler and was performed by flashing the lean solution to generate the steam feed which was introduced to the stripper column via a compressor. As illustrated in Fig. 4, the leaving lean solution from the stripper decreased its pressure through a flash valve to one bar and was flashed through a flash drum to produce the gaseous phase. This gaseous phase was composed mainly of water vapor, which was recompressed to two bar and reintroduced to the stripping column. Similar to the Base case, the liquid phase was cooled by the rich solvent and returned to the absorber. The optimized CO_2 mole fraction at the bottom of the stripper and rich and lean CO_2 loading are shown in Table 2.

3.2.6. LVR combined with absorber inter-cooling model (Case 5)

This process configuration illustrated in Fig. 4 combined the effects of absorber inter-cooling and the lean vapor recompression.

4. Results and discussion

4.1. CO_2 capture and compression plant

In this section, the CO_2 capture and compression units were divided into control regions to perform exergy balances over each control region and irreversibility calculations. Data for the streams from the simulations for the various cases are reported in Appendix A.

4.1.1. The total work demand of various CO_2 capture process configurations

The process configurations described in Section 3.2 were optimized with respect to low energy consumption. As suggested by Leites et al. (2003), the fundamental concept behind the modifications should imply the minimization of the driving forces along the columns and heat exchangers and the reduction of the wasted heat. Avoiding the additional driving forces and maximization of thermodynamic potentials were the key concepts regarded in optimization of energy consumption in these processes.

The total work demand for all the process configurations are given in Table 3. As listed, the total work demand of the capture and compression process consisted of the work equivalent of the regeneration energy that was in the form of steam to the reboiler, the power requirement for the pumps and the blower and the compressor in LVR configurations, and the CO_2 compression work demand.

Obviously, as the reboiler duty was decreased from the Base case to the last case, the total work demand for each case was decreased. By absorber inter-cooling modification (Case 1), less total work demand was achieved compared to Base case. Also split-flow (Case 2) modification led to less total work demand compared to Base case. So the interaction of these process modifications (Case 3) led to a significant improvement and less total work demand.

Table 3
Total work demand [MJ/kg CO_2] for the optimized process configurations.

	Base case	Case 1	Case 2	Case 3	Case 4	Case 5
Power production penalty for solvent regeneration	0.90	0.88	0.84	0.80	0.66	0.65
CO_2 compression work	0.33	0.33	0.33	0.33	0.33	0.33
Other work-pumps, blower	0.15	0.15	0.16	0.16	0.25	0.25
Total work	1.39	1.36	1.33	1.29	1.25	1.23

Table 4
Exergy efficiency (ψ_{CC}) for CO_2 capture and compression plant.

	Base case	Case 1	Case 2	Case 3	Case 4	Case 5
CO_2 capture process [%]	21.3	21.9	22.6	23.6	24.5	25.0
Compression process [%]	64.3	64.3	64.3	64.3	64.3	64.3
Total [%]	31.6	32.3	33.0	34.1	35.1	35.6

It should be mentioned that for the Cases 4 and 5, the compressor work needed for lean vapor recompression increased the work amount that is covered under the *Other work* term. Nevertheless, the major reduction of energy requirement of the reboiler caused the reduction of total work demand for Cases 4 and 5.

The CO_2 compression work demand remained constant since the capture rate was set at 90% of the CO_2 content of the entering flue gas that was kept constant in all cases.

4.1.2. Exergy efficiency

According to the second law of thermodynamics, the required work input for a reversible process is the minimum work input required to accomplish that process. The work input for real irreversible processes is always higher than the work input of theoretical reversible processes. For the current chemical absorption unit, the minimum reversible work of 90% separation of CO_2 from the power plant exhaust stream was calculated to 0.225 MJ/kgCO_2 on the basis of the approach of Cengel and Boles (2006). The minimum reversible work of compression of pure CO_2 stream from 1.1 bar to 110 bar was calculated as the exergy difference of the second and first states. Using the Peng and Robinson (1976) equation of state, the minimum work demand for compression of pure CO_2 to 110 bar and 30 °C was calculated to 0.213 MJ/kg CO_2. Alternatively, when using the improved equation of state by Span and Wagner (1996), the minimum work demand of the CO_2 compression resulted in 0.216 MJ/kg CO_2. Here, the former number was used for the consistency of calculations.

Considering the actual work demand from Table 3, the exergy efficiency of the CO_2 capture unit, the compression unit and the total exergy efficiency of the CO_2 capture and compression plant were presented in Table 4. Here, the exergy efficiency was defined as the ratio of minimum, theoretical-reversible work required to actual work required in the process, i.e. $\psi_{CC} = \dot{W}_{rev}/\dot{W}_{act}$.

As the results show, the total exergy efficiency increased from the Base case to the last case. The maximum increase in exergy efficiency was observed at 4.0 percentage points for Case 5.

4.1.3. Irreversibility rates

Eq. (3) was used for irreversibility calculations, and the control region was considered around each unit taking into account the exergy inflow and outflows to/from each control region.

Since the local driving forces were rather high and unevenly distributed along the absorber and stripper, their irreversibilities were high. In the stripper section, high amount of heat exchange in the reboiler with the associated large driving forces at the bottom of the stripping column was in favor of the stripping process of CO_2 from the amine solution. On the other hand, this also increased the irreversibilities in the stripper. As mentioned earlier, an even distribution of driving forces over the unit operations would be the optimal solution for decreasing irreversibilities. Table 5 shows the irreversibilities of process units for various process configurations.

As the total work demand of CO_2 capture and compression processes, including power production penalty due to steam use, was decreased from the Base case to Case 5, the irreversibilities were decreased predictably along the cases. The key parameters determining the irreversibility rates were the non-uniform temperature driving forces, work inputs to each control region, water and MEA make-up amounts and streams' composition changes. The latter parameter determined the chemical exergy of streams and affected the exergy balances over the units.

The comparison between cases without and with absorber inter-cooling shows the increased absorber and decreased stripper irreversibilities. For the absorber section, the supporting reason would be that because of inter-cooling effect, the temperature driving forces were higher, which would add up to the irreversible losses. Looking to Fig. 5, taking Base case and Case 1 for instance, the temperature profile of Case 1 for the absorber section shows higher temperature changes in the bottom section of the column since the cooled stream was fed close to the absorber bottom. These higher non-uniform temperature driving forces were in favor of higher separation process rates, however, resulted in increased exergy losses. The increased absorber exergy losses from the Base case to Case 3, i.e. the combination of split-flow and absorber inter-cooling modifications, could be explained with the same reason. Regarding temperature changes, the cooled *semi-rich* amine was returned to the middle of the absorber (Fig. 3), which caused higher non-uniform temperature driving forces. Moreover, the temperature distribution along the absorber stages, which is shown in Fig. 5, showed the highest temperature changes for Case 3 and the lowest temperature changes for the Base case and Case 4. This led to the highest absorber irreversibility rates for Case 3 and the lowest for the Base case and Case 4.

The increased rich loading at the bottom of the absorber was regarded as another effect of the absorber inter-cooling process configuration. This meant lower chemical exergy outflow of the rich amine solution from the absorber comparing to the case without inter-cooling and, consequently, resulted in the increase of exergy losses considering the exergy balance. A slight decrease in the chemical exergy of make-up streams was observed when cases with absorber inter-cooling was compared to cases without absorber inter-cooling, however it did not lead to a decrease in the irreversibility rates due to inter-cooling.

Table 5
Irreversibility [MJ/kg CO_2 separated] by unit sections for the CO_2 capture and compression plant.

	Base case	Case 1	Case 2	Case 3	Case 4	Case 5
Flue gas cooler	0.10	0.10	0.10	0.10	0.10	0.10
Blower	0.03	0.03	0.03	0.03	0.03	0.03
Absorption section	0.71	0.74	0.88	0.99	0.71	0.72
Rich/lean heat exchanger(s)	0.02	0.02	0.02	0.01	0.11	0.11
Stripper	0.60	0.54	0.38	0.24	0.26	0.19
Compression section	0.14	0.14	0.14	0.14	0.14	0.14
Total	1.60	1.57	1.54	1.51	1.35	1.29

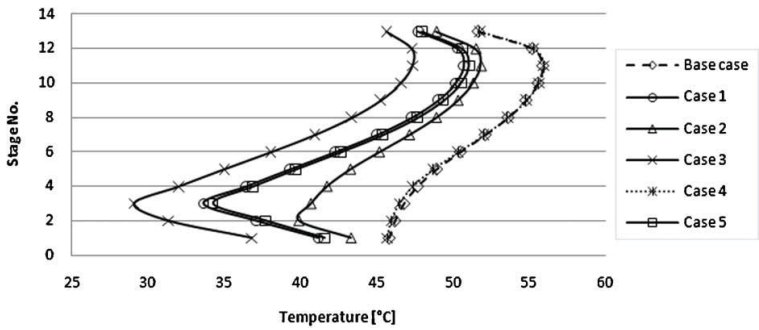

Fig. 5. Absorber temperature profile. Column stages were numbered from the bottom to the top.

It was clear from the results that the process modification of LVR would not increase the absorber irreversibility, i.e. the situation between the Base case and Case 4 and similarly for Cases 1 and 5. According to Fig. 5, the temperature profiles were close to each other for the mentioned cases, which meant that the absorber irreversibility results for the addressed cases would remain in the same range when adding the LVR modification to the capture process.

The results of irreversibility calculations for the stripper showed the lowest rates for Case 5.

It was observed that the absorber inter-cooling effect resulted in a reduction of stripper irreversibility rate. One of the effects of inter-cooling was regarded as increasing the rich loading. This meant lower exergy inflow of the rich amine solution to the stripper compared to the case without inter-cooling. Additionally, as the inter-cooling resulted in the decreased reboiler steam demand, the steam exergy flow to the stripper was less for the cases with inter-cooling, which resulted in lower exergy losses in the stripper.

For the cases with split-flow configuration, *semi-rich* amine streams (Fig. 3, Stream No. 15) were side-drawn from the stripper for the sake of lower reboiler duty. Since the portion of solution that was flown through the reboiler and thoroughly stripped of CO_2 was less than the cases without split-flow configuration, the reboiler duty and the steam exergy transfer to the reboiler was decreased and the stripper irreversibilities was decreased. Additionally, the low molar exergy inflows of rich amine to the top and middle of the stripper (Fig. 3, Stream Nos. 5 and 18) were among the other parameters which led to decrease the exergy losses. Moreover, the split-flow configurations enabled a more uniform temperature distribution of rich solution to the stripper, i.e. the split stream to the top of the stripper (Fig. 3, Stream No. 5) had lower temperature, and the split stream to the middle of stripper (Fig. 3, Stream No. 18) had higher temperature (Fig. 6). This means that the colder stream entered the colder part of the stripper, the exergy loss due to condensation of water vapor decreased and the hotter stream was fed to the bottom part of the stripper. This caused the decrease in the condenser exergy losses and accordingly the stripper exergy losses.

Comparing the cases without and with LVR, the results show a decrease in stripper irreversibilities for the cases with LVR. By the LVR modification, the heat of condensation of overhead water vapor at the stripper column was used as the heating media for the reboiler. The lean solution was flashed to produce steam that was compressed and re-introduced to the stripper. By this design, the total reboiler steam requirement was reduced. Hence, the steam exergy transferred to the stripper was diminished. This design resulted in lower lean solution temperature, which means that the available heat through rich/lean heat exchanger was less. This led to lower stripper feed temperature and consequently, less cooling duty was needed for the overhead vapor condensation. Although an additional work input was imposed to the system because of the vapor compressor, which accumulated to the stripper control region exergy inputs, the substantial decrease in the reboiler work demand led to less irreversibility for the cases with LVR.

Another parameter that affected the stripper exergy losses was the sudden temperature change at the stripper condenser and the return of cooled condensed solution to the stripper. The stripper temperature profile is shown in Fig. 6, and sudden temperature changes along the higher stages are observed. Along the modifications from the Base case to Case 5, the temperature differences at

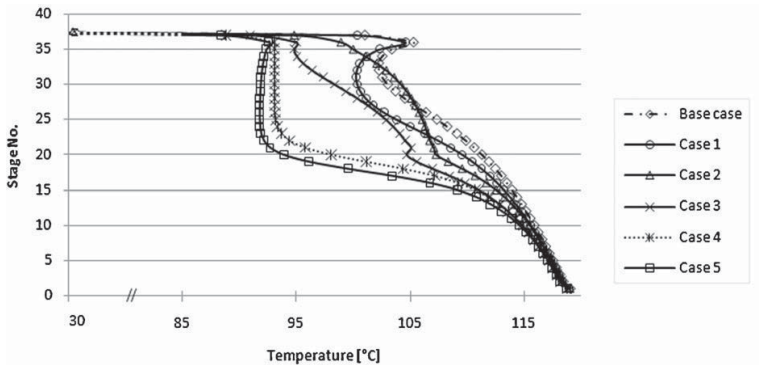

Fig. 6. Stripper temperature profile; column stages were numbered from the bottom to the top.

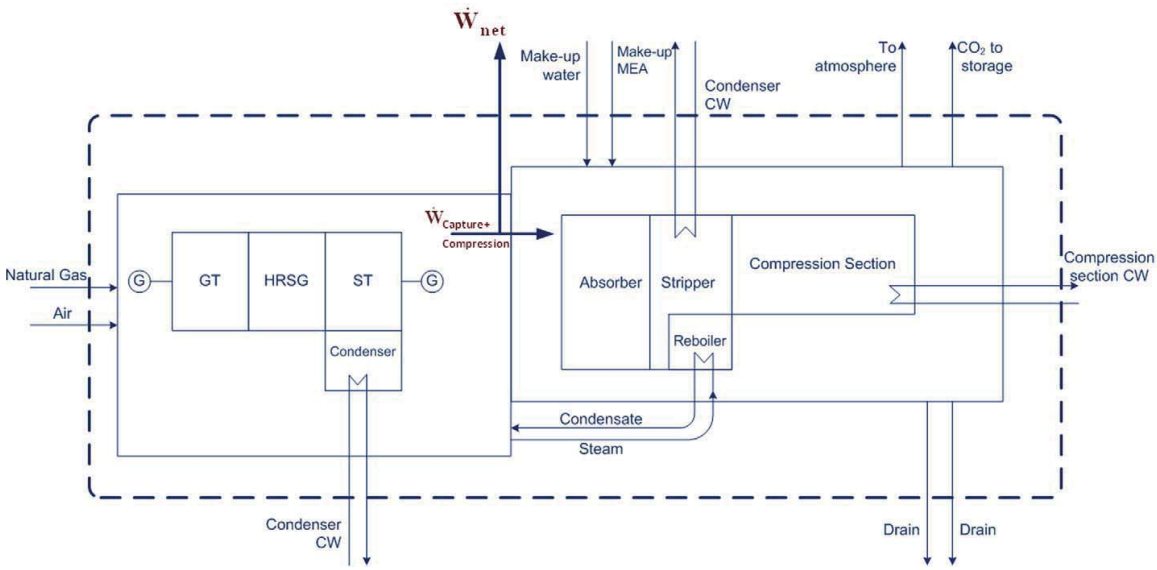

Fig. 7. Block scheme for the demonstration of inflow and outflow of exergy to/from the control region of NGCC with CO_2 capture and compression plants. The scheme does not show the path of streams inside the control region. The overall control region is shown by dashed line. CW here denotes the cooling water supply and return.

the top of the stripper were decreased gradually to more uniform and lower values, which demonstrated the reduction of exergy losses over the range of cases.

The irreversibilities for the flue gas cooler and blower remained unchanged along the process modifications from Base case to Case 5. Since the flue gas conditions were constant, these process units were unchanged, and the corresponding exergy balance over these units resulted in the same figures for all cases (Table 5). Moreover, the irreversibilities of the compression section were also constant, since the flue gas was constant along the process modifications and 90% of CO_2 from the flue gas was separated and sent to the compression section. Hence, the exergy balance calculations for the compression section resulted in the same amounts for all the process modifications.

4.2. Natural gas fired power plant

The exergy balance (Eq. (3)) was used over the power plant control region for the reference case, i.e. without the CO_2 capture, and other cases from the Base case to the fifth case, i.e. power plant coupled with the chemical absorption and compression plants. Fig. 7 illustrates the exergy streams to/from the control region. As listed in Table 3, $\dot{W}_{\text{capture + compression}}$ comprises the rich and lean amine pump work demands, the blower work demand, the vapor compressor work demand for Cases 4 and 5, and the CO_2 compression work demand. The results of exergy calculation for the power plant with CO_2 capture are shown in Table 6.

The energy analysis was done on the integration of each of the cases with the reference power plant and the results of net power plant efficiency (%LHV) have been presented by Amrollahi et al. (submitted for publication) for the same process modifications. It is stated that the total work demand for the CO_2 capture and compression plant was reduced from the Base case to Case 5 and the power plant efficiency penalty was decreased from 7.0 percentage points for the Base case to 6.2 percentage points for Case 5. Moreover, the net power plant work output was increased from the Base case to Case 5.

The net power plant work output, which is equivalent to exergy, and the pure pressurized CO_2 stream, which is a thermodynamic asset of the separation process, were considered as the exergy balance outputs over the control region. The exergy inputs and outputs combined with the irreversibility results, which were calculated in each subordinate control region, are presented in Table 6.

Table 6 shows the rational efficiency of the power plant with CO_2 capture and compression. It was increased from 48.5% for the Base case process configuration to 49.5% for the modified chemical absorption process configuration of lean vapor recompression with absorber inter-cooling. The cases were evaluated by the combination of power plant efficiency analysis and the exergy analysis and determined the modified chemical absorption process configuration of lean vapor recompression with absorber inter-cooling as the best choice. However, the main limitation of these improvements is the increase of complexity which, would lead to higher costs of design and operation.

4.3. Overall discussion

In the present study, exergy analysis was used to understand the effects of process-configuration modifications leading to improved performance. However, several other modifications could be triggered by the findings to further improve and optimize the current configurations.

As the inter-cooling individually and combination of inter-cooling with split-flow modification pointed out, the increased rich loading was in favor of CO_2 separation process by increasing the absorber driving forces. Thus increased rich loading led to lower rich-stream exergy, higher absorber exergy losses, lower reboiler work demand, lower stripper exergy losses and higher CO_2 capture exergy efficiency. This points towards process-configuration modifications with several steps of inter-cooling along the lower stages of the absorber.

By adding the rich-stream splits to the stripper, the stripper exergy losses are expected to decrease since the temperature driving force will be distributed more gradually along the stripper.

Table 6
Overall exergy balance results for the NGCC without and with post-combustion CO_2 capture (see Fig. 7).

	Reference plant without capture	Ref. plant + Base case	Ref. plant + Case 1	Ref. plant + Case 2	Ref. plant + Case 3	Ref. plant + Case 4	Ref. plant + Case 5
Exergy input[a] (MW)							
Fuel exergy	713.9	713.92	713.92	713.92	713.92	713.92	713.92
CW exergy to the stripper condenser	–	2.26	2.13	1.41	1.08	0.95	0.93
CW exergy to the compression section inter-coolers	–	0.93	0.93	0.93	0.92	0.93	0.94
Water + MEA make-up to the absorber	–	12.73	9.67	11.10	9.49	11.64	6.54
CW exergy to the lean amine cooler	–	1.57	1.03	1.11	0.51	1.54	1.07
CW exergy to the flue gas cooler	–	1.96	1.96	1.96	1.96	1.96	1.96
CW exergy to the absorber inter-coolers/split cooler	–		1.62	1.78	3.76		1.54
CW exergy to the power plant condenser	14.8	8.81	9.01	9.23	9.58	10.37	10.45
Exergy output (MW)							
Net power output[b]	384.3	336.30	337.49	338.44	340.42	341.09	341.78
Exergy of the separated and compressed CO_2	–	23.45	23.38	23.44	23.16	23.44	23.47
Irreversibility rates (MW)							
CO_2 capture and compression plant (from Table 5)	–	56.54	55.30	54.69	52.95	47.96	45.65
Compression section drains	–	0.36	0.36	0.36	0.36	0.36	0.36
Exergy to stack[c]	18.4	7.60	5.42	5.80	4.42	7.71	5.21
Flue gas cooler drain	–	2.89	2.89	2.89	2.89	2.89	2.89
Power plant	326.0	315.14	315.49	315.86	316.52	317.84	317.97
Rational efficiency, ψ (%)	52.7	48.5	48.7	48.8	49.1	49.2	49.5

[a] CW denotes the cooling water. CW exergy in this table is presented as the difference of physical exergy amounts of the supply and return cooling water to each unit.
[b] Net power output results was presented by Amrollahi et al. (2011).
[c] For the reference power plant, it was considered as the exergy of the released flue gas to the atmosphere. For cases with CO_2 capture, "Exergy to stack" is defined as the exergy outflow of stream leaving the top of the scrubber.

Table 7
Calculated exergy amounts for Base case and Case 1. Selected positions according to Fig. 2.

Stream no.	Pressure (bar)	Base case			Case 1		
		Temperature (°C)	Exergy (MW)	Exergy (kJ/kg CO_2)	Temperature (°C)	Exergy (MW)	Exergy (kJ/kg CO_2)
1	1.0	94.0	17.3	489.0	94.0	17.3	489.0
2	1.0	42.0	12.8	361.7	42.0	12.8	361.7
3	1.1	48.4	16.1	455.2	48.4	16.1	455.2
4	6.8	46.0	5206.6	146965.7	41.4	4915.7	139206.9
5	6.4	110.3	5313.5	149983.3	110.2	5025.1	142304.2
6	1.9	119.0	5315.4	150037.9	119.0	5027.9	142383.9
7	1.5	54.5	5207.9	147004.5	49.9	4918.0	139270.4
8	4.0	25.0	1.8	50.2	25.0	5.2	146.0
9	4.0	25.0	11.0	309.2	25.0	4.5	128.0
10	1.0	49.4	7.6	214.6	45.6	5.4	153.6
11	1.1	30.1	16.1	454.8	30.1	16.1	454.8
12	4.3	20.0	0.3	9.1	20.0	0.3	9.1
13	18.9	20.0	0.0	1.1	20.0	0.0	1.1
14	110	24.9	23.5	662.0	24.9	23.5	662.0

Table 8
Calculated exergy amounts for Case 2 and Case 3. Selected positions according to Fig. 3.

Stream no.	Pressure (bar)	Case 2			Case 3		
		Temperature (°C)	Exergy (MW)	Exergy (kJ/kg CO_2)	Temperature (°C)	Exergy (MW)	Exergy (kJ/kg CO_2)
1	1.0	94.0	17.3	489.0	94.0	17.3	489.0
2	1.0	42.0	12.8	361.7	42.0	12.8	361.7
3	1.1	48.4	16.1	455.2	48.4	16.1	455.2
4	6.5	43.5	2875.1	81197.7	37.0	2808.7	80284.5
5	6.1	98.2	2926.7	82656.0	96.0	2863.5	81848.5
6	1.9	119.1	4504.6	127217.2	118.9	4335.6	123926.5
7	1.5	52.0	4409.3	124528.2	45.5	4234.4	121034.6
8	4.0	25.0	4.6	128.7	25.0	8.7	249.3
9	4.0	25.0	6.5	184.8	25.0	0.8	22.1
10	1.0	46.7	5.8	163.7	43.5	4.4	126.4
11	1.1	30.1	16.1	454.7	30.1	15.9	454.6
12	4.3	20.0	0.3	9.1	20.0	0.3	9.1
13	18.9	20.0	0.0	1.1	20.0	0.0	1.1
14	110	24.9	23.5	662.0	24.9	23.5	662.0
15	1.8	106.7	2835.7	80086.8	104.5	2850.5	81477.6
16	1.4	53.7	2784.0	78624.7	49.2	2796.0	79919.4
17	6.5	43.5	4312.6	121796.6	37.0	4213.1	120426.7
18	6.1	109.5	4407.2	124467.8	108.3	4313.6	123297.9

Table 9
Calculated exergy amounts for Case 4 and Case 5. Selected positions according to Fig. 4.

Stream no.	Pressure (bar)	Case 4			Case 5		
		Temperature (°C)	Exergy (MW)	Exergy (kJ/kg CO_2)	Temperature (°C)	Exergy (MW)	Exergy (kJ/kg CO_2)
1	1.0	94.0	17.3	489.0	94.0	17.3	489.0
2	1.0	42.0	12.8	361.7	42.0	12.8	361.7
3	1.1	48.4	16.1	455.2	48.4	16.1	455.2
4	6.8	45.9	5139.7	145135.9	41.8	4898.5	138158.1
5	6.4	93.1	5215.8	147284.5	93.0	4978.1	140402.9
6	1.0	101.8	5222.3	147469.2	101.7	4986.2	140632.7
7	0.6	54.4	5142.2	145207.6	50.3	4902.8	138279.3
8	4.0	25.0	0.6	16.1	25.0	1.6	44.5
9	4.0	25.0	11.1	312.7	25.0	5.0	139.8
10	1.0	49.5	7.7	217.6	45.8	5.2	146.8
11	1.1	30.2	16.0	451.0	30.1	16.1	454.8
12	4.3	20.0	0.3	9.1	20.0	0.3	9.1
13	18.9	20.0	0.0	1.1	20.0	0.0	1.1
14	110	24.9	23.5	662.0	24.9	23.5	662.0

Simultaneously, taking a cooled-semi-rich side-stream from the stripper and returning it to the absorber will additionally increase the rich loading with the effects mentioned previously.

The combination of LVR and the split-flow configuration could be another interesting modification to be examined. The stage temperatures will be decreased at the top part of the stripper and gradually decreased along the stripper. Thus, the condensation exergy losses is reduced and more reduction in stripper exergy losses is expected.

The modified chemical absorption process configuration of LVR with absorber inter-cooling appeared as the best process according to lowest power demand and exergy losses. Yet, these modified process configurations would pay for energy savings with their higher investment costs. This necessitates the combination of

overall economical and technical analysis for the power plant with capture and compression to avoid costly and non-operable designs.

5. Concluding remarks

Exergy analysis was applied to evaluate the exergy efficiency of an NGCC power plant integrated with an optimized post-combustion CO_2 capture and compression plant. Six chemical absorption plant configurations for CO_2 capture were analyzed and compared according to their total work demand and their exergy losses. These cases comprised a Base case, Case 1 as the chemical absorption process with absorber inter-cooling, Case 2 as the chemical absorption process with split flow configuration, Case 3 as the chemical absorption process with absorber inter-cooling and split flow configuration, Case 4 as the chemical absorption process with lean vapor recompression (LVR) and Case 5 as the chemical absorption process with absorber inter-cooling and LVR.

Comparing Case 5 to the Base case, the reboiler energy consumption decreased from 3.74 MJ/kg CO_2 to 2.71 MJ/kg CO_2, and the total work demand for the CO_2 capture and compression plant was decreased from 1.39 MJ/kg CO_2 to 1.23 MJ/kg CO_2. Considering the minimum work requirement of separation processes, the exergy efficiency of the capture and compression plants was increased from 31.6% for the Base case to 35.6% for Case 5.

The irreversibility rates were calculated for each of the process sections of the CO_2 capture and compression plant and summed to the total irreversibility of the plant. The results showed decreased irreversibilities from 1.60 MJ/kg CO_2 for the Base case to 1.29 MJ/kg CO_2 for Case 5.

The findings from the process modifications were included but not limited to following expressions:

- The inter-cooling process modification would increase the absorber irreversibilities yet reversely, decreased the stripper irreversibilities. The absorber inter-cooling modification was combined with other modifications as an efficient method to decrease irreversibilities and the total work demand.
- The split-flow process modification led to a significant increase of absorber irreversibilities and a major decrease in the stripper exergy losses. The introduction of the cooled semi-rich side-stream to the absorber caused a significant increase in the absorber irreversibility. However, the total irreversibility was reduced comparing the cases with split-flow to the Base case and Case 1.
- The LVR process modification would not increase the absorber irreversibility, yet decreased the irreversibility associated to the stripper substantially. The heat of water vapor condensation was regained through the vapor compressor in the form of steam; thus the total work demand was decreased significantly.

The rational efficiency of the power plant with CO_2 capture and compression was evaluated for all of the cases. The results showed an increase in rational efficiency from 48.5% for the power plant integrated with the Base case chemical absorption process configuration to 49.5% for the modified chemical absorption process configuration of lean vapor recompression with absorber intercooling. The latter capture process was the best process with the lowest power demand, irreversibility amounts and the highest exergy efficiency.

Acknowledgments

This publication forms a part of the BIGCO2 project, performed under the strategic Norwegian research program Climit. The authors acknowledge the partners: Statoil, GE Global Research, Statkraft, Aker Clean Carbon, Shell, TOTAL, ConocoPhillips, ALSTOM, the Research Council of Norway (178004/I30 and 176059/I30) and Gassnova (182070) for their support.

Appendix A.

The details of the streams resulting from the simulations for each of the cases are reported here in Tables 7–9. The points that are selected to show in the tables consist of but are not limited to; flue gas entering the chemical absorption process, the exhaust gas which is leaving from the top of the scrubber, rich amine from the absorber and lean solution from the stripper, amine and water make-ups stream of captured CO_2 and stream of compressed CO_2.

References

Amrollahi, Z., Ertesvåg, I.S., Bolland, O., 2011. Thermodynamic analysis on post-combustion CO_2 capture of natural-gas-fired power plant. International Journal of Greenhouse Gas Control 5, 422–426.

Amrollahi, Z., Ystad, P.A.M., Bolland, O., Ertesvåg, I.S. Optimized process configurations of post-combustion CO_2 capture for natural-gas-fired power plant—power plant efficiency analysis. International Journal of Greenhouse Gas Control, submitted for publication.

Aroonwilas, A., Veawab, A., 2007. Integration of CO_2 capture unit using single- and blended-amines into supercritical coal-fired power plants: Implications for emission and energy management. International Journal of Greenhouse Gas Control 1 (2), 143–150.

Cengel, Y.A., Boles, M.A., 2006. Thermodynamics: An Engineering Approach, 6th edition. McGraw-Hill.

Ertesvåg, I.S., Kvamsdal, H.M., Bolland, O., 2005. Exergy analysis of a gas-turbine combined-cycle power plant with precombustion CO_2 capture. Energy 30, 5–39.

Geuzebroek, F.H., Schneiders, L.H.J.M., Kraaijveld, G.J.C., Feron, P.H.M., 2004. Exergy analysis of alkanolamine—based CO_2 removal unit with AspenPlus. Energy 29 (9/10), 1241–1248.

GT PRO version 19, 2009. Thermoflow Inc.

Hammond, G.P., Ondo Akwe, S.S., 2007. Thermodynamic and related analysis of natural gas combined cycle power plants with and without carbon sequestration. International Journal of Energy Research 31 (12), 1180–1201.

IEA, 2008. Carbon Dioxide Carbon and Storage (a Key Carbon Abatement Option). OECD.

Jassim, M.S., Rochelle, G.T., 2005. Innovative absorber/stripper configurations for CO_2 capture by aqueous monoethanolamine. Industrial & Engineering Chemistry Research 45 (8), 2465–2472.

Kotas, T.J., 1995. The Exergy Method of Thermal Plant Analysis. Krieger Publishing Company, Malabar, FL.

Leites, I.L., Sama, D.A., Lior, N., 2003. The theory and practice of energy saving in the chemical industry: some methods for reducing thermodynamic irreversibility in chemical technology processes. Energy 28, 55–97.

Lozza, G., Chiesa, P., 2002. Natural gas decarbonization to reduce CO_2 emission from combined cycles-Part II: steam-methane reforming. Journal of Engineering for Gas Turbines and Power 124 (1), 89–95.

Oyenekan, B.A., Rochelle, G.T., 2007. Alternative stripper configurations for CO_2 capture by aqueous amines. AlchE Journal 53 (12), 3144–3154.

Peeters, A.N.M., Faaij, A.P.C., Turkenburg, W.C., 2007. Techno-economic analysis of natural gas combined cycles with post-combustion CO_2 absorption, including a detailed evaluation of the development potential. Int J Green Gas Control 1 (4), 396–417.

Peng, D., Robinson, D.B., 1976. New 2-constant equation of state. Industrial & Engineering Chemistry Fundamentals 15, 59–64.

Pfaff, I., Oexmann, J., Kather, A., 2010. Optimised integration of post-combustion CO_2 capture process in greenfield power plants. Energy 35, 4030–4041.

Reddy, S., Gilmartin, J., Francuz, V., 2007. Integrated compressor/stripper configurations and methods. Patent No. WO/2007/075466. Fluor Technologies Corporation Fluor Technologies Corporation.

Romeo, L.M., Usón, S., Valero, A., Escosa, J.M., 2010. Exergy analysis as a tool for the integration of very complex energy systems: the case of carbonation/calcination CO_2 systems in existing coal power plants. International Journal of Greenhouse Gas Control 4, 647–654.

Schach, M.O., Schneider, R., Schramm, H., Repke, J.U., 2010. Techno-economic analysis of post-combustion processes for the capture of carbon dioxide from power plant flue gas. Industrial & Engineering Chemistry Research 49 (5), 2363–2370.

Span, R., Wagner, W., 1996. A new equation of state for carbon dioxide covering the fluid region from the triple-point temperature to 1100 K at pressures up to 800 MPa. Journal of Physical and Chemical Reference Data 25 (6), 1509–1596.

Szargut, J., Morris, D.R., Steward, F.R., 1988. Exergy Analysis of Thermal, Chemical and Metallurgical Processes. Hemisphere Publishing Corp, New York.

Tobiesen, A.F., Dorao, C.A., 2008. A simulation study of alternative process configurations for CO_2 absorption plant using CO2SIM. In: Proceedings of 9th International Conference on Greenhouse Gas Control Technologies, GHGT 9.
UniSim Design User Guide, 2008. Honeywell, R380 Release.
Valenti, G., Bonalumi, D., Macchi, E., 2009. Energy and exergy analyses for the carbon capture with the Chilled Ammonia Process (CAP). Energy Procedia 1, 1059–1066.
Yu, Y.S., Li, Y., Li, Q., Jiang, J., Zhang, Z.X., 2009. An innovative process for simultaneous removal of CO_2 and SO_2 from flue gas of a power plant by energy integration. Energy Conversion and Management 50, 2885–2892.
Zhang, N., Lior, N., 2008. Two novel oxy-fuel power cycles integrated with natural gas reforming and CO_2 capture. Energy 33, 340–351.